CHIMERIC RECEPTORS FOR DELIVERY OF T CELL COSTIMULATION

DEVELOPMENT OF NOVEL CHIMERIC RECEPTORS FOR DELIVERY OF COSTIMULATION TO TUMOR-REACTIVE ENGINEERED T CELLS

By ARYA AFSAHI, B.MSc. (HONS)

A Thesis
Submitted to the School of Graduate Studies in
Partial Fulfillment of the Requirements for the Degree

Master of Science

McMaster University

MASTER OF SCIENCE (2015)
(Medical Sciences)

McMaster University
Hamilton, Ontario

TITLE: Development of novel chimeric receptors for delivery of costimulation to tumor-reactive engineered t cells

AUTHOR: Arya Afsahi, B.M.Sc (University of Western Ontario)

SUPERVISOR: Dr. Jonathan L. Bramson

NUMBER OF PAGES: xiv, 120

Abstract

Introduction: Manipulation of the immune system to eliminate cancer, known as cancer immunotherapy, is an emerging field that has shown impressive clinical success and promise. Adoptive transfer of T cells engineered for tumor reactivity is an avenue of therapy for patients with previously untreatable disease. Our lab has developed a novel chimeric receptor, called a T cell antigen coupler (TAC), which redirects T cell cytotoxicity towards a tumor target. Although considerably effective, this receptor does not provide T cell costimulation necessary for optimal anti-tumor effectiveness.

Methods: We explored two methods to deliver costimulation to TAC-engineered T cells. First, we designed a receptor to be utilized in conjunction with the TAC in a dual receptor system. This chimeric costimulatory receptor (CCR) was generated by fusion of the T cell TIGIT and CD28 receptors. In our second approach, we investigated direct incorporation of costimulatory domains into the TAC design. To do so, we substituted in regions from the CD28 or 4-1BB costimulatory receptors.

Results: Three TIGIT/CD28 chimeras were successfully generated. Of these, two were well surface-expressed on primary human T cells. Despite testing of these receptors in several biological assays, we were unable to confirm functionality of these receptors in transmitting CD28 signals. We next generated the 4-1BB and CD28TAC variants. The 4-1BBTAC was poorly surface-expressed

and was difficult to introduce into T cells at high efficiency. The CD28TAC-variant was virtually absent from the T cell surface membrane. Further analysis indicated that the CD28TAC was retained in the endoplasmic reticulum (ER) and the 4-1BBTAC was produced at an extremely low amount.

Conclusions: Our investigation into delivery of costimulation through a novel CCR or TAC receptor was inconclusive. We recommend several optimizations to both receptor design and experimental analysis to further elucidate the potential of these receptors.

Acknowledgments

I would like to first and foremost give my sincere thanks and gratitude to my supervisor, Dr. Jonathan Bramson. This project and thesis would not be what it is today without your guidance and support. Your passion for science and discovery has inspired me in my own pursuit, and your endless help, motivation, and wealth of knowledge have been a guiding light in my research. Our lengthy discussions have helped shape me into the researcher I am today. I would also like to thank my committee members, Dr. Carl Richards and Dr. Manel Jordana, for their input, expertise, and direction on how to be the best scientist I can be.

To members of my lab, I would like to thank you for making this amazing research experience unforgettable. Not only have you supported me with your assistance and willingness to help, but the bonds and friendships we've made over long nights and experiments have kept me going through hard times. I would like to thank Dr. Heather VanSeggelen, Joni Hammill, and Daniela Tantalo. I can't express how much your friendship, help, and direction meant when I first came to Hamilton and the lab. To Dr. Alina Lelic and Robin Parsons, thank you for all of your scientific expertise, and for listening and encouraging me all those times I came to HITS to talk. I would like to also thank Dr. Galina Denisova, Ksenia Bezverbnaya, and Ken Mwawasi for their exceptional scientific knowledge and support. I couldn't have asked for a greater group of people to work with.

To my friends at MIRC, and the community as whole, the friendly atmosphere and wonderful resources have made my time my graduate studies exceptional. I want to thank my partners in crime, Sam Afkhami and Talveer Mandur. Thank you for listening to my rants, and for our shared experiences in the Medical Sciences program, I couldn't have done it without you guys.

To my wonderful parents, sister, and friends, thank you for everything, not only during my graduate studies, but throughout all of my studies. You have been amazing. Mom and Dad, thank you for your tireless support and love, I will always be grateful for all that you sacrificed for me, and all that you have taught me. It is through you two that I have been able to become the person I am today. To my dear sister, you have been so supportive, thank you for listening to my rants and always being there to listen and help.

Finally, I would like to give a special thank you to my girlfriend, Ashley Beaulieu. You're probably sick of hearing about T cells and cancer by now, but your incredible patience, support, and caring (and not to mention your gracious contribution of editing skills!) throughout this means the world to me. I cannot thank you enough. You have been my rock throughout all of this, keeping me on track and sane. I love you!

Table of Contents

Title Page.....i

Descriptive Note.....ii

Abstract.....iii

Acknowledgements.....v

Table of Contents.....vii

List of Figures and Tables.....ix

List of Abbreviations and Symbols xi

Declaration of Academic Achievement xiv

1.0 Introduction.....1

1.1 Cancer and its Etiology 1
1.2 Conventional Cancer Therapy……..2
1.3 Cancer and the Immune System……..5
1.4 T Cells: Potent Anti-Tumor Effectors……7
1.5 Cancer Immunotherapy……11
1.6 Adoptive Transfer of Engineered, Tumor-Redirected T cells……..15
1.7 The Impact of Costimulation on Engineered T cells……18
1.8 TIGIT Inhibitory Receptor and Ligand Distribution on Cancer Cells…..22

2.0 Central Question and Hypothesis……..23

3.0 Materials and Methods……..28

3.1 Cloning of Chimeric Constructs……..28
3.2 Generating Engineered T cells……32
3.2.1 Lentivirus Production……32
3.2.2 Engineering and Culture of Human Primary T cells……..34
3.3 Phenotypic Analysis of Cells……38
3.3.1 Flow Cytometric Analysis of Surface Marker Expression……38
3.3.2 Immunofluoresence……..39
3.4 Assessment of Engineered T cell CD28 Signaling……...41
3.4.1 Phospho-Flow Cytometry……41

3.4.2 Western Blot……..41
3.4.3 Multiple Myeloma Survival Assay……44
3.5 Functional Analysis of Engineered T cells……46
3.5.1 Intracellular Cytokine Staining……46
3.5.2 AlamarBlue Killing Assay……47

4.0 Results……49

4.1 TIGIT/CD28 Chimeric Costimulatory Receptor……...49
4.1.1 Design and Cloning of the TIGIT/CD28 Variants……...49
4.1.2 Generating Engineered Cells by Lentiviral Transduction…….55
4.1.3 Assessment of Signaling via TIGIT/CD28 Chimeras through Akt Phosphorylation……59
4.1.4 Assessment of Signaling via TIGIT/CD28 Chimeras through Multiple Myeloma Survival……69
4.1.5 Assessment of Signaling via TIGIT/CD28 Chimeras through Complementation of the CD4TAC Receptor……73
4.2 Costimulatory TAC Receptors……83
4.2.1 CD28TAC and 4-1BBTAC Design……..83
4.2.2 Phenotype and Cellular Localization……..87

5.0 Discussion……91

6.0 Conclusions……..103

7.0 Appendix……104

References……106

List of Tables and Figures

2.0 Central Question and Hypothesis

Figure 1. Schematic design of the recombinant receptors designed in the Bramson Lab……27

3.0 Materials and Methods

Table 1. A list of primers and their corresponding sequence used within this research……31

4.0 Results

Figure 2. Schematic diagram of construction of the TIGIT/CD28 chimeras……..52

Table 2. Amino acid sequence of TIGIT/CD28 chimeric receptors……..53

Figure 3. Transfer plasmids used to generate lentivirus for engineering of T cells with the TIGIT/CD28 chimeras……55

Figure 4. HEK293TM and primary human T cells variably express the TIGIT/CD28 chimeras……..57

Figure 5. Akt phosphorylation was not measurable by flow cytometry following stimulation with either soluble PMA ± Ionomycin or plate-bound anti-CD3/anti-CD28 antibodies……..60

Table 3. Summary of phospho-Akt (S473) flow cytometry attempts……...62
.
Figure 6. Stimulation with agonistic anti-CD28 produces the greatest Akt phosphorylation at 1 µg/mL……...63

Figure 7. Stimulation with agonistic anti-CD28 antibody induces greatest Akt phosphorylation when incubated for 120 minutes……..64

Figure 8. The TIGIT/CD28 variants do not show increased Akt phosphorylation in response to stimulation with rhCD155……..67

Figure 9. MM.1S cells are not suitable for assessment of CD28 signaling after transduction with lentivirus……71

Figure 10. Schematic diagram depicting the component origins of the HER2-CD4TAC……...74

Figure 11. Schematic of final transfer plasmids used to generate lentiviruses for coexpression of HER2-CD4TAC and TIGIT/CD28 chimeras……...75

Figure 12. TAC and TIGIT/CD28 are poorly expressed in primary T cells, but not HEK293TM cells……..77

Figure 13. The cancer cell lines A549, MDA-MB-231, LoxIMVI, and SKBR3 expresses CD155……...79

Figure 14. T cells transduced with both HER2-CD4TAC and TIGIT/CD28 chimera do not show enhanced IL-2 production compared HER2-CD4TAC alone when stimulated with tumor cells……....80

Figure 15. Inclusion of the TIGIT/CD28 CCR does not alter the cytokine expression profile of T cells expressing the HER2-CD4TAC……81

Figure 16. The TIGIT/CD28 chimeras do not affect the killing of tumor cells……..82

Figure 17. Schematic diagram depicting the construction of the modified TACs from the original HER2-CD4TAC components and parent CD28 or 4-1BB proteins……84

Table 5. Amino acid sequence of the modified TAC receptors……85

Figure 18. Final transfer plasmid designs used for generation of lentiviruses encoding either the HER2CAR, HER2-CD4TAC, HER2-CD28TAC, or HER2-4-1BBTAC……..86

Figure 19. Primary human T cells poorly express modified TAC receptors……...89

Figure 20. HER2-CD4TAC and HER2-CD28TAC, but not HER2-4-1BBTAC, expression is observable by western blot analysis……....90

Figure 21. Immunofluorescence microscopy of CAR- and TAC-transduced T cells……..91

7.0 Appendix

Figure S1. Lentiviruses containing the HER2-CD4TAC, and to a lesser degree the HER2-CD28TAC, contain the TAC receptor protein……..106

Figure S2. The cell line K562 expresses the surface antigens CD112 and CD155……107

List of Abbreviations and Symbols

α alpha

β beta

Δ delta

γ gamma

ε epsilon

ζ zeta

μ micro

ACT adoptive cell transfer

ALL acute lymphoblastic leukemia

APC(s) antigen-presenting cell(s)

aAPC(s) artificial antigen-presenting cell(s)

BSA bovine serum albumin

BV brilliant violet

CAR chimeric antigen receptor

CCR chimeric costimulatory receptor

CD# cluster of differentiation

cDNA complementary DNA

CLL chronic lymphocytic leukemia

cRPMI complete RPMI

CTL(s) cytotoxic T lymphocyte(s)

CTLA-4 cytotoxic T lymphocyte antigen-4

DAMP(s) danger associated molecular pattern(s)

DARPin designed ankyrin repeat protein

DC(s) dendritic cell(s)

DMEM Dulbecco's modified Eagle medium

DNA deoxyribonucleic acid

EF-1α elongation factor 1 alpha

ER endoplasmic reticulum

FACS fluorescence-activated cell sorting

FBS fetal bovine serum

HER2 human epidermal growth factor receptor 2

HLA human leukocyte antigen

IFN(s) interferon(s)

IL interleukin

ITIM immunoreceptor tyrosine-based inhibitory motif

mAb(s) monoclonal antibody(ies)

MEM minimum essential medium

MFI mean fluorescence intensity

MHC major histocompatibility complex

MOI multiplicity of infection

NGFR nerve growth factor receptor

PAMP(s) pathogen-associated molecular pattern(s)

PBMC(s) peripheral blood mononuclear cell(s)

PBS phosphate buffered saline

PCR polymerase chain reaction

PD-1 programmed death 1

PFA paraformaldehyde

PRR(s) pattern recognition receptor(s)

rh recombinant human

RNA ribonucleic acid

RPMI Roswell Park Memorial Institute

RRE rev response element

scFv single-chain variable fragment

T2A *Thosea asigna* virus 2A sequence

TAA(s) tumor-associated antigen(s)

TAC T cell antigen coupler

TBS Tris-buffered saline

TCR T cell receptor

TIGIT T cell immunoreceptor with Ig and ITIM domain

TM transmembrane

TNF tumor necrosis factor

VSV vesicular stomatitis virus

WT wild type

Declaration of Academic Achievement

The work presented and described in this thesis is a result of the combined effort of myself and Dr. Jonathan Bramson over the course of my Master's graduate studies. Together, we conceived the experimental design and approaches described, and I carried out the associated work. We interpreted the resulting data together, and drew conclusions where appropriate.

1.0 Introduction

1.1 Cancer and its Etiology

Cancer is a disease of many multicellular organisms characterized by the unrestricted growth and expansion of cells in local and distant sites. The properties that permit cell growth during embryogenesis and wound healing become dysregulated during carcinogenesis[1]. Carcinogenesis, first proposed by Nowell in 1976, is a process through which cells accumulate progressor mutations and undergo neoplastic transformation, acquiring the capacity to proliferate uncontrollably[2]. Neoplastic cells continuously arise as a byproduct of stochastic DNA errors, genetic predisposition, and environmental stimuli[3–5]. With regard to environmental stimuli, it is clear that a causal relationship exists between cigarette smoking and lung cancer[6], and a significant correlation between indoor tanning and certain skin cancers[7–9]. Cigarette smoke, which contains many known carcinogens[10], and ultraviolet light promote cancer by inducing mutations into the genome of cells. As cells become transformed and attain the ability to initiate tumor growth, a tumor niche that is conducive to their growth begins to form. This environment is comprised of accessory cells, such as fibroblasts and stromal cells, and vasculature that support tumor formation[11,12]. Depending on the tissue origin and the location of tumors and metastases, cancerous masses resulting from this unchecked growth may deprive local tissues of nutrients, secrete factors that disrupt natural physiology, or physically disrupt the function of organ systems. Each

of these mechanisms negatively affect the health of afflicted patients, ultimately contributing to untimely death.

Despite the impact cancer has had on humanity throughout history, attempts to treat the disease have been mostly ineffective until the past century[13]. Passing of the U.S. National Cancer Act in 1971 paved the road for increased research and, arguably, began the greatest concerted effort towards improved treatment of cancer[13]. However, in spite of such efforts, cancer remains the leading cause of death in Canada, accounting for roughly 30% of all deaths[14]. Two in five Canadians will develop cancer in their lifetime, and one in four will die from this disease[14]. The Canadian Cancer Society's Advisory Committee predicts that nearly 200,000 new cases of cancer will be diagnosed by the end of 2015, highlighting the prevalence and impact of this disease on Canadians.

1.2 Conventional Cancer Therapy

As cancer arises from our own tissues, the greatest challenge in treating the disease is the design of agents that discriminate cancerous tissue from healthy tissue. Furthermore, due to the stochastic and unstable nature of cancerous cells, cancer represents a group of similar diseases with considerable inter-tumor heterogeneity between patients, and intra-tumor heterogeneity within an individual[15–17]. This heterogeneity results in a level of variance between patients, where cancers of the same type and grading may differ and may therefore not respond to the same treatments[18]. Additionally, within any given patient, cancer

cell subpopulations arise that often diverge in their phenotype and gene expression as a result of this clonal heterogeneity. This presents a difficult situation where no single pharmacological or medical intervention may target all tumor cells. The level of diversity and heterogeneity between cancer types is, at least partially, dependent on the stability and level of somatic mutations present within the cancer cells. For example, lung cancers and melanoma often arise from considerable external carcinogenic factors, have the greatest number of somatic mutations, whereas cancers of the brain possess far fewer mutations[19]. Consequently, the notion that there exists a possible "cure to cancer" may be disingenuous given the highly complex and variable nature of the disease. Conventional therapies have attempted to address commonalities among tumors by either removing the cancerous tissue (surgery), destroying afflicted tissues (radiotherapy), or killing rapidly dividing cells (chemotherapy). Patient's lives have been extended using these therapies and, in some cases, their tumors have been put into complete remission.

Surgery was the earliest form of cancer treatment, gaining prominence in the early 19th century with the development of anaesthesia and antiseptic techniques, and peaking with radical surgeries where tissues were removed *en masse* in an attempt to capture all residual cancerous tissue[20]. These radical surgeries were no more effective than more conservative approaches that sought to preserve healthy tissue, and until the advent of radiotherapy and chemotherapy, many cancers remained untreatable. Today, surgery is an effective choice for

isolated or low-grade tumors, and cures may be achieved if no cancerous cells are left behind. However cancers may develop in, or metastasize to, sites that are not surgically accessible. This is particularly an issue in the case of metastases to the brain. Modern radiotherapy and chemotherapy allow treatment for a broader and more diverse range of cancers. Chemotherapy utilizes systemic delivery of cytotoxic chemicals that preferentially target and kill cancerous cells by exploiting their rapid division. Radiation therapy is a highly targeted treatment that delivers ionizing radiation to kill cancerous cells in a well-defined region [20]. Chemotherapy and radiotherapy may be utilized in conjunction with surgery as a pre-operative (known as *neo-adjuvant therapy*) or post-operative treatment (known as *adjuvant therapy*). Post-operative treatment with irradiation and chemotherapy following surgery has improved survival in the case of certain cancers, such as breast cancer[21]. In fact, many cancers today are treated with a combination therapy in hope that a multi-pronged approach will eliminate the chances of tumor escape and resurgence.

Although these conventional cancer therapies can be successful in low-grade, mid-grade, and sometimes advanced disease, these approaches often prove unproductive in the case of certain cancers, metastases, or relapsed disease[22,23]. Cancer recurrence and metastasis represent two of the largest hurdles to overcome. Despite seemingly successful treatment of primary tumors, previously disseminated tumor cells often remain dormant and hidden for a considerable length of time – even as long as decades – before emergence and

progression into active disease once again[24–26]. Selection processes and genetic changes are induced in these distal secondary tumors, and these aberrations promote resistance to previously effective chemotherapy or radiation therapy[27–29]. Thus, despite advances in targeted drug development, screening, and diagnosis, there is still an unmet clinical need for treatment of aggressive metastatic or relapsing drug-refractory disease. Paramount in developing innovative cancer therapeutics is the creation of a system or treatment that is effective in both finding and targeting disseminated cancer cells.

1.3 Cancer and the Immune System

The majority of organisms contain some form of immune system to combat entities that pose a threat to their well-being. The complexity of these systems can range from the relatively simple CRISPR/Cas system used to target bacteriophages and foreign DNA in prokaryotes[30], to the complex network of cells, tissues, and soluble mediators that have evolved in higher vertebrates to respond to pathogens and other dangers. In humans, with the exception of some privileged sites such as the eye[31], immune cells circulate and access tissues using the arteriovenous and lymphatic vessels in order to prevent pathogen entry and maintain health. Antigen presenting cells (APCs) of the innate immune system survey tissues, sampling both foreign and self-antigens with germ-line encoded pattern recognition receptors (PRRs). These receptors have evolved to detect pathogen- or danger-associated molecular patterns (PAMPs and DAMPs) as a

possible threat[32]. Recognition of these danger signals by the innate immune system initiates a cascade of events that lead to generation of an immune response. Phagocytic innate cells are rapidly recruited to eliminate pathogens and respond to danger. Meanwhile, additional processes begin to activate B and T lymphocytes of the adaptive branch of the immune system.

It is now abundantly clear that the immune system is tied in with both anti- and pro-tumor pathways, with ample evidence highlighting the ability of certain immune cells to “police” cell transformation and control neoplasms in a process known as immunosurveillance[33–35]. Due to a lack of supporting evidence, the concept of immunosurveillance received much criticism when first proposed in the mid-20th century by Burnet and Thomas[36]. However, several key studies examining the rate of cancer formation in immunodeficient mice, and in humans with reduced immune function, brought support to this hypothesis[36]. Transplant patients given immunosuppressive drug therapy to prevent rejection are at an increased risk of non-infection related cancers[37,38]. Additionally, immune cells can factor heavily into tumor relapse or progression to clinical disease. Examination of tumor biopsies from cancer patients has revealed that the level and cellular composition of immune infiltrates in the tumor biopsy correlate with prognostic outcome of many cancers[39,40]. These studies hint at the complicated interplay between the immune system and the growing tumor mass. Paradoxically, while immune cells can eliminate tumor cells, extrinsic tumor control by the immune system sculpts and selects for tumor cells able to evade and escape immune clearance, a process

known as immunoediting[35,41]. Thus, many cancers that arise are frequently poorly immunogenic due to the selection forces imposed by the immune system.

1.4 T Cells: Potent Anti-Tumor Effectors

Of the immune cells present in humans, the T lymphocyte (further referred to as a T cell) is one of the most potent cells with anti-tumor functionality. Each T cell bears an antigen receptor with unique specificity, known as a T cell receptor (TCR), which binds to a defined peptide antigen presented in the context of a major histocompatibility complex (MHC) molecule (pMHC). MHC molecules are cell-surface receptors classified as either class I or II based upon which subset of T cells they interact with[42]. In humans, all nucleated cells express class I MHC. However, only some cells, such as APCs, express class II MHC[42]. The peptides bound by MHC are derived from virtually any protein source, such as cellular, bacterial, or viral proteins, and are known as T cell antigens.

Development and maturation of T cells in the thymus is a complicated process that results in a cell with unique specificity and minimal self-reactivity[43]. This broad TCR diversity is a result of somatic recombination events that occur during T cell development where genomic segments of the TCR α and β chains are rearranged to generate novel sequences. Through this process, the immune system is able to generate T cell clones that are distinct in their reactivity, generating a population of cells capable of responding to nearly any protein antigen[43]. Following gene rearrangement, immature T cells are tested for the ability

to bind to pMHC. The ability to bind either MHC class I or II determines their differentiation to the $CD4^+$ or $CD8^+$ subset, respectively[44]. Once fully matured, naïve T cells egress from the thymus and begin to populate secondary lymphoid organs, where they remain until activation.

Dendritic cells (DCs) are the primary innate APCs, which activate naïve T cells. DCs constantly sample antigen in the periphery, returning to lymphoid tissues to present captured antigens to naïve T cells. However, TCR binding to pMHC alone is not sufficient to fully activate a naïve T cell. In addition to TCR stimulation, T cells require costimulatory signals to become fully activated. Costimulation provides secondary signals that integrate with TCR stimulation to reinforce activation, maintain survival, and promote differentiation to memory and effector T cells[45]. In the absence of costimulation, T cells will enter a state of hypo-responsiveness known as anergy[46]. CD28 is the prototypical costimulatory receptor present on naïve T cells, and is one of the most potent and well-studied costimulatory pathways[47,48]. The receptor forms a homodimer on the cell surface and transmits signals through its cytoplasmic tail upon binding of its ligands, CD80 and CD86[49]. Signaling through CD28 promotes survival and proliferation through promotion of the anti-apoptotic protein Bcl-X_L, inhibition of apoptotic pathways, and translocation of NFκB and NFAT transcription factors to the nucleus[49,50]. Growth and function are also supported through upregulation of glucose transport and glycolysis[51,52], increased cytokine (primarily IL-2) and chemokine expression[53,54], as well as expression of additional costimulatory receptors[54]. CD28 signaling is

also critical for stabilizing and synergizing with the TCR/CD3ζ signaling pathways to reduce the threshold for full activation[54] and expansion of memory cells[55,56]. There is some indication that CD28 also mediates qualitative, in addition to quantitative, transcriptional programs that are distinct from TCR/CD3ζ signaling[57].

Under steady state conditions, DCs remain immature and tolerogenic, and therefore do not activate naïve T cells to presented antigens, presumably as a mechanism of maintaining tolerance to self-antigens. However, the presence of danger signals in the periphery, such as DAMPs/PAMPs or signals from other immune cells, can activate DCs to become mature. Maturation of DCs results in upregulation of costimulatory ligands, such as CD80/86 that ligate CD28, needed to fully activate naïve T cells[58]. Once activated, T cells proliferate and the daughter cells acquire features of memory or effectors. Memory T cells are long-lived cells that retain the ability to rapidly proliferate and expand in response to antigenic-stimulation. Conversely, effector T cells are short-lived, functioning to circulate, identify, and delete pathogens or nascent neoplastic cells.

The greatest difference between $CD4^+$ and $CD8^+$ T cells is centered on their functionality and role in the immune system. In regards to tumoricidal activity, $CD8^+$ T cells are the primary mediators of tumor de-bulking. Known as cytotoxic T lymphocytes (CTLs), these T cells are highly efficient killers that recognize antigen presented in the context of MHC class I. Upon synapse formation with a tumor or virally-infected cell, CTLs rapidly initiate apoptotic or necrotic pathways in the target

cell. Furthermore, CTLs can bind and induce cell death in multiple target cells simultaneously, highlighting the capacity of these cells to act as serial killers[59]. During this process, the lytic machinery is spatiotemporally uncoupled from the antigen-stimulation synapse. This property allows CTLs to mediate bystander killing of antigen-negative surrounding cells[59,60], a characteristic that can contribute to the control of a heterogenous tumor population. To achieve killing, CTLs possess a variety of cytotoxic modalities, including both soluble-factor- and receptor-mediated mechanisms. Of these mechanisms, the granule-exocytosis pathway is a dominant mediator of cytotoxicity. Granules, containing the cytotoxic molecules perforin and granzyme, are polarized to the synapse and released into the cleft where they are able to induce lysis and/or apoptosis of target cells[61]. Additionally, $CD8^+$ T cells express Fas ligand, a death receptor ligand which results in induction of apoptosis in target cells upon binding to its receptor, Fas[61]. Conversely, $CD4^+$ T cells are more prominently involved with regulation of immune responses and cells, although they are infrequently capable of direct cytotoxicity[62,63]. These cells are further categorized into subsets with different functions and impact on anti-tumor immunity[64]. For example, T helper cells facilitate $CD8^+$ cytotoxic T cell anti-tumor responses[64]. Signals provided by helper $CD4^+$ T cells to APCs result in their activation and subsequent ability to prime naïve $CD8^+$ T cells[65]. In addition to their interaction with APCs, helper $CD4^+$ T cells also provide signals during primary activation of $CD8^+$ T cells that are critical in facilitating secondary expansion of $CD8^+$ memory T cells[66]. Helper T cells also

produce a number of key cytokines that regulate immune function and can mediate tumor control. T helper 1 $CD4^+$ T cells are producers of the cytokines TNFα and IFNγ. TNFα binding to TNF receptors on T cells functions to enhance their activation[67,68], and also facilitates recruitment of immune cells to tumors by improving vascular permeability[67]. IFNγ sensitizes tumor cells to T cell-mediated killing through upregulation of MHC I receptors[69,70].

1.5 Cancer Immunotherapy

T cells possess attributes and characteristics that make them desirable candidates for targeting and eliminating cancers. However, several factors limit the utility of these cells under normal physiological conditions. Among these are the restrictions placed on generation of natural anti-tumor cells. T cells can be powerful mediators of auto-immunity[71]. When direct against self-antigens, the highly cytotoxic and inflammatory nature of T cells can pose a threat to the integrity of the body. To prevent generation of auto-reactive T cells during development, T cell-precursors that have rearranged their TCR to react against a self-antigen are eliminated to prevent auto-immune disease. This process is known as central tolerance. A consequence of central tolerance is a limited generation of natural anti-tumor T cells. Because tumor cells arise from autologous healthy tissues, there are likely few T cells that can distinguish the tumor from healthy tissue due to central tolerance. With the exception of novel antigens produced as a result of genomic mutation, referred to as *neo-antigens*, and germ-line restricted antigens

expressed due to aberrant DNA methylation[72], many tumors remain largely non-immunogenic[73,74].

However, T cells and the immune system can be manipulated to overcome these limitations. Cancer immunotherapy is a rapidly expanding field that seeks to harness and direct the immune system to target and induce cancer regressions. The first documented approach to cancer immunotherapy was conducted by Dr. William Coley in the late 1890s[75]. Dr. Coley noted that in certain rare cases, cancer patients appeared to undergo sudden, unexpected resolution of their cancer following an infection. Coley performed a radical treatment on three of his patients in 1891 where he inoculated them with live streptococcal bacteria. Although two of these patients ultimately died, Dr. Coley confirmed that the presence of an infection can induce regression in some cancers. He continued to work on this treatment, creating what is known as “Coley’s Toxin” – a combination of heat-killed streptococcus and *Serratia marcescens* – and treated hundreds of cases[75]. We now appreciate that the infection triggered an immune response, and recruited immune cells also eliminated cancer cells through bystander killing. The presence of inflammatory factors produced in response to the pathogen may also have relieved some tumor-mediated immunosuppression and improved the functionality of tumor-specific T cells. This approach has been extended to treat bladder cancers in the past century, by injection of the tuberculosis vaccine BCG[76]. Although BCG treatment can produce regression of bladder cancer, it is not without

side-effects, the most severe of which is a systemic reaction similar to that of septic shock that requires intensive care[76].

One of the greatest examples of the power of cancer immunotherapy has been the recent creation of checkpoint blockade inhibitors that relieve T cell inhibition. These drugs are monoclonal antibodies (mAb) that block signaling of inhibitory receptors on activated T cells, relieving the negative T cell regulation that occurs in the tumor and draining lymphatics. Blockade of either PD-1 or CTLA-4, two T cell inhibitory receptors, has led to regression of previously untreatable advanced melanoma and improved survival of patients with numerous diseases, such as renal cancer, lung cancer, lymphoma)[77–82]. However, this form of therapy is most effective in the case of immunogenic cancers where anti-tumor T cells are already present, but in a state of hyporesponsiveness. Furthermore, current mAb therapy is a systemic treatment that is not restricted to relief of anti-tumor T cells alone and results in significant, albeit reversible, toxicity due to the presence of checkpoint receptor ligands present on regular tissues [83,84]. These toxicities are often mild or moderate in severity. However, immune-related adverse events of higher grade, such as colitis or hepatitis, may present and require medical intervention[84].

Another approach to circumvent the rarity of anti-tumor T cells has been through therapeutic vaccination against tumor-associated antigens (TAA). At the heart of cancer immunotherapy is the identification and choice of a suitable tumor

antigen. The risk of autoimmune sequelae due to cross-reactivity is an important consideration when choosing a target antigen. As T cells clonally expand, any cross-reactivity to a self-antigen may result in potentially serious adverse effects[85,86], although these effects may be attenuated[87]. Tumor antigens may be loosely categorized as either low- or high-tumor specificity[72]. Highly specific tumor antigens include neo-antigens and oncofetal antigens. However, identification of neo-antigens is a difficult and highly laborious task, and mutations are primarily restricted to the individual[73]. Historically, the majority of targeted tumor antigens have included over-expressed proteins, and differentiation antigens on non-essential tissues[72]. So far, truly effective therapeutic anti-cancer vaccines have proven elusive[88]. Our lab has investigated therapeutic adenovirus-based cancer vaccines and noted that the vaccine-induced T cells trigger an adaptive immunosuppression within the tumor that prevented sustained regression[89]. We suspect that this phenomenon explains the limited utility of vaccination strategies to fight cancer on their own. It is believed that a combination of therapeutic vaccination and checkpoint blockade may provide a therapy that is available for a broad range of patients, not simply those with immunogenic tumors, and produce more favorable outcomes. Clinical trials addressing this hypothesis are currently underway (ClinicalTrials.gov Identifier: NCT02263508 and NCT01740297).

1.6 Adoptive Transfer of Engineered, Tumor-Redirected T cells

Advances in genetic engineering and T cell culture have allowed clinicians and researchers to bypass some of the difficulties that exist in producing a robust, natural anti-tumor response – such as poor reactivity to tumor antigens – and exploit T cell clonal expansion, systemic circulation, and natural cytotoxic capabilities against neoplastic cells.

T cells harvested from peripheral blood mononuclear cells (PBMCs) can be engineered for tumor-reactivity, expanded *ex vivo*, and subsequently infused into the patient through a process called adoptive cell transfer (ACT). Through gene transfer technology, T cells can be engineered to express a tumor-directed receptor with chosen specificity and function. This approach has shown considerable promise in enhancing T cell tumoricidal activity, and can therefore be used to circumvent the rare production of anti-tumor T cells due to central tolerance. Moreover, evidence from our lab and others has indicated that the large number of T cells provided by ACT can overwhelm the adaptive response of the tumors and produce tumor regression[90,91].

Usage of e*x vivo* culture and gene engineering allows a highly tailored approach to producing a very defined and characterized T cell product. This methodology permits customization of the final product at both the cellular and population level. T cell subset composition appears to be a key determinant in success of therapy, and it is now evident that choice of T cell subset greatly affects

the efficacy of ACT[92]. Recent evidence suggests less differentiated cultures engraft better and produce the greatest anti-tumor efficacy[93]. Thus, at the population level, T cell cultures can be customized to achieve the ideal composition. However, the principle component in engineered T cell therapy is the redirection of T cells through expression of a tumor-directing receptor.

The two primary methods of T cell redirection involve engineering expression of either a known TCR or a chimeric antigen receptor (CAR). T cells engineered to express a known tumor-reactive TCR are functionally similar to natural T cells. These cells recognize antigens in an MHC-dependent manner and therefore require patients to have the proper human leukocyte antigen (HLA; the human MHC genes) composition. TCR-engineered T cells represent a viable strategy to target tumors, and the latest studies describing the challenges and successes of this platform are reviewed in more detail by Bonini and Mondino[94]. However, tumors often exhibit MHC I downregulation[95] and antigen processing defects[96,97] which prevent TCR-based recognition. CAR-technology utilizes a myriad of binding moieties and so does not encounter this issue. Because of this we have chosen to focus our attention to examining CAR-technology and chimeric receptors. CARs are synthetic hybrid molecules comprised of an extracellular binding moiety (and sometimes linker) attached to an intracellular signaling endodomain through a transmembrane (TM) domain. Described first in 1993 by Eshhar *et al.*, the earliest first generation CAR against a tumor target consisted of a scFv specific to the human epidermal growth factor receptor 2 (HER2), a

differentiation antigen that is often overexpressed on breast cancers[98,99], linked to the ζ chain of CD3 or the γ subunit of the Fc receptor[100,101]. CARs effectively link binding of native, surface-expressed antigens to T cell activation in an MHC-independent manner, circumventing antigen processing and presentation. Furthermore, CARs also allow for binding of non-canonical T cell epitopes, such as carbohydrates or glycolipids, expanding the range of tumor antigens available for targeting. The most crucial facets of CAR design lie in the choices of antigen target and signaling motif incorporated into the CAR, as these components are the primary drivers of T cell targeting and activation. Although scFv molecules are predominately utilized for antigen binding, other binding domains such as the extracellular portion of the natural killer and T cell cytotoxic receptor NKG2D[102–104], or repeat proteins such as designed ankyrin repeat proteins (DARPins; Bramson lab, manuscript submitted) have been employed in CAR design. Perhaps the most impressive display of CAR-T cell potential was shown in a recent trial utilizing an anti-CD19 CD3ζ-4-1BB CAR for the treatment of relapsed or refractory acute lymphoblastic leukemia (ALL), a form of cancer that is virtually untreatable with current approved therapies[105]. Twenty-five patients aged 5-22 and five patients aged 26-60 were treated with these T cells, and an impressive 27 patients displayed complete remission post CAR-T cell therapy, with 67% of these individuals remaining in remission at 6 months. The trial saw an overall survival rate of 78% at 6 months[105].

1.7 The Impact of Costimulation on Engineered T cells

Upon infusion, engineered T cells must survive adoptive transfer to engraft, then expand and persist to display optimal anti-tumor efficacy. Furthermore, the tumor microenvironment is a harsh setting for infiltrating lymphocytes, containing inhibitory soluble factors and cells, such as regulatory T cells and myeloid-derived suppressor cells[106–108]. T cells within the tumor microenvironment may, over time, enter a state of exhaustion. Exhausted T cells express inhibitory receptors, become hyporesponsive to stimulation, and have reduced cytotoxic and effector function[109]. In addition to the immunosuppressive factors present, tumor cells often express ligands of T cell coinhibitory receptors. In opposition to costimulation, coinhibition provides negative regulation on activated T cells that limit their function and cytotoxicity[110,111]. These negative signals within the tumor present a strong barrier to therapy. This is underscored by the clinical success of checkpoint blockade inhibitors attenuating signaling through co-inhibitory ligands CTLA-4 and PD-1[77–80].

To adequately prepare engineered T cells for the tumor microenvironment, provision of costimulatory signals can enhance the hardiness, persistence, survivability, and proliferation of these cells[112–115]. A study of 14 patients with relapsed refractory chronic lymphocytic leukemia (CLL) highlights the importance of engraftment and persistence of the T cells in ACT. Using anti-CD19 CD3ζ-4-1BB CAR cells, the authors found that expansion and persistence of these cells correlated with an objective response[116].

There are several methods by which costimulation may be provided to T cells through genetic engineering. The most widely utilized approach has been to include costimulatory signaling endodomains in the structure of the chimeric receptor, as seen in conventional second and third generation CARs[117]. Currently, a number of CAR designs incorporating different costimulatory endodomains are under investigation. These include, but are not limited to, CD28[114,115,118], 4-1BB[119,120], OX40[119,121], CD27[122], or ICOS[119,123]. These studies demonstrate the improvements in anti-tumor efficacy when costimulatory signaling domains are included.

Inclusion of the CD28 TM and cytoplasmic tail is one the most widely utilized CAR designs incorporating costimulatory endodomains. CAR-T cells containing the CD28 endodomain show enhanced IL-2 secretion, proliferation, survivability, and persistence in both pre-clinical models[115,118] and lymphoma patients[114] when compared directly to an equivalent CD3ζ first generation CAR. A recent publication by Condomines *et al*. highlights the possible advantage of including the CD28 costimulatory domain in the design of a CAR, rather than through the natural pathway[124]. This study examined T cells engineered with either a first generation CD3ζ CAR, the same CD3ζ CAR and CD80, or a second generation CD28-CD3ζ CAR. The authors' investigation concluded that CD28 costimulation through the CAR provided greater benefit over constitutive expression of costimulatory ligand CD80, which is capable of providing both auto- and trans-costimulation when engineered for expression in T cells[125]. The authors explain the probable

mechanism behind this phenotype is that CD28 signaling through the CAR bypasses the ability of the coinhibitory receptor CTLA4 to form a high-affinity interaction with CD80 and outcompete CD28, thus averting inhibitory signaling. Interestingly, one report investigating a second generation CD3ζ-CD28 CAR found that inclusion of CD28 reduced the anti-tumor efficacy of the CAR-T cells in their model due to CD28-mediated IL-2 production preferentially supporting expansion of regulatory T cells within the tumor[126]. Conversely, other studies have highlighted the importance of CD28 signaling in overcoming the suppressive effects of regulatory T cells[127] and the anti-inflammatory cytokine TGF-β[112].

An alternative approach to providing costimulation is through use of a dual receptor system that splits the primary TCR/CD3ζ activation signal to one receptor and the costimulatory signal to a second, chimeric costimulatory receptor (CCR) targeting a secondary tumor antigen – akin to natural T cell signaling. One of the earliest reports of such a CCR described a fusion protein consisting of a GD2-specific scFv fused to the CD28 hinge, transmembrane, and cytoplasmic tail[128]. This receptor provided survival and proliferative advantages to transduced primary T cells. An added advantage of a split receptor system is the ability to attenuate one or both receptors and, in turn, require ligation of both receptors for full T cell activation. With proper choice of target antigens, this method of T cell redirection can further enhance specificity to tumor cells. Kloss and colleagues have elegantly shown this experimentally by transducing T cells with a PSCA-specific CD3ζ CAR and a PSMA-specific CD28-4-1BB CCR and showing that T cell activation and

cytotoxicity only occurs when target cells express both antigens[129]. The crux of the authors' method lay in finding a PSCA-specific scFv that was a suboptimal activator of T cells. When this suboptimal scFv was not utilized, the engineered T cells were able to respond to cells expressing the PSCA alone. This study highlights two direct benefits to this approach, the first of which is in the absence of a tumor-specific antigen, less optimal antigens may be utilized. Secondly, T cell cytotoxicity is further restricted to a specific expression profile that can be fine-tuned to tumor cells.

Despite the considerable number of studies investigating different CAR designs, few have done head-to-head comparisons between costimulatory domains. A study conducted by Zhong *et al.* found that combination of CD28 and 4-1BB resulted in an additive improvement[130], whereas Milone *et al.* found that CD3ζ-4-1BB has a greater anti-leukemic effect *in vivo* when compared directly to CD3ζ-CD28 CARs targeting CD19[131]. A recent study investigating functional differences between second generation CARs incorporating CD28, ICOS, or 4-1BB found that incorporation of CD28 with an IgG4 hinge conferred substantial auto-proliferative capacity, which is a potential safety concern [132]. Ultimately, it remains unclear which costimulatory domain, or combination of domains, provides the greatest functional advantage to CAR-engineered T cells[133]. Given the conflicting evidence on the benefits and downsides of different endodomains, it may be that the choice is dependent on the target antigen, CAR structure, or cancer being treated, and will ultimately be determined in clinical trial testing.

1.8 TIGIT Inhibitory Receptor and Ligand Distribution on Cancer Cells

TIGIT is a recently identified coinhibitory receptor[134] belonging to the CD28 family expressed on NK, activated-, memory-, and regulatory-T cells[135]. TIGIT is able to bind the nectin and nectin-like adhesion molecules CD155 and CD112[136]. Similar to CD28, TIGIT is a type 1 transmembrane cell surface protein containing a single IgV ectodomain However, TIGIT contains two ITIM motifs on its intracellular domain which are believed to be important in inhibitory signaling[136,137]. TIGIT is expressed on the cell surface as a monomer, dimer, or oligomer, but binds its primary ligand, CD155, as a dimer[137]. This interaction takes place through a lock-and-key motif present on TIGIT and CD155[137]. Interestingly, TIGIT has a counter receptor that acts as an activating/stimulatory receptor, CD226. In this regard, the TIGIT/CD226 dynamic is highly analogous to CTLA-4/CD28 in expression, affinity, and function[136,138]. TIGIT ligands are highly associated and upregulated on a number of primary human cancers. CD155 and CD112 are upregulated on colorectal[139] and ovarian carcinomas[140], and breast and ovarian cancers[141], respectively. Furthermore, both CD155 and CD112 are upregulated on acute myeloid leukemias[142], myeloma[143], some lymphoblastic leukemias[142] and neuroblastomas[144], as well as many cancer cell lines[145]. This high ligand expression seems counterintuitive at first, as tumors would normally seek to downregulate activating ligands on their cell surface. However, the affinity of TIGIT for CD155 and CD112 is greater than that of CD226[138], and evidence from NK cells shows that chronic CD155 exposure by some primary cancers downregulates

CD226 expression, curbing the antitumor response[146]. CD155 has also been shown to augment tumor cell invasiveness and dispersal, suggesting a potential role in metastasis[147,148]. Finally, the effects of TIGIT on antagonizing T cell anti-tumor function is most evident by studies investigating the correlation of TIGIT on anti-tumor T cells, and the improvements seen by blocking signaling with an antagonistic mAb. Expression of TIGIT on $CD8^+$ T cells is well correlated with infiltration of primary solid tumors such as melanoma[149], and blockade with anti-TIGIT mAb increases functionality[149–151].

2.0 Central Question and Hypothesis

The field of engineered-T cell therapy has rapidly grown and expanded in the past several years, and impressive results from clinical trials utilizing anti-CD19 CARs highlight the potential of this form of treatment. The Bramson lab is developing a number of novel recombinant receptors that redirect T cells to tumors as an alternative to conventional CARs. These receptors, collectively termed T cell Antigen Couplers (TAC) are distinct from CARs as they do not rely on artificial signaling domains for activation. Instead, the TAC receptor redirects the native TCR via an scFv specific to CD3ε (**Figure 1A**). The TAC receptor also contains the CD4 hinge, TM, and cytoplasmic domain to recruit the receptor to lipid rafts and associate with Lck, an essential kinase in TCR signaling and activation (**Figure 1A**). Although not yet proven, we believe the mechanism of action of the TAC relies on ligation of multiple TAC receptors to a target cell, resulting in clustering of TAC-TCR/CD3 complexes to initiate natural signaling through the endogenous machinery by bringing Lck within proximity of TCR complexes. As this approach does not rely on synthetic signaling endodomains, we believe it is functionally closer to natural T cell activation.

This TAC prototype, which is specific to the HER2 antigen (HER2-CD4TAC) has a number of potential advantages over conventional CARs. The HER2-CD4TAC receptor has shown increased potency/killing of tumor lines *in vitro* in comparison to a conventional second generation CAR employing the same binding domain with CD3ζ and CD28 endodomains. Furthermore, TAC-engineered T cells

appear to produce less inflammatory cytokines (Bramson Lab, unpublished data) than CAR-T cells, which may be beneficial in avoiding the toxicities associated with cytokine release syndrome seen in CAR-T cell therapy[105]. However, the HER2-CD4TAC does not transduce any kind of costimulatory signal, which is constructive to anti-tumor efficacy of adoptively transferred T cells. Given the clear improvements of costimulation on the functionality of CAR-engineered T cells, we logically hypothesized that provision of costimulation to our TAC-engineered T cells would be equally advantageous, as the current TAC receptor is analogous to first generation CD3ζ CARs.

We first sought to develop a bipartite receptor system incorporating a chimeric costimulatory receptor. To this end, we investigated a chimeric receptor composed of the TIGIT extracellular binding domain fused to the TM and cytoplasmic tail of CD28 (**Figure 1B**). The nearly ubiquitous expression of TIGIT ligands on adenocarcinomas and certain hematological malignancies makes utilization of TIGIT as a targeting moiety attractive. Additionally, since CD28 requires divalent ligation for proper signaling[152,153], we predict that TIGIT will match well in this regard, as TIGIT also normally functions as a homodimer. A chimeric receptor utilizing the binding domain of TIGIT to transmit costimulatory signals thus has twofold potential advantages: 1) exploit ligands that are highly associated with cancers to provide for enhanced tumor targeting, 2) convert a normally inhibitory signal in the tumor microenvironment to a costimulatory signal to enhance survival and function of adoptively transferred T cells.

Second, we also investigated alteration of the HER2-CD4TAC receptor to replace the CD4 components with equivalent portions of CD28 or 4-1BB, a design similar to second generation CARs. As CD28 directs mobilization of lipid rafts and Lck to the central region of the immunological synapse, and is itself recruited to these regions[154–156], integration of CD28 in the TAC receptor may confer similar activation properties to the T cell as the HER2-CD4TAC, while additionally generating costimulatory signals. It should be noted that the CD28-Lck interaction is not of high affinity[157], but sustained clustering of TCR complexes by using the high affinity tumor antigen targeting moiety in the TAC design may be enough to achieve activation. We are also investigating the functionality of 4-1BB in place of CD4, as the 4-1BB signaling has been shown to be highly complementary to CAR-T cell function.

Accordingly, the central goal of this research is to investigate and develop methods to provide costimulatory signals to TAC-engineered T cells. We hypothesize that a modified TAC or dual receptor system will be able to enhance the antitumor capabilities of TAC-T cells *in vitro.*

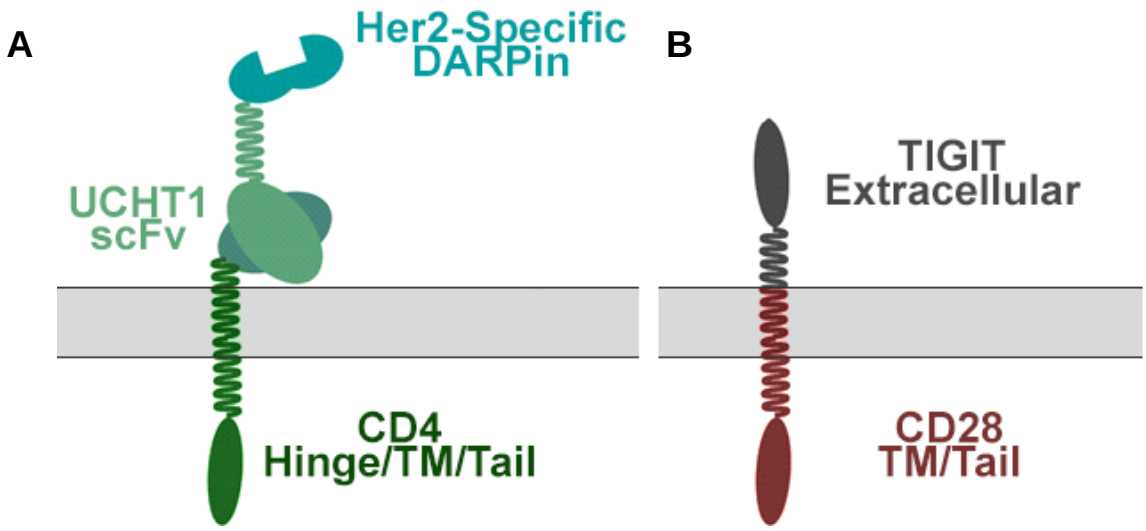

Figure 1. Schematic design of the recombinant receptors designed in the Bramson Lab. ***A*** The HER2-CD4TAC receptor used to transduce activation signals. ***B*** The TIGIT/CD28 chimera under investigation as a chimeric costimulatory receptor.

3.0 Materials and Methods

3.1 Cloning of Chimeric Constructs

The three TIGIT/CD28 construct variants were cloned by stitch PCR with overlapping primers. The human TIGIT and CD28 template cDNAs were available in various plasmids within the lab, thus construction of the recombinant genes was accomplished through a number of standard molecular cloning techniques. The modified sequences were created by PCR amplification using custom oligos, and subsequent ligation and sub-cloning into the pCCL vector.

The TIGIT/CD28*a* construct was created through three PCR reactions. The TIGIT extracellular domain (amino acids 1-141) was amplified using Bramson Lab pCCL plasmid #744 with primers F.pCCL and R.TIG28 (**Table 1**). F.pCCL anneals upstream of a codon-optimized TIGIT isoform one sequence (UniProtKB Q495A1). Reverse primer R.TIG28 contains the 5' portion of the CD28 transmembrane region, generating an annealing region for stitch PCR. The CD28 portion containing the transmembrane and cytoplasmic region of isoform one (UniProtKB P10747, amino acids 153-220) with a 3' *NheI* site was similarly amplified using plasmid #744 with primers F.TIG28 and R.CD28.NheI (**Table 1**). Forward primer F.TIG28 contains the 3' end of TIGIT's extracellular region and the 5' portion of the CD28 transmembrane for annealing, and the reverse primer R.CD28.NheI contains the 3' cut site. These two PCR products were then used as templates to create the final construct using primers F.pCCL and R.CD28.NheI. The TIGIT/CD28*a* was

then sub-cloned into the pCCL vector under the EF-1α promoter using cut sites *AscI/NheI*.

The TIGIT/CD28*b* was constructed similarly, however, using different primer sets. The TIGIT/CD28*b* TIGIT extracellular region (amino acids 1-141) attached with the 3' portion of the CD28 extracellular domain (amino acids 140-152) was amplified using plasmid #744 as template, with forward and reverse primers F.pCCL and R.TIG28.Add (**Table 1**). The reverse primer contains the additional sequence within the oligo. The remainder of the CD28 transmembrane and cytoplasmic region (amino acids 153-220) was amplified in a separate PCR reaction using primers F.TIG28.Add.Sub (**Table 1**) and R.CD28.NheI. The two PCR products were used to create the final construct using primers F.pCCL and R.CD28.NheI. The gene was then sub-cloned into pCCL as above.

The TIGIT/CD28*c* construct was generated in the same manner as the TIGIT/CD28*a* and TIGIT/CD28*b* constructs using the #744 plasmid as template. Primers F.pCCL and R.TIG.CD28.Sub (**Table 1**) were used to amplify a segment of DNA containing the TIGIT extracellular region with deletion of amino acids 128-141 (amino acids 1-127) and the 3' region of the CD28 extracellular domain (amino acids 140-152). A separate PCR reaction with primers F.TIG28.Add.Sub and R.CD28.NheI was used to amplify the CD28 transmembrane and cytoplasmic region (amino acids 153-220). The two PCR products were used as templates in stitch PCR to produce the final TIGIT/CD28*c* gene using primers F.pCCL and R.CD28.NheI. The gene was then sub-cloned into pCCL as before.

Dual expression of HER2-CD4TAC and TIGIT/CD28 constructs within T cells was achieved by cloning each recombinant gene into the pCCL vector with a self-cleaving picornavirus 2A peptide sequence between the two proteins; in this particular case, we employed the *Thosea asigna* virus 2A sequence (T2A). The peptide sequence was inserted with flanking AgeI and KpnI sites (5' ACCGGTGGCAGCGGCGAGGGCAGAGGCTCCCTGCTGACCTGCGGGGACG TGGAAGAGAATCCTGGCCCTGGCACCAGCGGTACC 3). The HER2-CD4TAC was amplified from Bramson Lab plasmid #741 using primers F.AscI.TAC and R.TAC.AgeI (**Table 1**). These primers removed the stop codon at the end of the TAC construct and replaced the NheI site with AgeI to allow placement into the upstream region of the T2A vector using the AgeI site. The TIGIT/CD28 construct was amplified using the respective variant in pCCL with primers F.KpnI.TIGIT (**Table 1**) and R.CD28.NheI, allowing placement into the downstream portion of the T2A vector using the *KpnI/NheI* sites.

Primer Name	Sequence (5' – 3')
F.pCCL	CACACTGAGTGGGTGGAGAC
R.TIG28	CACCAGCACCCAAAATGGGATCTGAAACCT
F.TIG28	AGGTTTCAGATCCCATTTTGGGTGCTGGTG
R.CD28.NheI	TATATGCTAGCTCAGGAGCGATAGGCTGCGAAGTCG
R.TIG.28.Add	GGGCTTAGAAGGTCCGGGAAATAGGGGACTTGGACAAAGTGGGATCTGAAACCTGGCCC
F.TIG28.Add.Sub	CTTTGTCCAAGTCCCCTATTTCCCGGACCTTCTAAGCCCTTTTGGGTGCTGGTGGTGGT
R.TIG.28.Sub	GGGCTTAGAAGGTCCGGGAAATAGGGGACTTGGACAAAGCAGCACCTCCAGGAAAATTC
F.AscI.TAC	CCAGTGAATTCGGCGCGCCATGGATTTCCAGGTCCAGATTTTCT
R.TAC.AgeI	ATATATACCGGTAATGGGTGAACAGGTCTTCTGGAAT
F.KpnI.TIGIT	ATATATGGTACCATGCGCTGGTGTCTGCTGCTGATTT

Table 1. A list of primers and their corresponding sequence used within this research.

3.2 Generating Engineered T cells

3.2.1 Lentivirus Production

Self-inactivating, non-replicative lentivirus used to transduce primary human PBMCs was produced via a third generation system as described by Didier Trono and Luigi Naldini[158,159]. This system produces a non-virulent lentiviral vector considered bio-safe due to a number of modifications to the packaging and genome of the virus. Briefly, this system dispenses with non-essential HIV-1 accessory genes *nef, vpu, vif,* and *vpr* coding for virulence factors, and maintains only the *rev, gag,* and *pol* genes necessary for virion production. The HIV-1 *env* envelope gene is replaced with the Vesicular Stomatitis Virus (VSV) envelope glycoprotein, VSV-G, to broaden tropism and increase hardiness of the virus for ultracentrifugation[160]. This system separates the genome amongst three packaging plasmids – pMD2.G encoding VSV-G, pRSV-Rev encoding HIV-1 Rev, and pMDLg/pRRE encoding HIV-1 Gag and Pol under the Rev Response Element (RRE) – and a transfer plasmid with the LTRs necessary for integration flanking the construct of interest. This split-genome configuration, and complementation of Rev in *trans*, ensures only cells transfected with all plasmids will produce virions. Replacement of the wild type 5' LTR with a chimeric LTR containing a constitutive promoter, such as that of cytomegalovirus (CMV), prevents the need for the Tat protein to transcribe from the 5' LTR. Finally, a deletion within the U3 region of the 3' LTR destroys the promoter when transferred to the 5' LTR upon integration. Thus, only the DNA flanked by the LTRs (i.e. DNA in the transfer plasmid

containing the recombinant protein(s) and any promoters), and not the viral packaging and structural genes, is carried by the virion for integration. Following integration, the chimeric LTR is no longer functional and transcription only occurs through internal promoters contained within the vector genome.

Lentivirus was prepared by plating 3 x 15 cm dishes (NUNC) with $8x10^6$ low passage HEK293TM cells/dish in 20 mL HEK293TM maintenance media (DMEM, 10% heat-inactivated fetal bovine serum, 10 mM HEPES, 2 mM L-glutamine, 100 U/mL penicillin + 100 µg/mL streptomycin) 24 hours prior to transfection. One hour prior to transfection, media was carefully replaced with 12 mL HEK293TM transfection media (DMEM, 10% heat-inactivated fetal bovine serum, 10 mM HEPES, 2 mM L-glutamine, 0.1 mg/mL normocin), after which the packaging plasmids pRSV-Rev (6.25 µg), pMD2.G (9 µg), pMDLg-pRRE (12.5 µg) and the transfer plasmid pCCL containing the construct (32 µg) in 4 mL Opti-MEM (Gibco) were incubated with 120 µL Lipofectamine 2000 (Life Technologies) in 4 mL Opti-MEM. Cells were then transfected with the 8 mL transfection solution per dish. Twelve to sixteen hours after transfection, media was replaced with 12 mL HEK293TM maintenance media supplemented with sodium butyrate (1 mM final).

Media containing lentivirus particles was collected after 48 hours, centrifuged at 2000 g to pellet cellular debris, and filtered through a 0.45 µm PES filter. Lentivirus was then concentrated at 28,000 RPM in an Optima L-90K (Beckman Coulter) ultracentrifuge using the SW 32 Ti rotor (Beckman Coulter), resuspended in ice cold 1x PBS and maintained at -80°C. Viral titer was

determined by serial dilution and transduction of 30,000 HEK293TM cells. HEK293TM cells were plated in 0.5 mL HEK293TM maintenance media per well of a 24-well plate (Falcon) and either mock transduced with 0.5 mL media or 0.5 mL lentivirus dilution ($2x10^{-3}$ to $2x10^{-6}$) 3 hours after plating. After 4 days of incubation, transduced HEK293TM cells were harvested by pipetting, and then washed with FACS (fluorescence-activated cell sorting) buffer containing 2 mM EDTA. Viral titer in transducing units per mL was quantified by determining the % truncated nerve growth factor receptor $(\Delta NGFR)^+$ via flow cytometry using an anti-NGFR-PE antibody (BD Biosciences). Cells were stained at room temperature in 50 µL FACS buffer with 2 mM EDTA for 30 minutes, then run on a BD LSR II or BD FACSCanto flow cytometer. Data is gated on the PE histogram using the unstained non-transduced as the negative, and the $\%\Delta NGFR^+$ is determined by subtracting the value of the stained non-transduced. Titer in TU/mL is calculated using the formula: titer (TU/mL) = (30,000 * dilution factor * $\%\Delta NGFR^+$)/100. The dilution factor closest to 10% ΔNGFR positivity is used.

3.2.2 Engineering and Culture of Human Primary T cells

Human PBMCs were isolated from healthy donors by Ficoll-Paque separation through Leucosep tubes. Briefly, 50 mL Leucosep tubes (VWR) with 15 mL Ficoll-Paque PLUS (GE Healthcare Life Sciences) were centrifuged at 1500 RCF to pass Ficoll-Paque through the porous filter. Plasma was removed from fresh donated blood collected in heparin sulphate tubes by centrifugation at 500 RCF for 5 minutes and subsequent removal of the yellow upper layer. Up to 15 mL

of blood was then transferred to a Leucosep tube and matched with an equal volume of PBS. PBMCs were separated from other cellular components by centrifugation at 1500 RCF for 10 minutes (no break). A white buffy coat present between the top and middle layer contained the PBMCs. As much of the top layer, containing any remaining plasma and platelets, was gently removed taking care not to disturb the buffy coat. The remaining solution containing the PBMCs was decanted into a 50 mL tube, topped off with PBS, and centrifuged at 500 RCF for 10 minutes to pellet cells. Cells were then resuspended in ~20 mL PBS and counted by Trypan Blue exclusion on a hemocytometer. PBMCs were pelleted a final time at 500 RCF for 5 minutes, resuspended in cold heat-inactivated human AB serum (Corning, cat# 35-060-CI) and then slowly given an equal volume of freezing media (80% human AB serum with 20% DMSO). PBMCs were then aliquoted to previously chilled cryovials, transferred to -80°C overnight, and finally stored in vapor phase liquid nitrogen until needed.

To produce engineered T cells, PBMCs were first thawed in a 37°C water bath and the thawed cell suspension was added dropwise to 7 mL base T cell media (RPMI 1640 (Gibco), 10% heat-inactivated fetal bovine serum, 2 mM L-glutamine, 10 mM HEPES, 0.5 mM sodium pyruvate, 1x non-essential amino acids (Life Technologies; cat# 11140-050), 55 μM β-mercaptoethanol, 100 U/mL penicillin + 100 μg/mL streptomycin) and pelleted at 500 RCF for 5 minutes. Cells were then carefully resuspended in 1 mL base T cell media and counted by hemocytometer. The cells were suspended at a concentration of $1x10^6$ cells/mL

with base T cell media, recombinant human IL-2 (Peprotech cat# 200-02) and IL-7 (Peprotech cat# 200-07) were added to a final concentration of 100 U/mL and 10 ng/mL, respectively. Cultures were initiated by aliquoting 100ul of the cell suspension per well of a tissue-culture treated, round-bottom 96-well plate (Falcon). Human T-Activated αCD3/αCD28 Dynabeads (Life Technologies cat# 11131D) were used at 0.8:1 bead to cell ratio to activate T cells within the PBMC mixture and induce proliferation. Following the manufacturer guidelines, beads were washed utilizing the MPC-S magnet (Life technologies cat# A13346), and resuspended in T cell media with IL-2 and IL-7. An aliquot of 100 µL of the Dynabead activator was mixed with the cells in each well. Cells were incubated overnight at 37°C with 5% CO_2 and ambient oxygen tension. After 18-24 hours of incubation, lentivirus was added to the culture by carefully removing 110 µL of medium from each well and adding the lentivirus at the appropriate multiplicity of infection (MOI) in a volume of 10 µL PBS gently to the center of the well without disturbing the cell pellet. Following 24 hours of incubation, 100 µL of T cell media supplemented with IL-2 and IL-7 was added per well. Cells were assessed daily for growth. Once the white T cell halo surrounding the red core of beads reached ~2-2.5 mm in diameter, the contents of each well was transferred to a well of a 24-well plate. This was accomplished by carefully transferring the cell pellet, undisturbed, into 900 µL of cytokine-supplemented T cell medium. T cells were monitored daily until the wells were ~90-95% confluent. At this point, T cells were transferred to a T-25 flask standing upright and 1 mL fresh T cell media with

cytokines was added. Cells were counted every 2-3 days, and fed and scaled to larger flasks accordingly to maintain a density of ~$1.0x10^6$ cells/mL. Experiments were typically performed after 14 days of T cell culture.

3.3 Phenotypic Analysis of Cells

3.3.1 Flow Cytometric Analysis of Surface Marker Expression

All lentiviral vectors utilized within this research encode a truncated low-affinity nerve growth factor receptor (ΔNGFR) under the control of the human CMV promoter to be used as a marker of transduction. For the purposes of phenotyping by flow cytometry, cells were counted by hemocytometer and $0.5x10^6$ cells were used for staining procedures. Cells were washed with 2 mL FACS buffer (PBS + 0.5% bovine serum albumin (BSA)) and stained with a cocktail of antibodies in 50 µL FACS buffer for 30 minutes at room temperature. When Brilliant Violet (BV) fluorophore-conjugated antibodies were used within the staining cocktail, FACS buffer was replaced with 50 µL Brilliant Violet stain buffer (BD Biosciences). When staining for HER2-specific CAR/TAC expression, cells were first incubated with 250 ng recombinant human HER2 Fc Chimera protein (R&D Systems, cat #1129-ER) per stain for 30 minutes at room temperature. When staining tumor lines, the FACS buffer was supplemented with 2.5 mM EDTA. Anti-human antibodies used for this research were: anti-CD4-AlexaFluor700 (eBioscience, cat #56-0048-82), anti-CD4-Pacific Blue (BD Pharmingen, cat #558116), anti-CD8-PerCP-Cy5.5 (eBioscience 45-0088-42), anti-CD8-AlexaFluor700 (eBioscience 56-0086-82), anti-CD112-PE (BD Pharmingen, cat #551057), anti-CD155-PE (eBioscience, cat #12-1550), anti-NGFR-BV421 (BD Pharmingen, cat #562582), anti-NGFR-PE (BD Pharmingen, cat #557196), anti-human IgG (Fcγ)-PE (Jackson ImmunoResearch, cat #109-115-098), anti-pAkt (S473)-AlexaFluor 488 (BD Phosflow, cat #560404),

and anti-TIGIT-APC (eBioscience, cat #17-9500-41). Cells that were exposed to lentivirus were fixed using PFA (2% final) for 15 minutes at room temperature after antibody stain.

Cells stained for flow cytometry were filtered using a 35 µm nylon mesh snap cap polystyrene tube (Corning) just prior to running on a BD FACSCanto or LSR II flow cytometer. Flow data was analyzed using FlowJo software (FlowJo, LLC).

3.3.2 Immunofluorescence

A 4% w/v paraformaldehyde (PFA) solution was first made by dissolving 2 g PFA (Sigma, cat #P6148) in 38.5 mL dH_2O with 2 µL 10 M sodium hydroxide over low heat. Ten milliliters 10x PBS and 1.5 mL 1 M sucrose were added; pH was adjusted to ~7-7.5. Solution was filter sterilized through a 0.2 µm filter and stored at 4°C for up to 1 week.

To prepare T cells for immunofluorescence, $1.5x10^6$ cells were pelleted at 500 RCF for 5 minutes, the supernatant was decanted, and the cells were fixed using 100 µL 4% PFA for 20 minutes on ice. Cells were then washed with 2 mL FACS buffer, and initially stained with mouse anti-human c-Myc (BD Pharmingen, cat #51-1485GR, 1:20 dilution) in 50 µL 1x Perm/Wash per stain, for 30 minutes on ice. Cells were then fixed/permeabilized with 100 µL Cytofix/Cytoperm (BD Biosciences), washed with 2 mL 1x Perm/Wash buffer (BD Biosciences), and then stained with mouse anti-human c-Myc and rabbit anti-calnexin (Abcam, cat #

ab22595, 1:150 dilution) antibodies in 50 µL 1x Perm/Wash per stain, for 30 minutes on ice. Cells were washed once with 2 mL 1x Perm/Wash and stained with goat anti-mouse IgG (H+L)-AlexaFluor 488 (Life Technologies, cat #A11029, dilution 1:100) and goat anti-rabbit IgG (H+L)-AlexaFluor 594 (Life Technologies, cat #A11012, dilution 1:100) secondary antibodies in 50 µL 1x Perm/Wash buffer for 30 minutes on ice. Cells were again washed with 2 mL 1x Perm/Wash and finally stained with Hoechst 33342 (Life Technologies, cat #H3570, 1:1000) for 20 minutes on ice. A final wash with 2 mL 1x Perm/Wash first, then with 2 mL FACS buffer, before cells were resuspended in 1 mL FACS and transferred to a 1.5 mL microcentrifuge tube. Stained cells were pelleted at 500 RCF for 5 minutes at 4°C, then the supernatant was carefully drawn off without disturbing the pellet and cells were resuspended in 1 drop VectaShield (Vector Labs, cat #H-1000). Five microliters were mounted on a glass slide and cells were imaged using a Life Technologies EVOS FL Auto Cell Imaging System using the Texas-Red, DAPI, and YFP Light Cubes, and data was analyzed using Volocity Software (Perkin Elmer).

3.4 Assessment of Engineered T cell CD28 Signaling

3.4.1 Phospho-Flow Cytometry

Two million T cells were stimulated utilizing either PMA (Sigma, cat #P8139), with or without Ionomycin, or plate-bound anti-CD3 (eBioscience, cat #16-0037-85), with or without anti-CD28 (eBioscience, cat #16-0289-85). Soluble reagents were mixed with T cells in a round-bottom 96-well plate to a total volume of 200 µL in base T cell media to begin stimulation. Plate-bound reagents were diluted in PBS to desired concentration in 200 µL final, incubated at 4°C overnight on the U-bottom 96-well plate, before 2x wash with 200 µL PBS and subsequent addition of T cells.

Following stimulation, cells were fixed and permeabilized to facilitate entry of phosphorylation-specific antibodies as described in the optimized protocol[161]. Briefly, 16% PFA was directly added to cells to a final concentration of 1.5% at the end of stimulation for 10 minutes at room temperature. Cells were then pelleted at 500 RCF, resuspended vigorously in 500 µL methanol/10^6 cells and incubated on ice for 20 minutes. Cells were finally washed twice with 3 mL FACS buffer and stained as per the staining protocol in 3.3.1.

3.4.2 Western Blot

As above, round-bottom 96-well plates were coated with plate-bound stimuli (200 µL final volume) overnight at 4°C. Reagents for stimulation used within this study were: anti-CD3 mAb (eBioscience, cat #16-0037-85), anti-CD28 mAb

(eBioscience, cat #16-0289-85), and recombinant human CD155 (R&D Systems, cat #2530-CD). Half a million T cells were utilized per well of stimulation. After stimulation, T cells were pelleted and immediately resuspended in 40 µL sample buffer (2% SDS, 50 mM Tris pH 6.8, 0.02% Bromophenol blue, 1% β-mercaptoethanol, 10% glycerol, in water) containing 1x phosphatase inhibitor cocktail (Cell Signaling Technologies, cat #5870), transferred to a 1.5 mL microcentrifuge tube and boiled for at least 20 minutes. Samples were then stored at -20°C or used right away.

Resolving gel was prepared (10% acrylamide/bis 29:1 solution (Bio-Rad, cat #161-0156), 0.375 M Tris pH 8.8, 0.1% SDS, 0.1% ammonium persulfate (APS), 0.1% TEMED, in water with APS and TEMED added last) within a 1.5 mm gel cast. Resolving gel was polymerized over 15 minutes. A 5% stacking gel (5% acrylamide/bis 29:1 solution (Bio-Rad, cat #161-0156), 63 mM Tris pH 6.8, 0.1% SDS, 0.1% APS, 0.1% TEMED, in water with APS and TEMED added last) was then polymerized on top over 30 minutes. Twenty microliters, or $0.25x10^6$ cells, of pre-boiled sample was loaded per well and electrophoresis performed in transfer buffer (0.3% w/v Tris-HCl pH 8.3, 1.44% w/v Glycine, 0.1% SDS, in water) at 200 V for 1 hour.

Proteins were transferred to nitrocellulose membrane (Pall, cat #66485) using the electrophoretic wet method of transfer, the theory of which is described by Kurien and Scofield[162]. Briefly, a sandwich was made in which the protein gel, facing the cathode, was in contact with the nitrocellulose membrane, surrounded

by three layers of blotting paper and a support pad on each side. The transfer assembly was placed into a tank with Towbin transfer buffer (0.3% w/v Tris-HCl pH 8.3, 1.44% w/v glycine, 20% v/v methanol, in water) and an ice pack, and transfer was performed at 400 mA for 70 minutes.

Following completion of the transfer, the nitrocellulose membrane was blocked for 1 hour at room temperature using a 1:1 ratio of 1X TBS (Tris Buffered Saline) and Odyssey Blocking Buffer (LI-COR Biosciences, cat #LIC-927-4000). Following block of the membrane, the blot was incubated at 4°C overnight with primary antibodies diluted in 1:1 mixture of 1X TBS-T (0.2% Tween-20) and Odyssey Blocking Buffer. Primary antibodies used within this research were: mouse anti-β-actin (Sigma, cat #A5441), chicken anti-β-actin (Abcam, cat #ab13822), rabbit anti-pAkt (S473) (Cell Signaling Technologies, cat #4060), rabbit anti-pAkt (T308) (Cell Signaling Technologies, cat #2965), rabbit anti-HIV-1 p24 (Abcam, cat#ab63913), and mouse anti-c-Myc (BD Pharmingen, cat #51-1485GR). Following incubation with primary antibodies, the blot was washed three times for 5 minutes with 1x TBS-T (0.1% Tween20). Secondary antibodies diluted in 1:1 mixture of 1X TBS-T (0.2% Tween-20) and Odyssey Blocking Buffer were incubated for 2 hours at room temperature. Secondary antibodies used in this study were: IRDye 800CW goat anti-mouse IgG (H+L) (LI-COR Biosciences, cat #926-32210), IRDye 680RD donkey anti-chicken IgG (H+L) (LI-COR Biosciences, cat #926-68075), IRDye 800CW goat anti-rabbit IgG (H+L) (LI-COR Biosciences, cat

#926-32211), IRDye 680LT goat anti-mouse (LI-COR Biosciences, cat #926-68020). The blot was finally washed three times as above.

Probed blots were imaged using a LI-COR Biosciences Odyssey 9120 Infrared Imaging System and analyzed using Image Studio Lite software (LI-COR Biosciences).

3.4.3 Multiple Myeloma Survival Assay

The multiple myeloma cell line MM.1S was cultured in CellGro RPMI 1640 (Corning, cat #10-040-CV) containing 10% FBS, 2 mM L-glutamine, 10 mM HEPES, 1x non-essential amino acids (Life Technologies; cat# 11140-050), 1 mM sodium pyruvate, 100 U/mL penicillin, 100 µg/mL streptomycin – termed MM.1S media. In the absence of serum, these cells begin to die unless provided with CD28 signaling. When supplemented with anti-CD28 functional antibody in the absence of serum, they remain viable. Beckman Coulter anti-CD28 mAb was reconstituted at 0.5 mg/mL using 400 µL sterile water. Once reconstituted, this antibody was kept at 4°C for 1 month maximum. After this period the antibody no longer rescues the cells.

To collect the MM.1S cells from cell culture flasks, the medium was removed and replaced with 1X citric saline (0.135 M potassium chloride, 0.015 M sodium citrate). The flask was incubated at 37°C until cells were no longer adherent. The MM.1S cells were collected into a conical tube, pelleted and washed three times with 10 mL of the respective media for the necessary conditions – MM.1S media

with or without serum. After the wash steps, cells were resuspended at $0.5x10^6$ cells/mL in their respective media for their culture conditions. MM.1S cells were then seeded at $0.1x10^6$ cells/well in 200 µL, in triplicates. For the anti-CD28 mAb-treated wells, reconstituted Beckman Coulter anti-CD28 was added to a final concentration of 20 µg/mL.

Cells were incubated at 37°C for 48 hours, after which cells were harvested from the wells by vigorous pipetting. Cells were then stained using Molecular Probes LIVE/DEAD Fixable Near-IR Dead Cell stain (Life Technologies, cat #L10119), as per manufacturer's instructions, and %dead cells was measured as a function of emission within the APC-Cy7 channel on a BD FACSCanto or LSR II cytometer. MM.1S cells cultured in serum were used as a positive control for the LIVE/DEAD stain through acid killing. Cells were incubated with an equivalent volume of 1 M HCl (0.5 M final) for 5 minutes at room temperature, then stained with LIVE/DEAD stain.

3.5 Functional Analysis of Engineered T cells

3.5.1 Intracellular Cytokine Staining

T cells were stimulated for 4 hours at 37°C using either plate-bound antigen (described in Section 3.4.1) or tumor cells. Antigens used for plate-bound stimulation were: recombinant human HER2 Fc chimera (R&D Systems, cat #1129-ER) at 200 ng/well, recombinant murine Rae-1β Fc chimera (R&D Systems, cat #1198-RA) at 200 ng/well. T cells ($0.75x10^6$ T cells per well) were added to each well in 100 µL complete RPMI (cRPMI; RPMI 1640, 10% FBS, 2 mM L-glutamine, 55 nM β-mercaptoethanol, 10 mM HEPES, 100 U/mL penicillin + 100 µg/mL streptomycin) and brought up to 200 µL with cRPMI containing 0.2 µL GolgiPlug (BD Biosciences, cat #555029) and 15 µL anti-CD107a antibody (BD Pharmingen, cat # 555800). When tumor cells were used $0.6x10^6$ T cells were mixed with $0.15x10^6$ tumor cells were added to a total of 100 µL, then brought up to 200 µL with cRPMI containing 0.2 µL GolgiPlug and 15 µL anti-CD107a antibody.

At the end of the stimulation period, 50 µL of 0.02 M EDTA was added to each well and incubated for 15 minutes at room temperature. Cells were spun down at 500 RCF, resuspended in 200 µL cRPMI, and kept at 4°C in tinfoil overnight. Unless otherwise noted, plates were centrifuged at 500 RCF for 5 minutes to pellet cells. Supernatant was removed using a vacuum manifold (V&P Scientific, cat # VP 180), and cells were washed twice with 200 µL FACS buffer.

Wells were then given 50 µL/well of surface stain cocktail and incubated on ice for 30 minutes. Antibodies used for surface stain were: CD3-QDot605 (Life Technologies, cat #Q10054), CD4-AlexaFluor700 (eBioscience, cat #56-0048-82), CD4-Pacific Blue (BD Pharmingen, cat #558116), CD8-PerCP-Cy5.5 (eBioscience 45-0088-42), and/or CD8-AlexaFluor700 (eBioscience 56-0086-82). Cells were then washed twice more with FACS buffer, then fixed and permeabilized using 100 µL/well Cytofix/Cytoperm reagent (BD Biosciences, cat #554722) on ice for 20 minute. Cells were then washed using 1x Perm/Wash solution (BD Biosciences, cat #554723). Cells were then stained using antibodies for intracellular cytokines in 50 µL of 1X Perm/Wash buffer. Antibodies used for the intracellular stain were: IFNγ-APC (BD Pharmingen, cat #554702), IL-2-PE (BD Pharmingen, cat #554566), and TNFα-PE-Cy7 (BD Pharmingen, cat #557647). Cells were then washed twice with 1X Perm/Wash buffer, resuspended in 200 µL FACS buffer, and filtered into 35 µm nylon mesh snap cap tubes prior to running on a BD LSR II flow cytometer. Data was analyzed by FlowJo software (FlowJo LLC) and SPICE 5 (National Institute of Allergy and Infectious Disease).

3.5.2 AlamarBlue Killing Assay

Tumor cells were plated in triplicates in a flat-bottom 96-well plate ($1.25x10^4$ cells in 100 µL cRPMI per well) 16-18 hours prior to co-culture with T cells. Additional wells were included that had no tumor cells or media alone to serve as background controls.

We evaluated effector:target ratios ranging from 0.25:1 to 8:1. T cells were counted, resuspended in base T cell media to a concentration of $1x10^6$ cells/mL, and serial dilutions were prepared to achieve the needed effector:target ratio. T cells were then added at a volume of 100 µL per well and incubated at 37°C for 6 hours. Tumor cell only and media only wells were given 100 µL of base T cell media in place of T cells.

AlamarBlue Viability reagent (Life Technologies, cat #DAL1100) was prepared by diluting in cRPMI to make a 10% solution, kept warm at 37°C. Media was aspirated from wells using the vacuum manifold, then wells were rinsed three times with 200 µL warm PBS. The 10% AlamarBlue solution was then added at 100 µL/well and the plate was incubated at 37°C for 3 hours.

The plate was then read using a Tecan Safire plate reader under the fluorescence top mode using the following settings: $\lambda_{excitation}$ 530 nm, $\lambda_{emission}$ 595 nm, 10 flashes, 3x1 Xline reads per well, and a gain of 100. %Viability is derived through the following formula: ((Emission – Background)/(Tumor cell alone – Background)) * 100%.

4.0 Results

4.1 TIGIT/CD28 Chimeric Costimulatory Receptor

4.1.1 Design and Cloning of the TIGIT/CD28 Variants

In our endeavor to provide TAC-engineered T cells with a means of receiving costimulation, we first investigated the creation of a novel CCR to be expressed in conjunction with the TAC receptor. Given the structural similarities between TIGIT and CD28, we hypothesized a fusion protein comprised of these two receptors will successfully transmit CD28 costimulatory signals through ligation of CD155 and/or CD112 by the TIGIT binding domain. In design of the novel TIGIT/CD28 chimeric protein, our initial challenge lay in the choice of fusion site, as inclusion or exclusion of specific regions could potentially affect both the stability and the ability of such a molecule to transduce CD28 signals upon ligation. Since we could not predict *a priori* which structure would be preferred, we generated multiple cDNAs encoding TIGIT/CD28 variants to maximize the likelihood of producing a functional receptor. We chose to pursue three variants, which differ in the regions of TIGIT and CD28 that were included in the final protein sequence.

In the case of TIGIT/CD28*a,* the entire TIGIT extracellular domain (residues 1-141) was fused to the CD28 transmembrane region and cytoplasmic tail (residues 153-220), as adapted from the sequence homology analysis of Levin *et al.*[135]. Based on published data regarding the TIGIT homodimer structure[137] and

CD28 signaling in CARs[163], we believed that this structure would successfully bind TIGIT ligands and retain the ability to bind CD28 signaling components.

Two other variants were designed where the fusion point was shifted. The human CD28 molecule contains a conserved cysteine residue (C141) proximal to the membrane that is important in stabilization of a homodimer structure through an interchain disulfide linkage. Although the exact signaling mechanism of CD28 is not fully understood, it is postulated that dimerization facilitates occupancy of the receptor's on/off kinetics and is important in enhancing function[164,165]. We speculated that inclusion of this short region (CD28 residues 140-152) within the TIGIT/CD28 chimera would aid in dimerization of the chimeric receptor and bring the cytoplasmic tails closer for signaling. A previous study investigating the use of the CD28 hinge versus that of the IgG1 hinge in a CD28TM/tail-CD3ζ CAR found the CD28 hinge resulted in greater surface expression[166]. Crystal structures of both TIGIT (PDBe entries 3Q0H, 3RQ3, 3UDW, and 3UCR) and CD28 (PDBe entry 1YJD) lack this region proximal to the membrane, and bioinformatic analysis using DisEMBL presents this region as potentially disorganized, suggesting that it may be an unstructured linker. However, because of the limited structure data on the membrane-proximal region of both TIGIT and CD28, as well as how CD28 binding results in signaling, we opted to investigate two constructs: TIGIT/CD28*b,* which fused the entire TIGIT extracellular domain (residues 1-141) to the CD28 interchain disulfide region, TM, and cytoplasmic tail (residues 140-220); and TIGIT/CD28*c,* which joined the TIGIT extracellular domain truncated at the membrane proximal

region (residues 1-128) to the same CD28 interchain disulfide region, TM, and cytoplasmic tail component (residues 140-220). **Figure 2** provides a schematic rearrangement of TIGIT and CD28 into the TIGIT/CD28 chimeras. **Table 2** outlines the respective amino acid sequences of the TIGIT/CD28 chimeras.

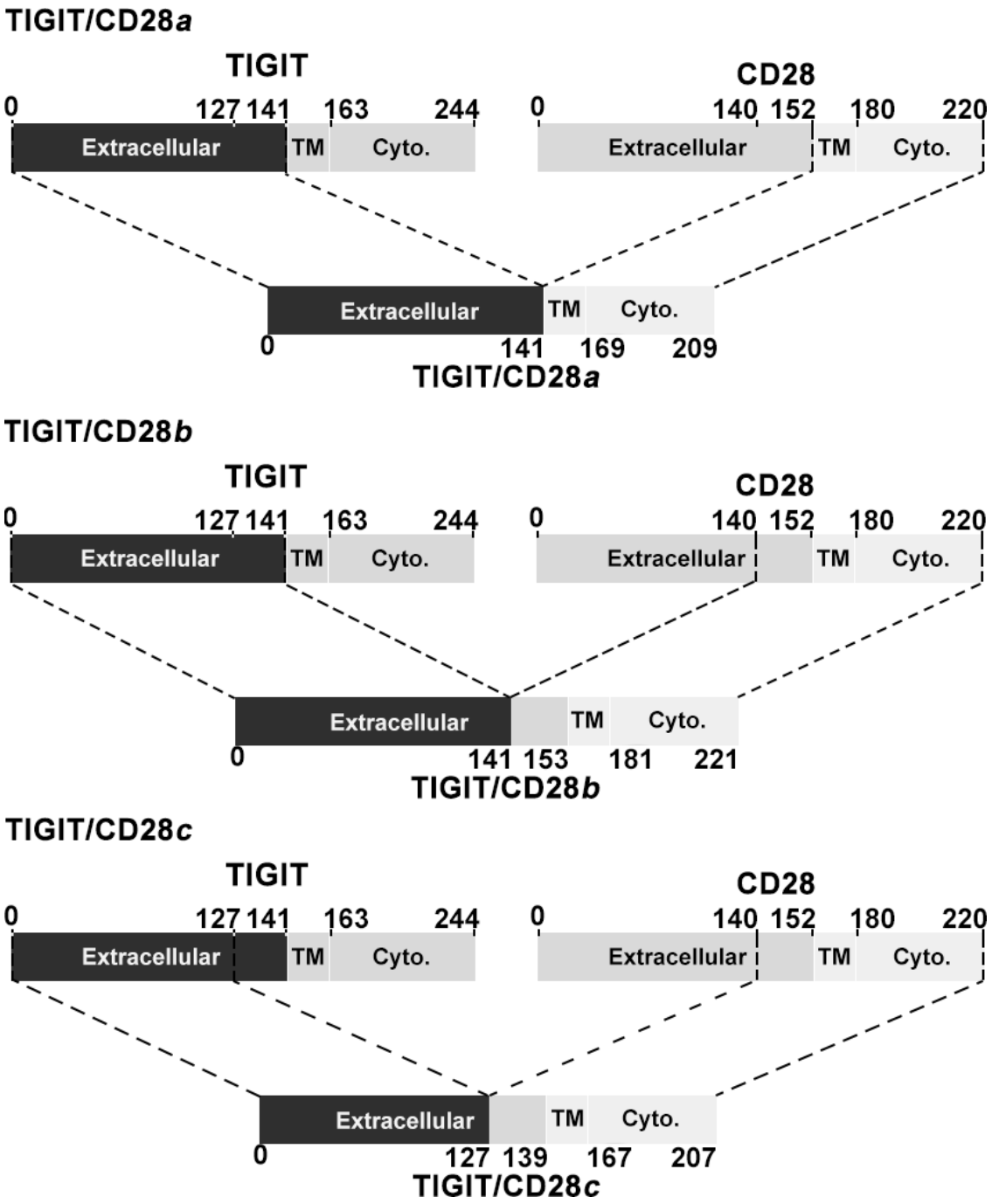

Figure 2. Schematic diagram of construction of the TIGIT/CD28 chimeras. Molecular schematic outlining the generation of the TIGIT/CD28 chimeras from the TIGIT and CD28 parents proteins indicating extracellular domain, hinge, transmembrane (TM), cytoplasmic tail regions, and the relevant amino acid residue number.

Construct	Amino Acid Sequence
TIGIT/CD28*a*	*MRWCLLLIWAQGLRQAPLASGMMTGTIETTGNISAEKGGSIILQ CHLSSTTAQVTQVNWEQQDQLLAICNADLGWHISPSFKDRVAP GPGLGLTLQSLTVNDTGEYFCIYHTYPDGTYTGRIFLEVLESSV AEHGARFQIP*FWVLVVVGGVLACYSLLVTVAFIIFWV<u>RSKRSRL LHSDYMNMTPRRPGPTRKHYQPYAPPRDFAAYRS</u>
TIGIT/CD28*b*	*MRWCLLLIWAQGLRQAPLASGMMTGTIETTGNISAEKGGSIILQ CHLSSTTAQVTQVNWEQQDQLLAICNADLGWHISPSFKDRVAP GPGLGLTLQSLTVNDTGEYFCIYHTYPDGTYTGRIFLEVLESSV AEHGARFQIPLCPSPLFPGPSKP*FWVLVVVGGVLACYSLLVTVA FIIFWV<u>RSKRSRLLHSDYMNMTPRRPGPTRKHYQPYAPPRDFA AYRS</u>
TIGIT/CD28*c*	M*RWCLLLIWAQGLRQAPLASGMMTGTIETTGNISAEKGGSIILQ CHLSSTTAQVTQVNWEQQDQLLAICNADLGWHISPSFKDRVAP GPGLGLTLQSLTVNDTGEYFCIYHTYPDGTYTGRIFLEVLCPSP LFPGPSKP*FWVLVVVGGVLACYSLLVTVAFIIFWV<u>RSKRSRLLH SDYMNMTPRRPGPTRKHYQPYAPPRDFAAYRS</u>

Table 2. **Amino acid sequence of TIGIT/CD28 chimeric receptors.** Sequence provided with: extracellular portion italicized, hinge in teal, transmembrane region in red, intracellular region underlined, and conserved CD28 cysteine highlighted in yellow.

4.1.2 Generating Engineered Cells by Lentiviral Transduction

The three TIGIT/CD28 variants were each cloned into the pCCL transfer plasmid containing a truncated nerve growth factor receptor (ΔNGFR) used as a transduction marker under the EF-1α and CMV promoters, respectively. Schematics of these plasmids used to generate non-replicative, self-inactivating lentivirus are shown in **Figure 3**. pCCL ΔNGFR was used to prepare negative control lentivirus to measure the effects, if any, of viral transduction on the T cell population (**Figure 3**).

Primary human PBMCs cultured in the presence of recombinant human IL-2 and IL-7 were transduced with lentiviruses expressing the various TIGIT/CD28 fusion proteins. Surface expression of the TIGIT/CD28 chimeric receptors on the T cells was measured after 14 days of culture by flow cytometry. Cells were gated on $CD4^+$ and $CD8^+$ (**Figure 4A).** Overall, T cells co-expressed both ΔNGFR and TIGIT for the TIGIT/CD28*a* and *b* variants, with $CD4^+$ T cells having greater expression than $CD8^+$ T cells. Conversely, despite high ΔNGFR surface levels, indicating a high level of transduction, there was little TIGIT expression on T cells transduced with the TIGIT/CD28*c* variant (**Figure 4B**). A similar phenotype was seen when HEK293TM cells were transduced with the TIGIT/CD28*c* chimera (**Figure 4C**) suggesting that the lack of surface expression was due to a trafficking defect of the chimeric protein.

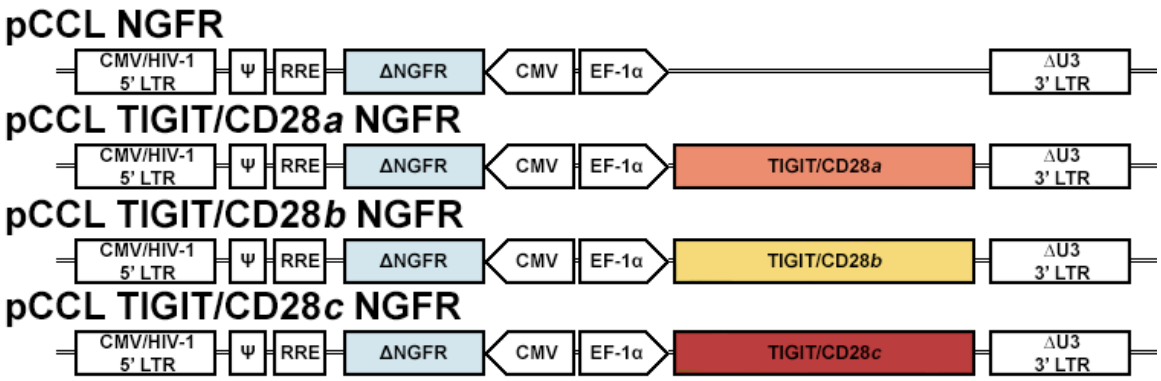

Figure 3. Transfer plasmids used to generate lentivirus for engineering of T cells with the TIGIT/CD28 chimeras. Schematic diagram of pCCL transfer plasmids used for generation of lentiviruses. Chimeric CMV/HIV-1 5' LTR containing CMV promoter; Ψ Packaging element; RRE rev response element; CMV minimal hCMV promoter; EF-1α human elongation factor 1 alpha promoter; ΔU3 3' LTR self-inactivating 3' LTR.

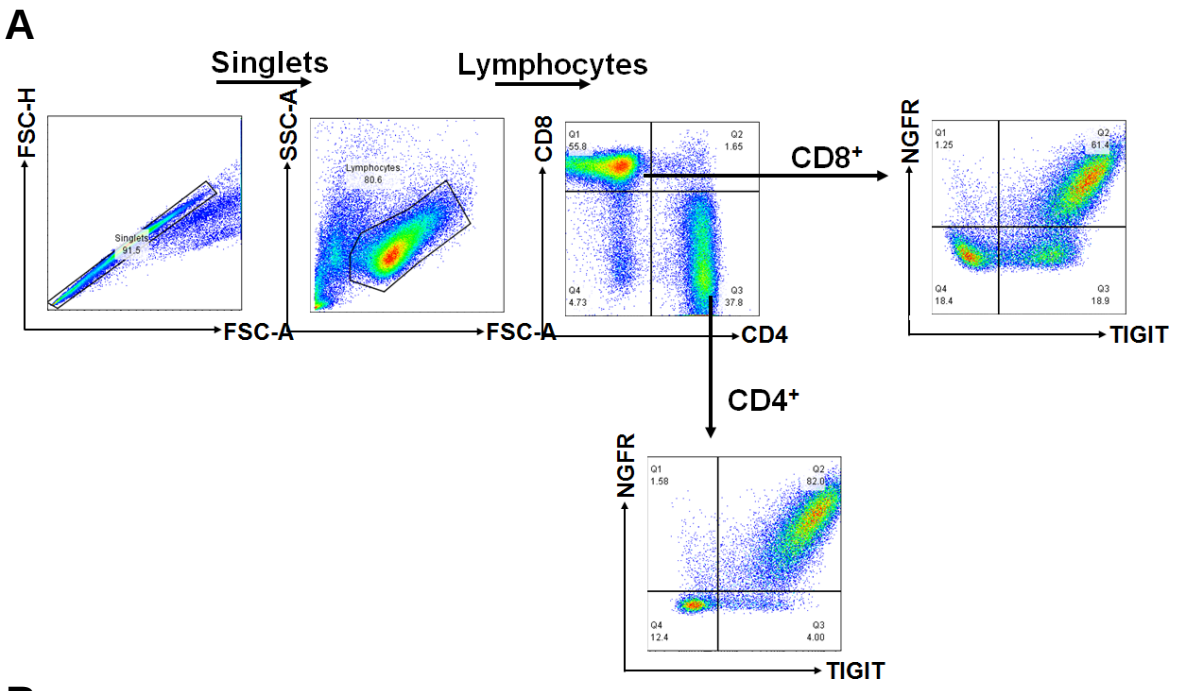
A
Singlets
Lymphocytes
FSC-H
FSC-A
SSC-A
FSC-A
CD8
CD4
CD8⁺
NGFR
TIGIT
CD4⁺
NGFR
TIGIT
B
CD4⁺
CD8⁺
%Positive Cells
100
80
60
40
20
0
%NGFR⁺TIGIT⁺
Total %NGFR⁺
TIGIT/CD28a
TIGIT/CD28b
TIGIT/CD28c
TIGIT/CD28a
TIGIT/CD28b
TIGIT/CD28c

C

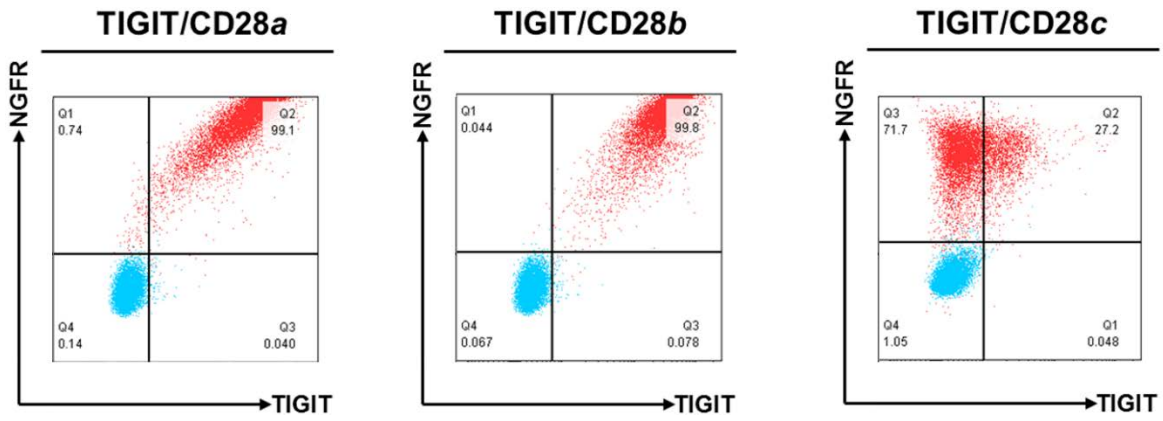

Figure 4. HEK293TM and primary human T cells variably express the TIGIT/CD28 chimeras. ***A*** Representative gating strategy for T cell phenotypic analysis. ***B*** Thawed PBMCs from healthy donors were transduced at an MOI of 10 and cultured for 14 days before staining with anti-TIGIT-APC, anti-NGFR-PE, anti-CD4-PacificBlue, and anti-CD8-AlexaFluor700. Results are pooled from two separate experiments utilizing two different donors. ***C*** HEK293TM cells transduced with TIGIT/CD28 chimeras were stained with anti-TIGIT-APC and anti-NGFR-PE.

4.1.3 Assessment of Signaling via TIGIT/CD28 Chimeras through Akt Phosphorylation

To characterize the functional properties of the TIGIT/CD28 chimeric receptor variants in transducing CD28 signals, we chose to monitor activation of the PI3K/Akt pathway as many of the effects of CD28 costimulation in T cells are mediated through the serine/threonine kinase Akt[50,167–169]. Full activation of Akt relies on phosphorylation of residues serine 473 and threonine 308 by mTORC2 and PDK1, respectively[170,171]. To this end, T cells transduced with the TIGIT/CD28 variants were stimulated and subsequently assayed for activation of Akt.

The phosphorylation status of proteins can be examined on a per cell basis with flow cytometry utilizing phosphorylation-specific antibodies[161,172]. Using this method we first assessed Akt phosphorylation in T cells in response to stimulation. TIGIT/CD28-transduced primary T cells were stimulated with both soluble and plate-bound reagents to determine effective controls. The phorbol ester, PMA, is recommended by BD Biosciences for induction of Akt phosphorylation at S473 in human PBMCs. Despite several attempts using both primary T cells and Jurkat E6-1 cells, this technique remained technically challenging and, with the exception of two outliers, only small, variable increases in phosphorylation were detected (**Figure 5 and Table 3**).

An alternate strategy to measure Akt phosphorylation is western blot analysis. First, we titrated the concentration of anti-CD28 functional antibody, as well as the length of stimulation, to determine the optimal conditions needed for

phosphorylation at both residues S473 and T308, and to determine a positive control. Stimulation with 1 µg/mL anti-CD28 for 2 hours resulted in the greatest Akt activation (**Figure 6 and 7**). This stimulation condition was incorporated into stimulation of TIGIT/CD28 variant-transduced T cells with 1 µg/mL anti-CD3 +/- anti-CD28 or 10 µg/mL rhCD155. Stimulation of TIGIT/CD28-transduced T cells by anti-CD3 and the TIGIT ligand, rhCD155, did not objectively increase Akt phosphorylation at either residues over stimulation with anti-CD3 alone or anti-CD3 with anti-CD28 (**Figure 8**).

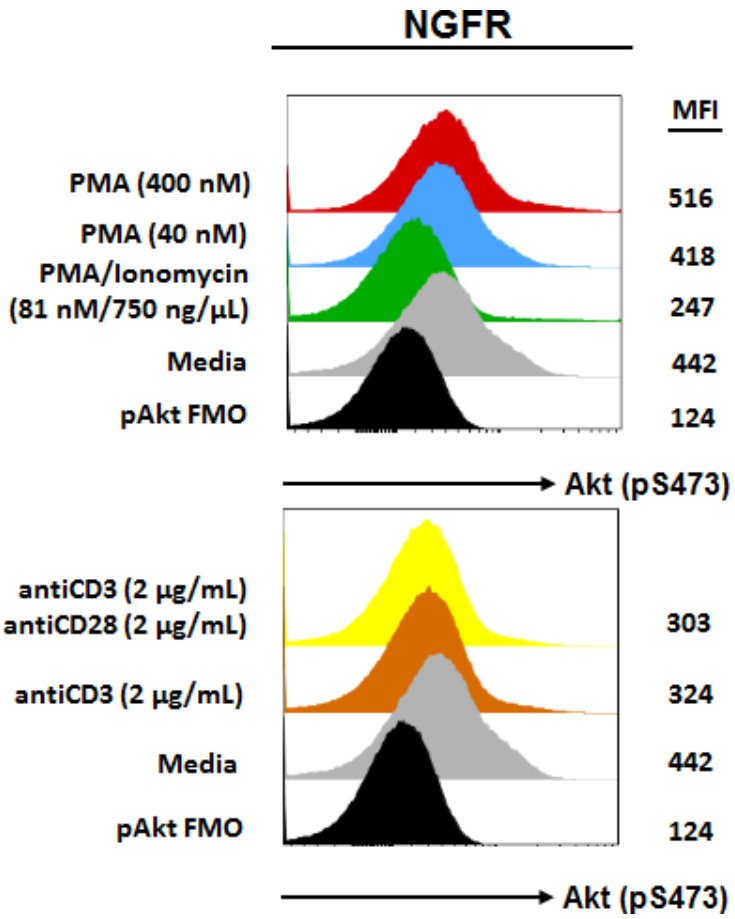

Figure 5. Akt phosphorylation was not measurable by flow cytometry following stimulation with either soluble PMA ± Ionomycin or plate-bound anti-CD3/anti-CD28 antibodies. A representative sample of phospho-specific flow cytometry. ΔNGFR-transduced primary human T cells were cultured for 19 days after which $2x10^6$ cells were stimulated for 30 minutes before fix/perm and staining with anti-Akt (pS473)-Alexa Fluor488.

Cell	Cell Age (Days)	Stimulus	Plate Bound or Soluble	Stim. Length	pAkt Antibody Dilution and Incubation Time	pAkt S473 ΔMFI
TIGIT/ CD28*a* T cells	13	Media	Soluble	30 min	1:25 30 minutes	0
		2 µg/mL anti-CD3				22
		2 µg/mL anti-CD3 2 µg/mL anti-CD28				1867
		2 µg/mL anti-CD3 5 µg/mL rhCD155				84
		40 nM PMA				60
ΔNGFR T cells	13	Media				0
		2 µg/mL anti-CD3				20
		2 µg/mL anti-CD3 2 µg/mL anti-CD28				25
		2 µg/mL anti-CD3 5 µg/mL rhCD155				19
		40 nM PMA				87
TIGIT/ CD28*a* T cells	19	DMSO/Media		2 hrs		0
		40 nM PMA				50
		400 nM PMA				85
		81 nM PMA 752 ng/µL Ionomycin				-153
		2 µg/mL anti-CD3				-79
		2 µg/mL anti-CD3 2 µg/mL anti-CD28				-88
		2 µg/mL anti-CD3 5 µg/mL rhCD155				-65
		2 µg/mL anti-CD3 10 µg/mL rhCD155				-65
		2 µg/mL anti-CD3 20 µg/mL rhCD155				-110
ΔNGFR T cells	19	DMSO/Media				0
		40 nM PMA				-31
		400 nM PMA				61
		81 nM PMA 752 ng/µL Ionomycin				-190
		2 µg/mL anti-CD3				-144
		2 µg/mL anti-CD3 2 µg/mL anti-CD28				-164
		2 µg/mL anti-CD3				-169

		5 µg/mL rhCD155				
		2 µg/mL anti-CD3 10 µg/mL rhCD155				-160
		2 µg/mL anti-CD3 20 µg/mL rhCD155				-250
TIGIT/ CD28*a* Jurkat	N/A	Media	Plate	30 min		0
		2 µg/mL anti-CD3				106
		2 µg/mL anti-CD3 2 µg/mL anti-CD28				110
		2 µg/mL anti-CD3 10 µg/mL rhCD155				94
ΔNGFR Jurkat		Media				0
		2 µg/mL anti-CD3				320
		2 µg/mL anti-CD3 2 µg/mL anti-CD28				52
		2 µg/mL anti-CD3 10 µg/mL rhCD155				118
TIGIT/ CD28*a* Jurkat		Media			1:2.5 1 hour	0
		2 µg/mL anti-CD3				-44
		2 µg/mL anti-CD3 2 µg/mL anti-CD28				748
		2 µg/mL anti-CD3 10 µg/mL rhCD155				72

Table 3. Summary of phospho-Akt (S473) flow cytometry attempts. Indicated cells were stimulated using either plate-bound or soluble stim for the indicated length of time. Upon completion cells were immediately fixed and permeabilized by 1.6% PFA and 100% methanol, respectively. Cells were then analyzed for phospho-Akt by flow cytometry. N/A, not applicable.

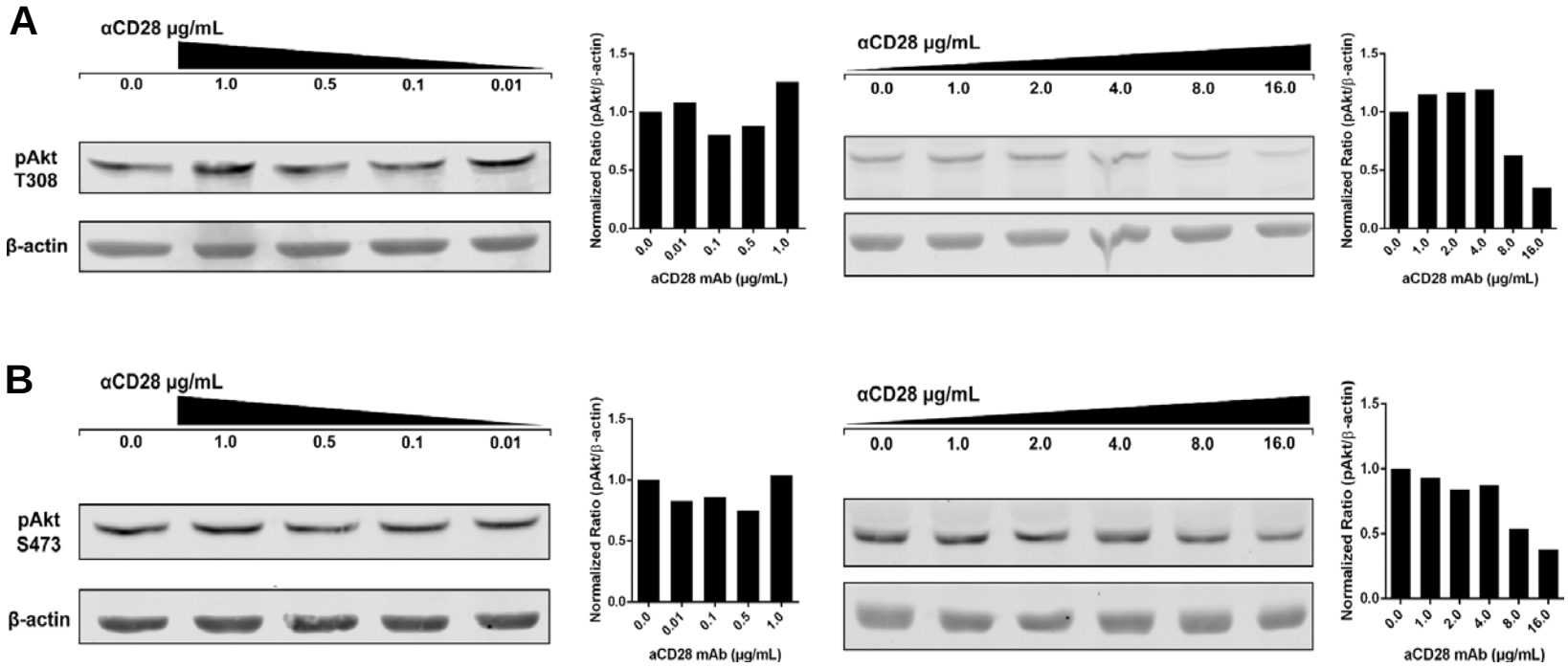

Figure 6. Stimulation with agonistic anti-CD28 produces the greatest Akt phosphorylation at 1 μg/mL. T cells were stimulated for 30 minutes with a range of plate-bound anti-CD28 functional antibody concentrations. Half a million cells were loaded per well on a 10% acrylamide gel. Samples were then transferred to a nitrocellulose membrane and blotted with 1:5000 chicken anti-β-actin and ***A*** 1:1000 rabbit anti-Akt pS473 or ***B*** 1:500 rabbit anti-Akt pT308 primary. Signal intensity was calculated as a ratio of pAkt/β-actin, and was normalized to the vehicle control.

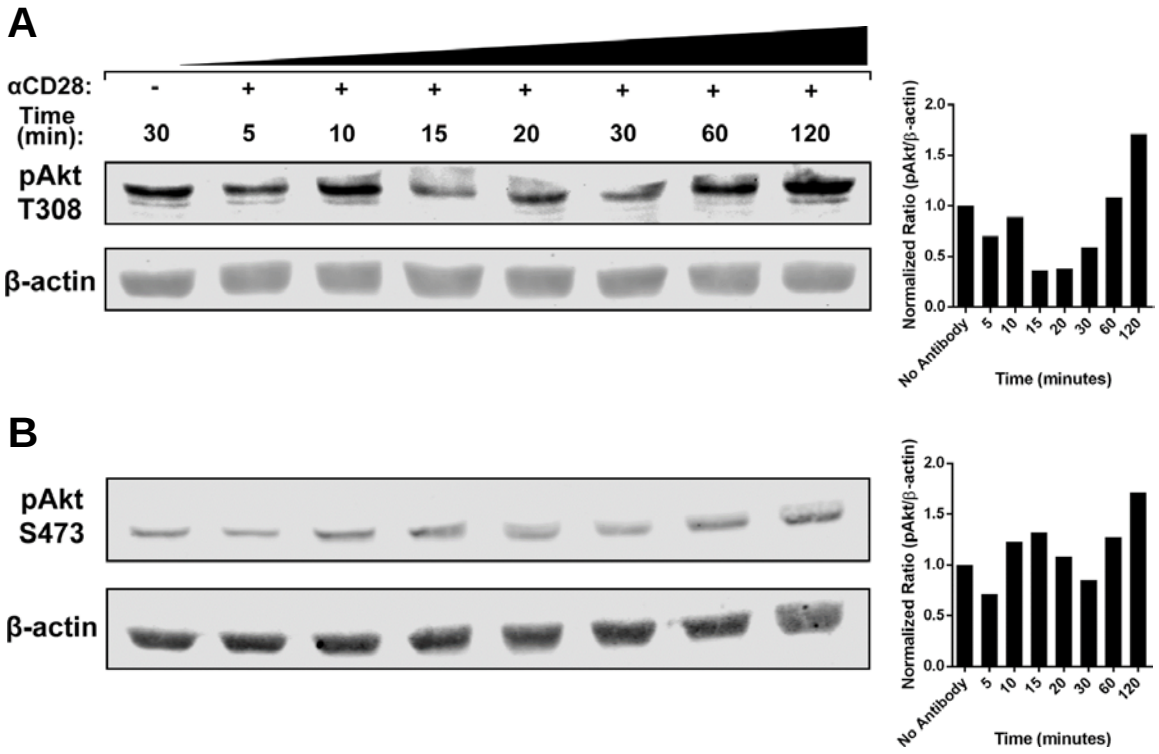

Figure 7. Stimulation with agonistic anti-CD28 antibody induces greatest Akt phosphorylation when incubated for 120 minutes. T cells were stimulated with 2 µg/mL plate-bound anti-CD28 over a time course. Half a million cells were loaded per well on a 10% acrylamide gel. Samples were then transferred to a nitrocellulose membrane and blotted with 1:5000 chicken anti-β-actin and ***A*** 1:1000 rabbit anti-Akt pS473 or ***B*** 1:500 rabbit anti-Akt pT308 primary. Signal intensity was calculated as a ratio of pAkt/β-actin, and was normalized to the vehicle control.

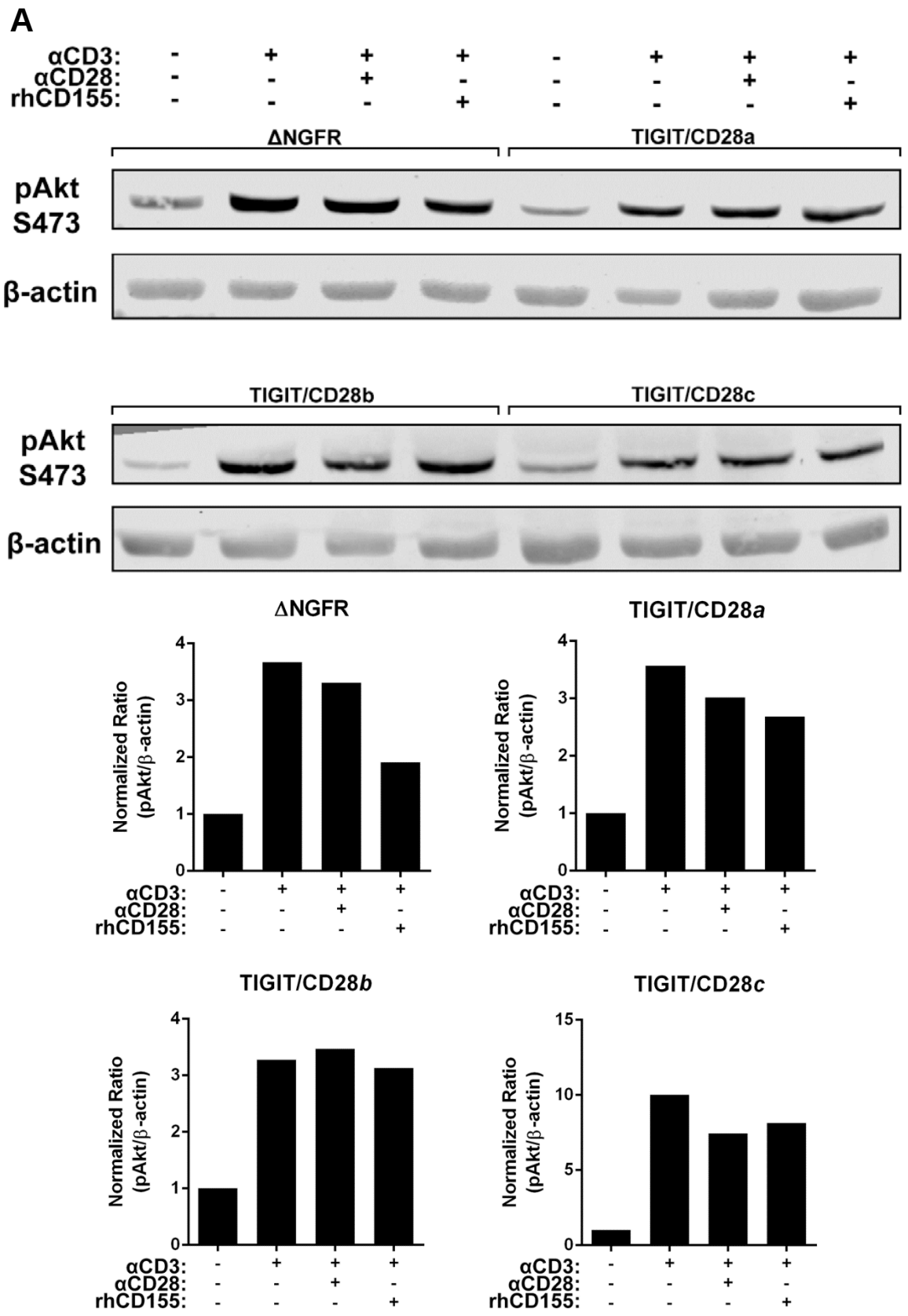
A
αCD3: - + + + - + + +
αCD28: - - + - - - + -
rhCD155: - - - + - - - +
ΔNGFR
TIGIT/CD28a
pAkt S473
β-actin
TIGIT/CD28b
TIGIT/CD28c
pAkt S473
β-actin
ΔNGFR
TIGIT/CD28a
Normalized Ratio (pAkt/β-actin)
αCD3: - + + +
αCD28: - - + -
rhCD155: - - - +
TIGIT/CD28b
TIGIT/CD28c

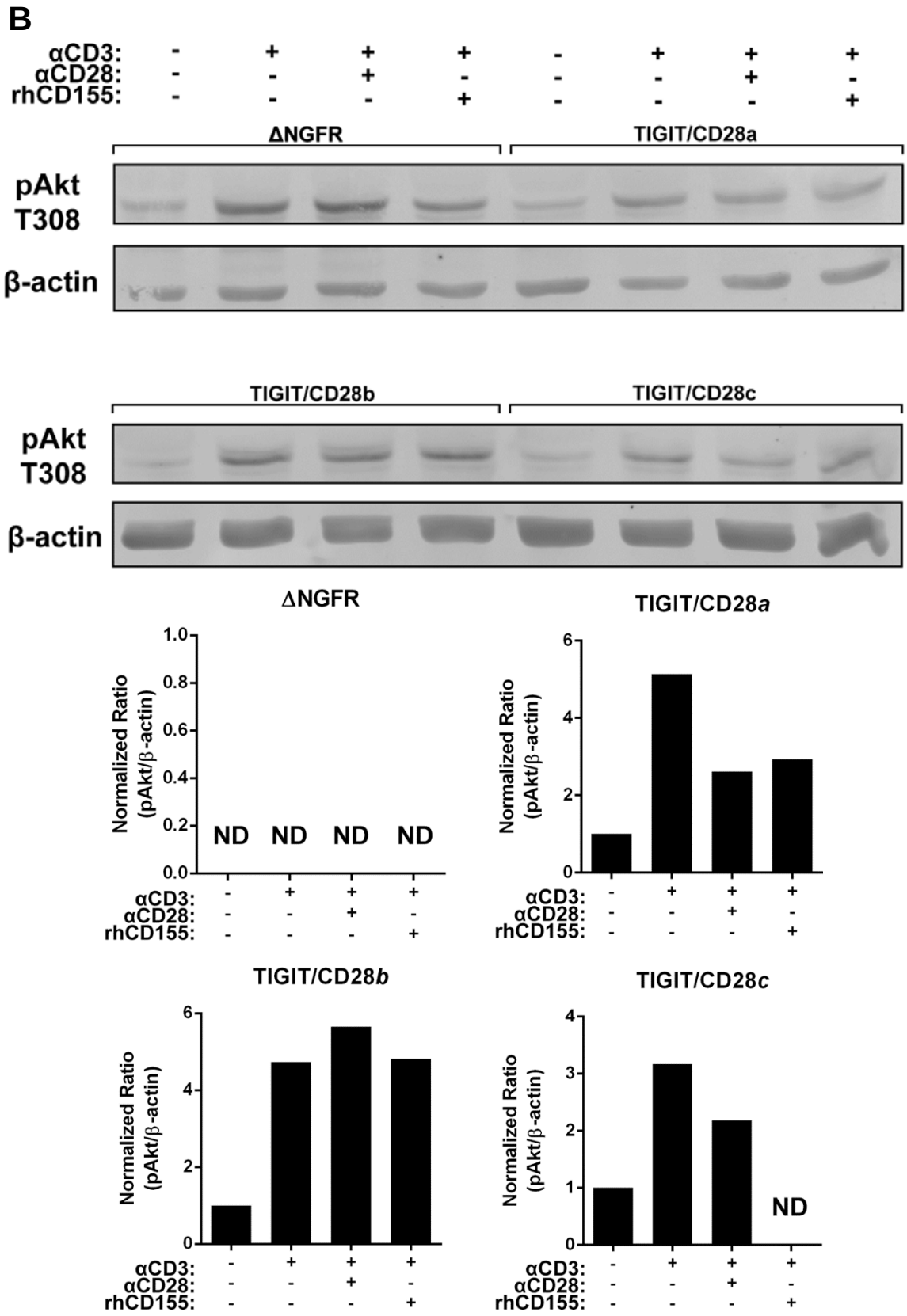
B
αCD3: - + + + - + + +
αCD28: - - + - - - + -
rhCD155: - - - + - - - +
ΔNGFR
TIGIT/CD28a
pAkt T308
β-actin
TIGIT/CD28b
TIGIT/CD28c
pAkt T308
β-actin
ΔNGFR
Normalized Ratio (pAkt/β-actin)
ND ND ND ND
TIGIT/CD28a
TIGIT/CD28b
TIGIT/CD28c
ND

Figure 8. The TIGIT/CD28 variants do not show increased Akt phosphorylation in response to stimulation with rhCD155. ΔNGFR (MOI 5) and TIGIT/CD28 chima T cells (MOI 25) were stimulated with anti-CD3 (1 µg/mL) with/without anti-CD28 (1 µg/mL) or rhCD155 (10 µg/mL) for 2 hours. Half a million cells were loaded per well on a 10% acrylamide gel. Samples were then transferred to a nitrocellulose membrane and blotted with 1:5000 chicken anti-β-actin and ***A*** 1:1000 rabbit anti-Akt pS473 or ***B*** 1:500 rabbit anti-Akt pT308 primary. Signal intensity was calculated as a ratio of pAkt/β-actin, and was normalized to the vehicle control. ND, not determined.

4.1.4 Assessment of Signaling via TIGIT/CD28 Chimeras through Multiple Myeloma Survival

Although our molecular assessment suggested that the TIGIT/CD28 fusions may not be activating the CD28 pathway, we wanted to employ an alternate method to confirm this lack of function. *In vivo*, the stroma surrounding multiple myeloma cells provides important survival factors and signals. One such signal is mediated via ligation of CD28 on the multiple myeloma cell[173,174]. In lieu of the stroma, multiple myeloma cell lines *in vitro* receive NFκB survival signals from growth factors contained in serum, such as IGF-1[173]. In the absence of these serum factors, multiple myeloma cells do not survive well in culture. However, CD28 signaling is able to compensate and rescue cells starved of serum[173]. Furthermore, it has been determined that CD28's pro-survival effect in multiple myeloma is partially driven through the PI3K/Akt pathway[175]. Using this knowledge, we investigated whether we could exploit multiple myeloma cell survival *in vitro* to examine signaling via the TIGIT/CD28 chimeric receptors.

MM.1S myeloma cells cultured in the absence of serum display reduced viability; however, the viability can be recovered by culturing in the presence of anti-CD28 mAb (**Figure 9A**). MM.1S cells were subsequently transduced with lentiviruses encoding the ΔNGFR construct or the TIGIT/CD28*a* construct, to test whether viral transduction influences the assay. We generated two MM.1S variant lines (named *ΔNGFR MM.1S* and *TIGIT/CD28*a *MM.1S*) that expressed high levels of both ΔNGFR and wild type CD28 (**Figure 9B**); we selected the cells in bulk to

avoid clonal heterogeneity. Interestingly, the TIGIT/CD28*a* MM.1S cells only displayed slight expression of the chimera (**Figure 9B**). Surprisingly, ΔNGFR- and TIGIT/CD28*a*-transduced MM.1S cells were more resistant to the effects of serum starvation and didn't show any responsiveness of the inclusion of anti-CD28 in the culture (**Figure 9C**). Further, we also tested the effect of the TIGIT ligand rhCD155 on MM.1S cells to determine whether the triggering ligand would affect MM.1S survival. Again, we were surprised to find that rhCD155 could rescue MM.1S cells to the same extent as anti-CD28 (**Figure 9D**). These latter observations were consistent and demonstrated that MM.1S cells would be not a suitable bioassay for measuring Akt activation via CD28 signaling.

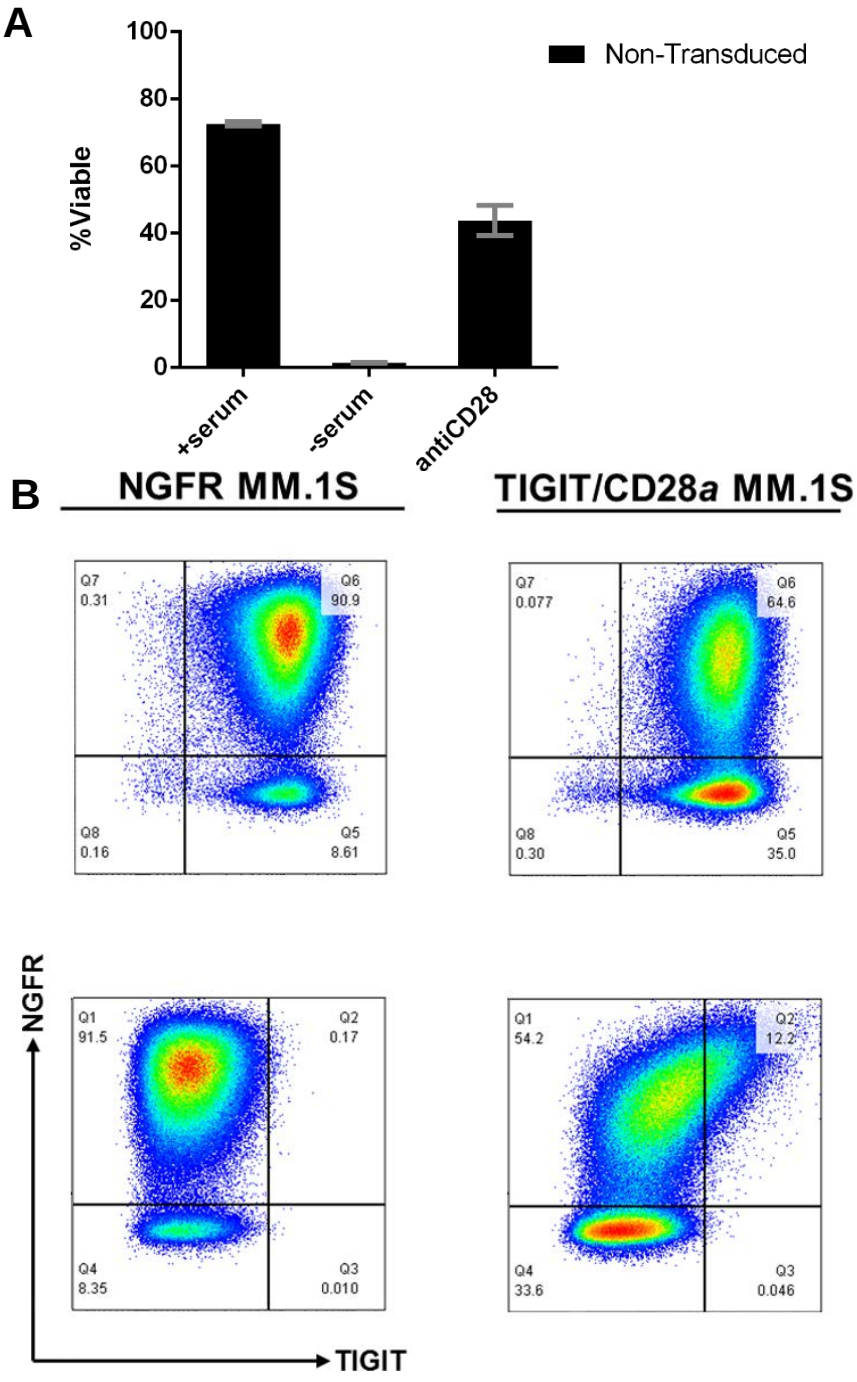
A
100
80
60
40
20
0
%Viable
Non-Transduced
+serum
-serum
antiCD28
B
NGFR MM.1S
TIGIT/CD28a MM.1S
Q7
0.31
Q6
90.9
Q8
0.16
Q5
8.61
Q7
0.077
Q6
64.6
Q8
0.30
Q5
35.0
NGFR
Q1
91.5
Q2
0.17
Q4
8.35
Q3
0.010
Q1
54.2
Q2
12.2
Q4
33.6
Q3
0.046
TIGIT

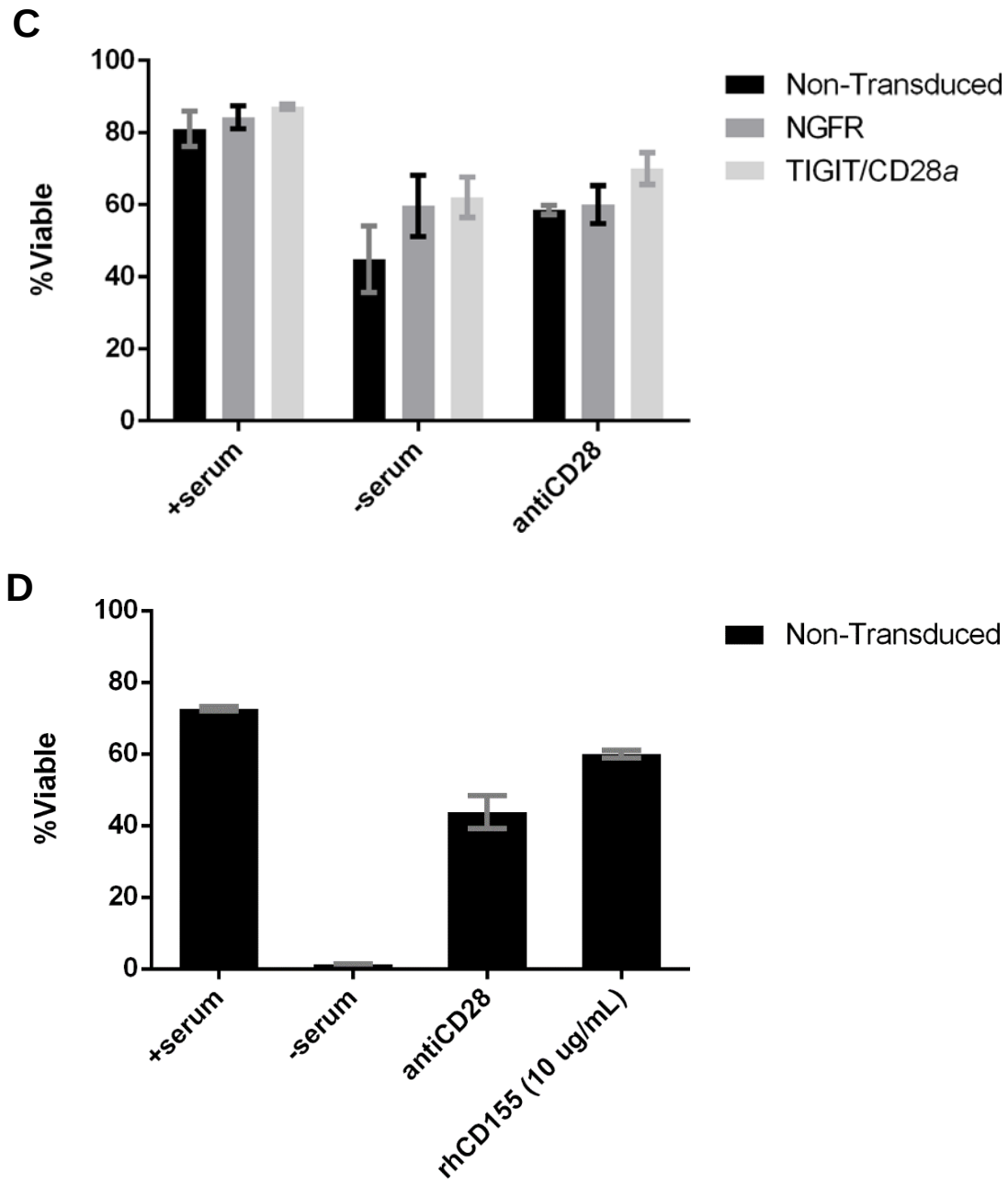

Figure 9. MM.1S cells are not suitable for assessment of CD28 signaling after transduction with lentivirus. ***A*** Non-transduced T cells were tested for viability after 48 hours of serum starvation with or without anti-CD28 mAb ***B*** MM.1S cells transduced with ΔNGFR-encoding lentivirus at an MOI of 2 were measured on flow cytometry for ΔNGFR and CD28 expression. ***C*** ΔNGFR-transduced and non-transduced MM.1S cells were tested for viability after 48 hours of serum starvation with or without anti-CD28 mAb. ***D*** As in *A*, however cells were additionally stimulated with rhCD155. Results presented in each panel are from a single experiment done in triplicate, respectively.

4.1.5 Assessment of Signaling via TIGIT/CD28 Chimeras through Complementation of the CD4TAC Receptor.

As stated previously, the key goals of this research is to develop a receptor capable of delivering costimulatory signals (i.e. signal 2) to complement the signal 1 provided by the novel TAC receptors developed in the Bramson lab. Therefore, to directly address this hypothesis, we opted to examine the impact of co-expression of the TIGIT/CD28 chimeric receptors with the prototypic HER2-CD4TAC receptor in human T cells. To this end, we engineered lentivirus vectors to co-express the HER2-CD4TAC with each of the TIGIT/CD28 chimeric receptors in primary human T cells. The lentivirus-transduced T cells were then exposed to targets that expressed both the TAC receptor ligand and the TIGIT/CD28 receptor ligand to determine whether co-ligation engendered functional improvements that would be expected from augmented CD28 signaling, such as increased IL-2 production[53,167].

Given the limited sequence room available within the pCCL transfer plasmid, introduction of a third promoter cassette was not feasible. To achieve co-expression of the HER2-CD4TAC (**Figure 10** and **Table 4**) and TIGIT/CD28 chimeras within a cell, we employed a 2A sequence from *Thosea asigna* virus (T2A), which is a short viral peptide sequences that result in cleavage of a peptide bond within the sequence due to ribosomal skip[176]. This method allows for expression of two genes under a single promoter. The HER2-CD4TAC and

TIGIT/CD28 variants were fused via T2A connector within the pCCL vector and used in generating lentivirus (**Figure 11**).

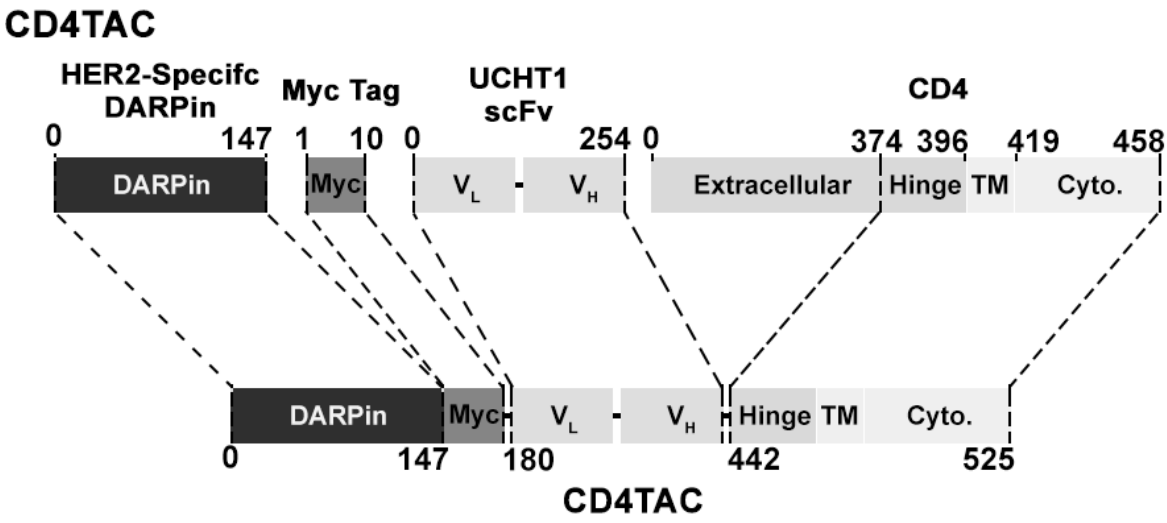

Figure 10. Schematic diagram depicting the component origins of the HER2-CD4TAC. Molecular schematic outlining the generation of the HER2-CD4TAC from parent proteins indicating extracellular DARPin, Myc tag, UCHT1 scFV, CD4 hinge, transmembrane (TM), cytoplasmic tail regions, and the relevant amino acid residue number.

Construct	Amino Acid Sequence
HER2-CD4TAC	*MDFQVQIFSFLLISASVIMSRGSDLGKKLLEAARAGQDDEVRILMA NGADVNAKDEYGLTPLYLATAHGHLEIVEVLLKNGADVNAVDAIG FTPLHLAAFIGHLEIAEVLLKHGADVNAQDKFGKTAFDISIGNGNE DLAEILQKLNEQKLISEEDLNPGGGGGSGGGGSGGGGSGGGGS GSMDIQMTQTTSSLSASLGDRVTISCRASQDIRNYLNWYQQKPD GTVKLLIYYTSRLHSGVPSKFSGSGSGTDYSLTISNLEQEDIATYF CQQGNTLPWTFAGGTKLEIKGGGGSGGGGSGGGGSGGGGSEV QLQQSGPELVKPGASMKISCKASGYSFTGYTMNWVKQSHGKNL EWMGLINPYKGVSTYNQKFKDKATLTVDKSSSTAYMELLSLTSED SAVYYCARSGYYGDSDWYFDVWGQGTTLTVFSTSGGGGSLESG QVLLESNIKVLPTWSTPVQPMALIVLGGVAGLLLFIGLGIFFCVRCR HRRRQAERMSQIKRLLSEKKTCQCPHRFQKTCSPI*

Table 4. Amino acid sequence of the HER2-CD4TAC receptor. Sequence provided with: extracellular portion italicized, DARPin in black, Myc tag in maroon, linker in grey hinge in teal, transmembrane region in red, and intracellular region underlined.

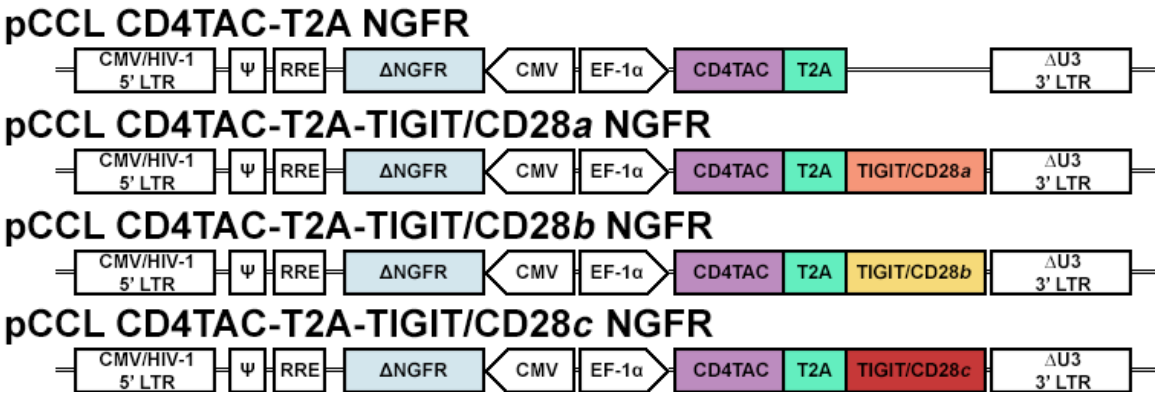

Figure 11. Schematic of final transfer plasmids used to generate lentiviruses for coexpression of HER2-CD4TAC and TIGIT/CD28 chimeras. Schematic diagram of pCCL transfer plasmids used for generation of lentivirus. Chimeric CMV/HIV-1 5' LTR containing CMV promoter; Ψ Packaging element; RRE rev response element; CMV minimal hCMV promoter; EF-1α human elongation factor 1 alpha promoter; ΔU3 3' LTR self-inactivating 3' LTR.

The functionality of the T2A connector was validated by transduction of HEK293TM cells with lentivirus containing the HER2-CD4TAC-T2A-TIGIT/CD28 CCR cassette. Transduced HEK293TM cells show high co-expression of the HER2-CD4TAC and the TIGIT/CD28 *a* and *b* variants (**Figure 12A)**. Similar to our previous results (**Figure 4**), the TIGIT/CD28*c* variant was poorly expressed on the cell surface (**Figure 12A**).

T cells were transduced with lentivirus at an MOI of 10 and cultured for 14 days before phenotypic analysis by flow cytometry to determine TAC and CCR expression. The HER2-CD4TAC-T2A-T cells were poorly transduced with <10% $\Delta NGFR^+$, and HER2-CD4TAC-T2A-TIGIT/CD28*a*, *b*, and *c* each show very poor transduction, all below 9% $\Delta NGFR^+$ (**Figure 12B**, mean±SD $\Delta NGFR^+$ $CD4^+$: 7.6%±1.8, $\Delta NGFR^+$ $CD8^+$: 6.6%±1.5). Although the overall transduction of all four of the TAC cultures was quite low, the HER2-CD4TAC-T2A-TIGIT/CD28*a* variant did reveal a TAC^+ $TIGIT^+$ $\Delta NGFR^+$ population, indicating that all 3 genes were being co-expressed in the transduced cells. T cells engineered with TIGIT/CD28*b* and TIGIT/CD28*c* had no measurable expression of TIGIT on the $\Delta NGFR^+$ TAC^+ population indicating that the chimeric protein was not being expressed.

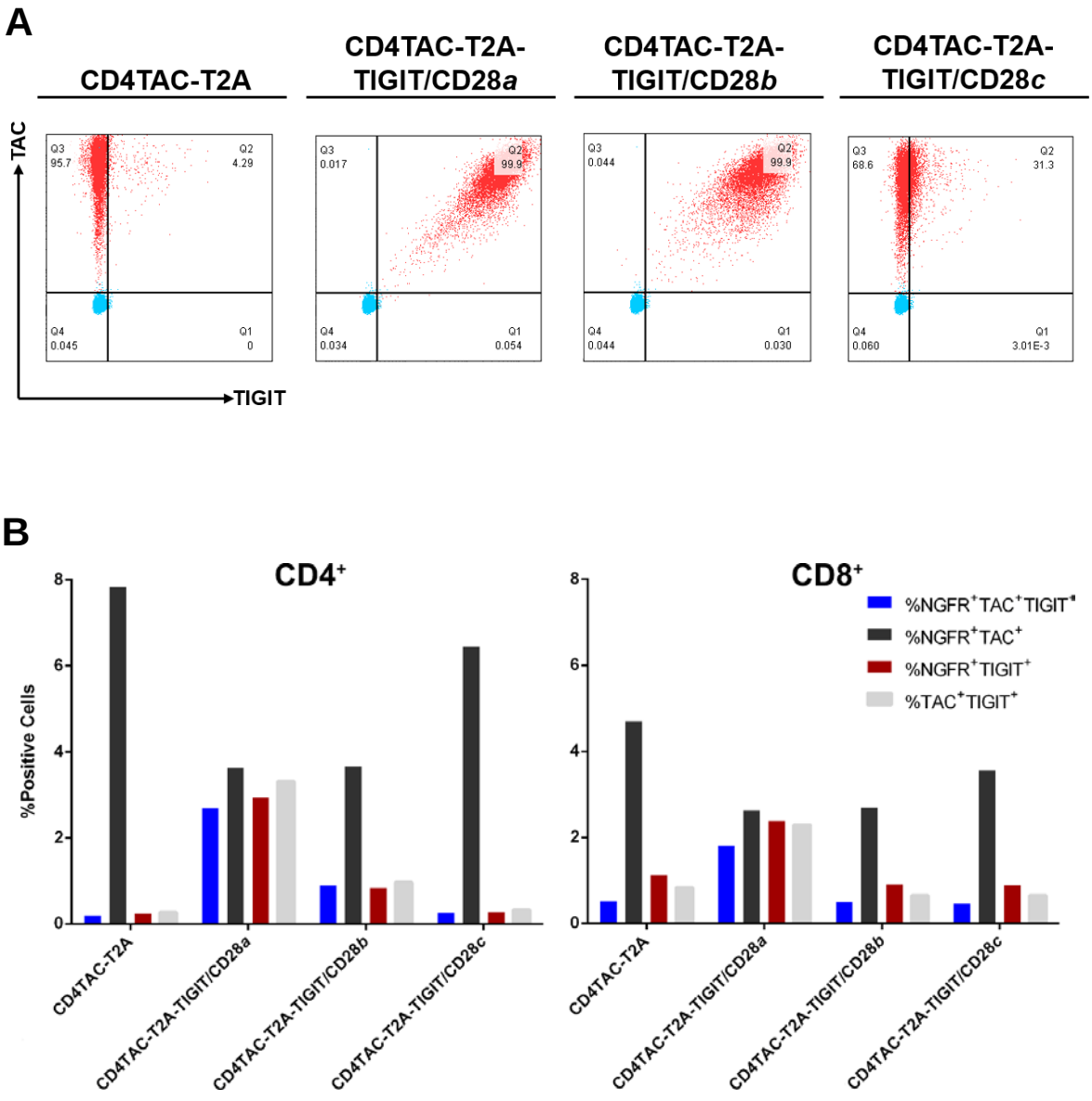

Figure 12. TAC and TIGIT/CD28 are poorly expressed in primary T cells, but not HEK293TM cells. ***A*** HEK293TM cells transduced with lentivirus encoding TAC-T2A with or without TIGIT/CD28 were stained for expression of HER2-CD4TAC and TIGIT. Blue and red dots represent non-transduced and transduced cells, respectively. ***B*** Primary human T cells transduced using lentivirus at an MOI 10 were cultured for 14 days before staining with anti-CD4-AlexaFluor 700, anti-CD8-PerCP-Cy5.5, anti-NGFR-BV421, anti-TIGIT-APC, and HER2 Fc/anti-human IgG-PE.

Despite the poor HER2-CD4TAC and TIGIT/CD28 expression, we evaluated cytokine production in response to stimulation with tumor cells. Tumor lines previously determined to be $HER2^+$ (A549, MDA-MB-231, SKBR3) or $HER2^-$ (LoxIMVI) within the lab were stained for CD155 expression. All tumor lines tested had high expression of CD155, and less so CD112 (**Figure 13**, and data not shown). T cells were incubated with A549 lung carcinoma and SKBR3 breast adenocarcinoma cells at a 4:1 T cell:tumor cell ratio for 4 hours and cytokine expression was investigated (**Figure 14** and data not shown). The inclusion of the TIGIT/CD28 chimeras failed to augment the level of IL-2 production or the number of IL-2 producing cells (**Figure 14**). Additionally, neither degranulation, as measured by CD107a surface expression, nor the percent of $IFN\gamma^+TNF\alpha^+$ double producing cells were influenced by coexpression of the HER2-CD4TAC and TIGIT/CD28 chimera in comparison to the HER2-CD4TAC alone. The overall cytokine and degranulation profile of the engineered-T cells was not altered by the presence of the TIGIT/CD28 CCRs (**Figure 15**). Finally, the killing activity HER2-CD4TAC-T2A-TIGIT/CD28-T cells were also tested in a 6 hour killing assay utilizing AlamarBlue Viability reagent as a measure of metabolic activity. Once again, there was little discernable difference seen with incorporation of the TIGIT/CD28 CCRs with the HER2-CD4TAC when co-cultured with A549, SKBR3, and MDA-MB-231 tumor cell lines (**Figure 16**).

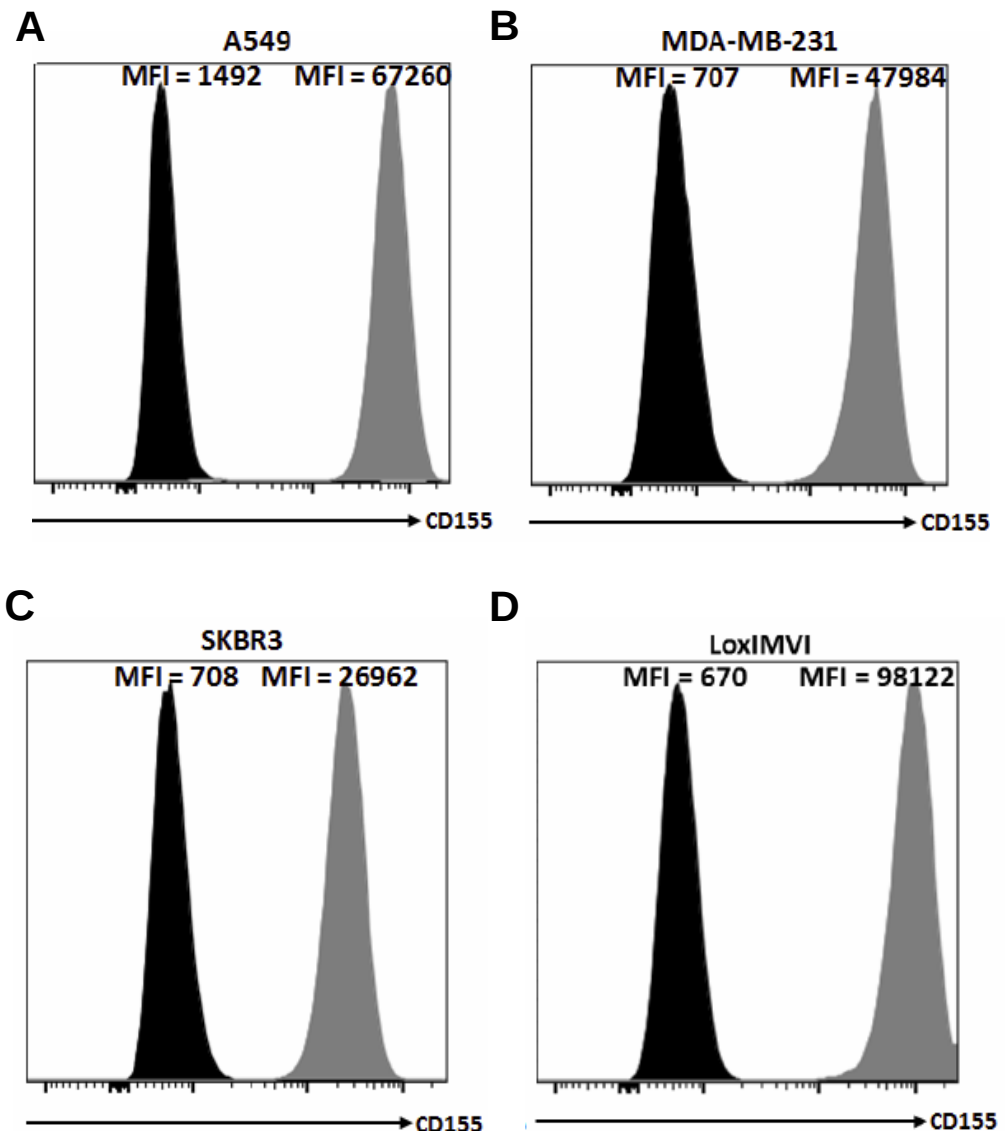

Figure 13. The cancer cell lines A549, MDA-MB-231, LoxIMVI, and SKBR3 expresses CD155. ***A*** A549 lung carcinoma, ***B*** MDA-MD-231 breast adenocarcinoma, ***C*** SKBR3 breast adenocarcinoma, and ***D*** Lox IMVI melanoma tumor cells were lifted utilizing 1x citric saline, washed, and stained with anti-CD155 PE antibody prior to flow cytometric analysis.

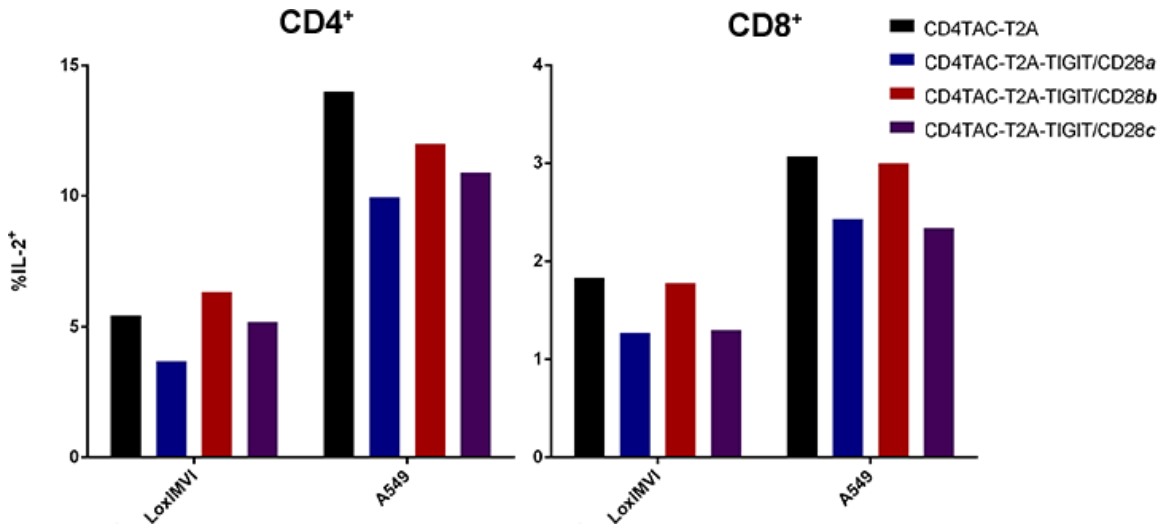

Figure 14. T cells transduced with both HER2-CD4TAC and TIGIT/CD28 chimera do not show enhanced IL-2 production compared HER2-CD4TAC alone when stimulated with tumor cells. T cells were co-cultured with tumor cells at a 1:4 ratio for 4 hours. Cells were permeabilized and fixed with BD Cytofix/Cytoperm before staining for cytokine expression. $HER2^-$ LoxIMVI and $HER2^+$ A549 served as negative and positive stimuli, respectively.

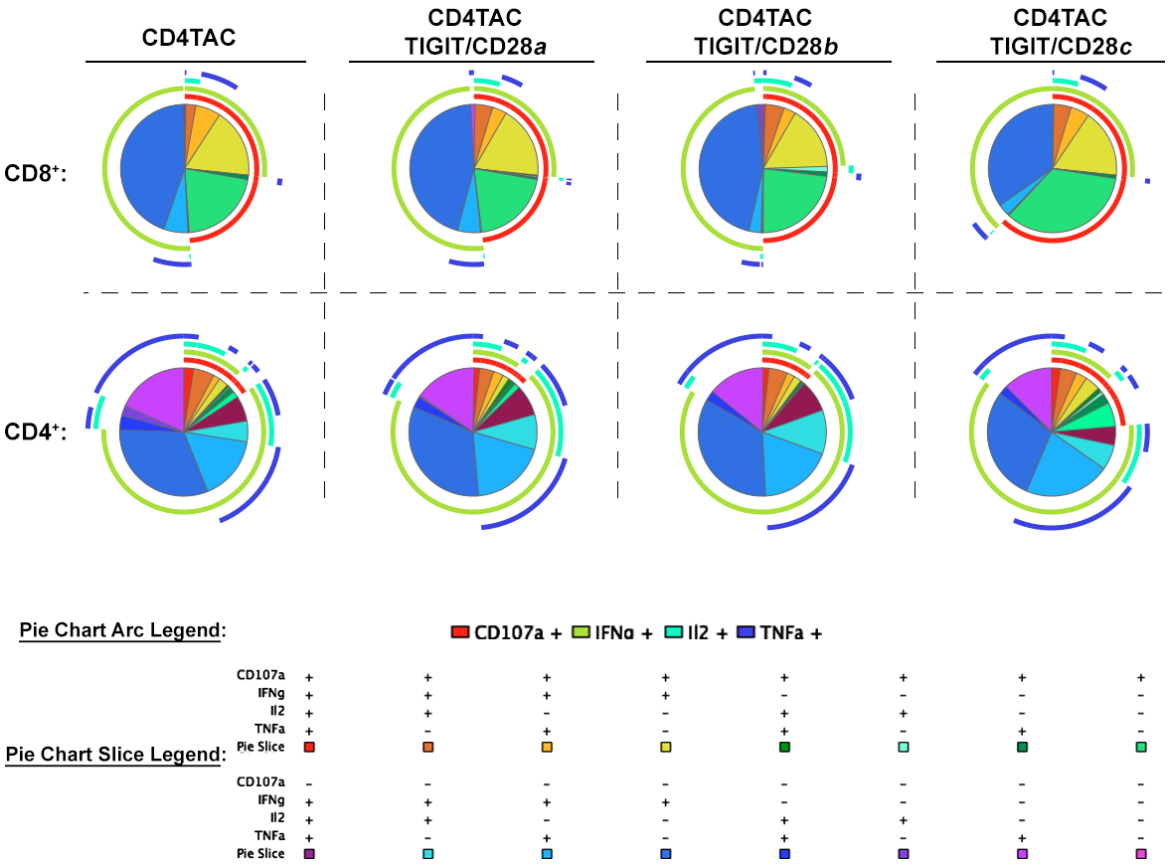

Figure 15. Inclusion of the TIGIT/CD28 CCR does not alter the cytokine expression profile of T cells expressing the HER2-CD4TAC. T cells were co-cultured with A549 lung carcinoma cells at a 1:4 ratio for 4 hours. Cells were permeabilized and fixed with BD Cytofix/Cytoperm before staining for cytokine expression. Data was analyzed by FlowJo software and parameters were processed through SPICE 5 software with threshold set to 0 to determine cytokine and degranulation express profile. Data is shown as $CD8^+$ and $CD4^+$ populations.

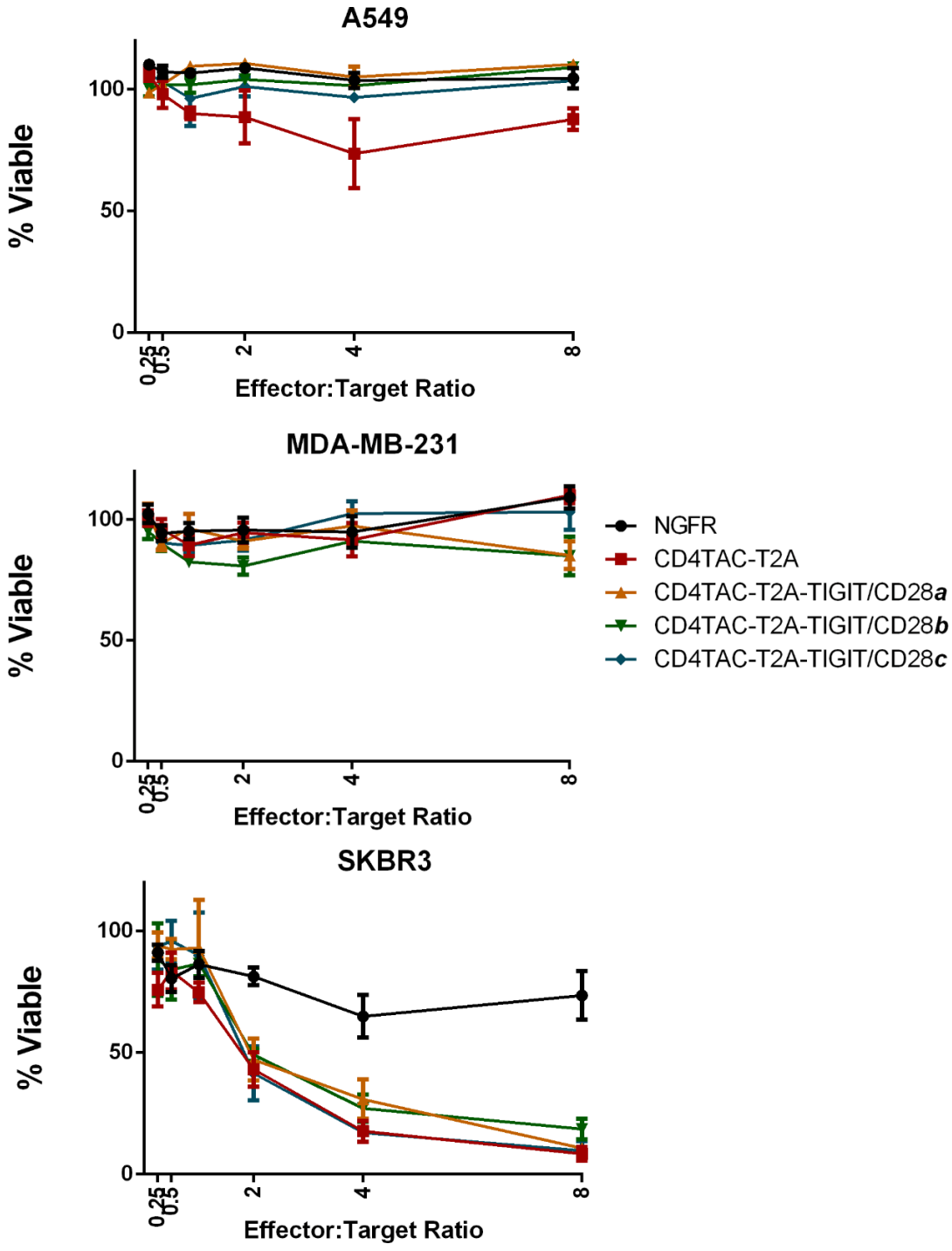

Figure 16. The TIGIT/CD28 chimeras do not affect the killing of tumor cells. 12,500 tumor cells were plated 18 hours prior to co-culture with T cells at a range

of effector:target ratios. After 6 hours, viability of tumor cells was assessed with Alamar Blue viability reagents. Results are from one experiment done in triplicate.

4.2 Costimulatory TAC Receptors

4.2.1 CD28TAC and 4-1BBTAC Design

An alternate strategy to delivery of costimulatory signals to TAC-engineered T cells would be to include the CD28 or 4-1BB costimulatory domains within the TAC receptor itself, akin to conventional CARs. However, a key difference here would be the absence of signal 1 domains from the TAC, which is provided by the natural TCR, in this case. A former lab member, Dr. Rajanish Giri, designed two fusion proteins where the CD4 domains from the TAC prototype were replaced by the linker, transmembrane and cytoplasmic domains of CD28 and 4-1BB to generate TAC variants we named *HER2-CD28TAC* and *HER2-4-1BBTAC*, respectively (**Figure 17** and **Table 5**). The extracellular portion of CD28 selected as the ”linker” in HER2-CD28TAC was chosen based on the crystal structure (PDBe entry 1YJD) and disorganized protein analysis program DisEMBL. There is currently no published crystal structure of 4-1BB, so bioinformatic modeling was used to determine a potential unstructured region.

The targeting moiety utilized in all three of the TAC receptors is a HER2-specific DARPin protein of picomolar affinity[177] and was cloned in with a Myc tag. HER2-CD28TAC- and HER2-4-1BBTAC-encoding lentiviruses were prepared as in section 1 (**Figure 18**).

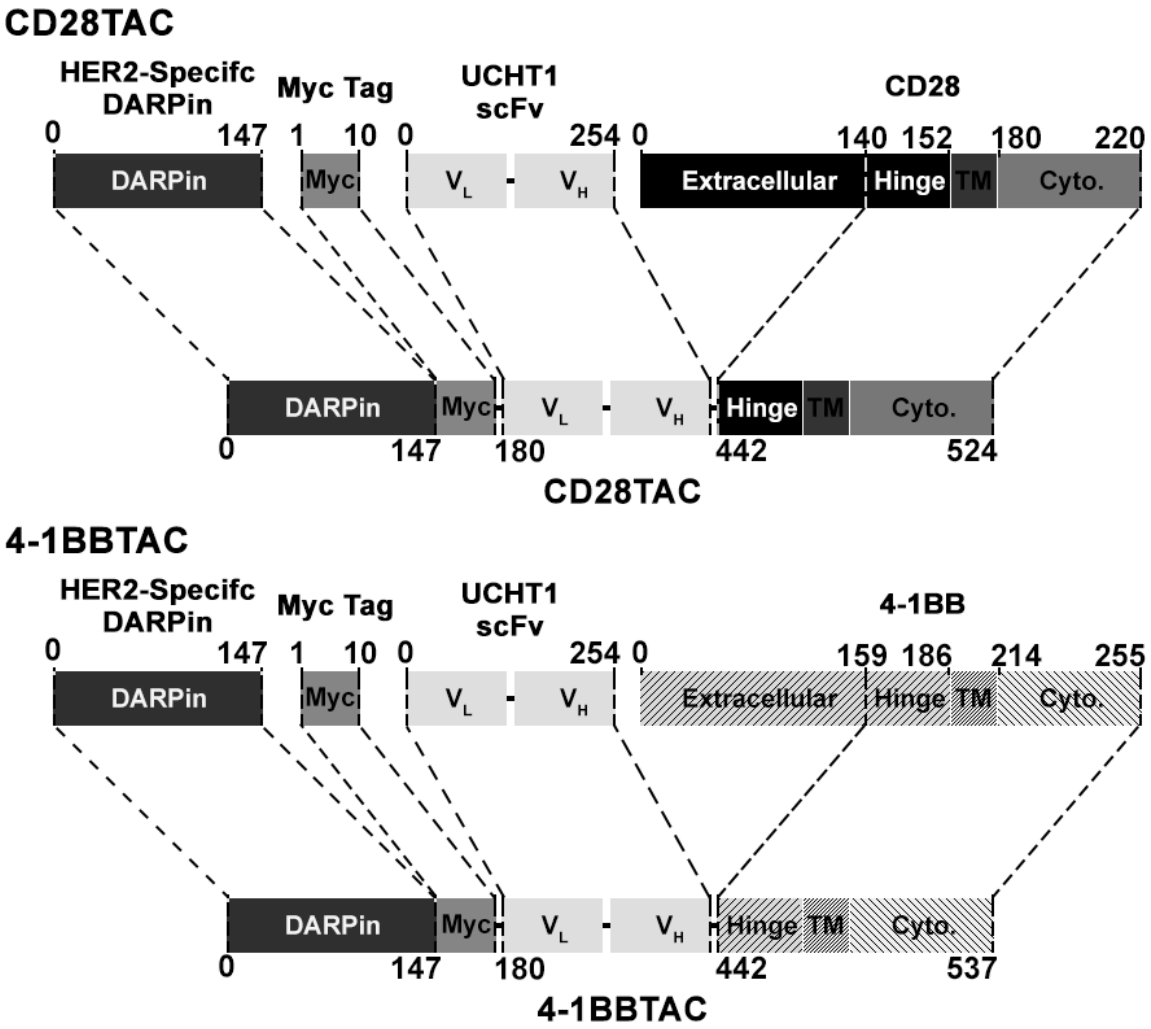

Figure 17. Schematic diagram depicting the construction of the modified TACs from the original HER2-CD4TAC components and parent CD28 or 4-1BB proteins. Molecular schematic outlining the generation of the HER2-CD4TAC from parent proteins indicating extracellular DARPin, Myc tag, UCHT1 scFV, CD4 hinge, transmembrane (TM), cytoplasmic tail regions, and the relevant amino acid residue number.

Construct	Amino Acid Sequence
HER2-CD28TAC	*MDFQVQIFSFLLISASVIMSRGSDLGKKLLEAARAGQDDEVRILMA NGADVNAKDEYGLTPLYLATAHGHLEIVEVLLKNGADVNAVDAIG FTPLHLAAFIGHLEIAEVLLKHGADVNAQDKFGKTAFDISIGNGNE DLAEILQKLNEQKLISEEDLNPGGGGGSGGGGSGGGGSGGGGS GSMDIQMTQTTSSLSASLGDRVTISCRASQDIRNYLNWYQQKPD GTVKLLIYYTSRLHSGVPSKFSGSGSGTDYSLTISNLEQEDIATYF CQQGNTLPWTFAGGTKLEIKGGGGSGGGGSGGGGSGGGGSEV QLQQSGPELVKPGASMKISCKASGYSFTGYTMNWVKQSHGKNL EWMGLINPYKGVSTYNQKFKDKATLTVDKSSSTAYMELLSLTSED SAVYYCARSGYYGDSDWYFDVWGQGTTLTVFSTSGGGGSLEKH LCPSPLFPGPSKPFWVLVVVGGVLACYSLLVTVAFIIFWVRSKRS RLLHSDYMNMTPRRPGPTRKHYQPYAPPRDFAAYRS*
HER2-4-1BBTAC	*MDFQVQIFSFLLISASVIMSRGSDLGKKLLEAARAGQDDEVRILMA NGADVNAKDEYGLTPLYLATAHGHLEIVEVLLKNGADVNAVDAIG FTPLHLAAFIGHLEIAEVLLKHGADVNAQDKFGKTAFDISIGNGNE DLAEILQKLNEQKLISEEDLNPGGGGGSGGGGSGGGGSGGGGS GSMDIQMTQTTSSLSASLGDRVTISCRASQDIRNYLNWYQQKPD GTVKLLIYYTSRLHSGVPSKFSGSGSGTDYSLTISNLEQEDIATYF CQQGNTLPWTFAGGTKLEIKGGGGSGGGGSGGGGSGGGGSEV QLQQSGPELVKPGASMKISCKASGYSFTGYTMNWVKQSHGKNL EWMGLINPYKGVSTYNQKFKDKATLTVDKSSSTAYMELLSLTSED SAVYYCARSGYYGDSDWYFDVWGQGTTLTVFSTSGGGGSLEPS PADLSPGASSVTPPAPAREPGHSPQIISFFLALTSTALLFLLFFLTL RFSVVKRGRKKLLYIFKQPFMRPVQTTQEEDGCSCRFPEEEEGG CEL*

Table 5. **Amino acid sequence of the modified TAC receptors.** Sequence provided with: extracellular portion italicized, DARPin in black, Myc tag in maroon, linker in grey hinge in teal, transmembrane region in red, and intracellular region underlined.

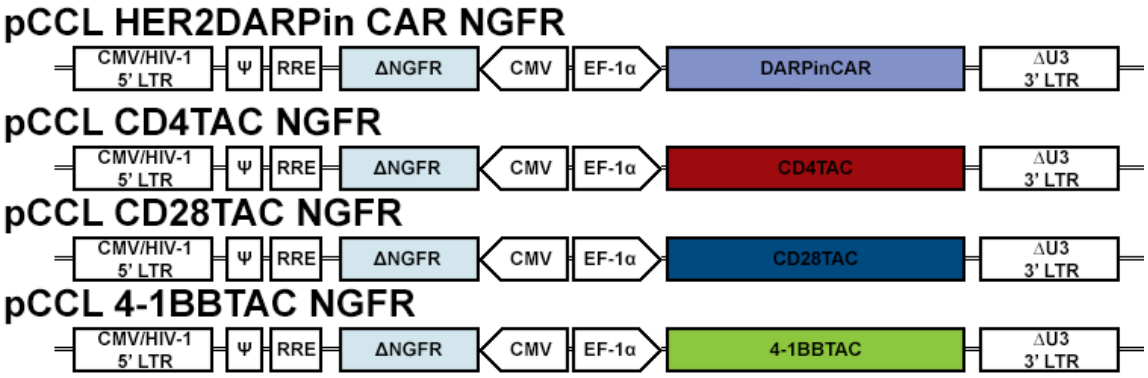

Figure 18. Final transfer plasmid designs used for generation of lentiviruses encoding either the HER2CAR, HER2-CD4TAC, HER2-CD28TAC, or HER2-4-1BBTAC. Schematic diagram of transfer plasmids used to generate lentiviral vectors for expression of chimeric constructs I. Chimeric CMV/HIV-1 5' LTR containing CMV promoter; Ψ Packaging element; RRE rev response element; CMV minimal hCMV promoter; EF-1α human elongation factor 1 alpha promoter; ΔU3 3' LTR self-inactivating 3' LTR.

4.2.2 Phenotype and Cellular Localization

To determine if the replacement of CD4 with CD28 or 4-1BB within the TAC design imparts any functional improvements to these cells, we sought to compare the new chimeras to the standard HER2-CD4TAC.

T cells transduced with HER2CAR or HER2-CD4TAC receptors displayed high surface expression of their respective receptors by flow cytometry (**Figure 19A**). T cells transduced with the HER2-4-1BBTAC displayed a relatively lower expression of the TAC receptor (**Figure 19A**). The modified HER2-CD28TAC, however, had an expression profile different than that of the HER2-CD4TAC or HER2-4-1BBTAC. Despite the high transduction of HER2-CD28TAC as seen by ΔNGFR expression, the HER2-CD28TAC receptor itself is poorly expressed, as seen by the weak double positive population (**Figure 19A**). However, the HER2-CD28TAC appears to be expressed at a low level on the surface of most cells (**Figure 19B**). The overall expression of the receptors, as seen by MFI, decreases in order from HER2CAR, HER2-CD4TAC, HER2-4-1BBTAC, to the HER2-CD28TAC receptor (**Figure 19B**). Further assessment of the HER2-CD28TAC and HER2-4-1BBTAC for TNFα, IFNγ, and IL-2 production upon stimulation with plate-bound recombinant HER2 Fc antigen showed negligible cytokine production (data not shown)**.**

Given the low surface expression of the HER2-CD28TAC, we questioned whether the chimeric receptor was possibly being retained within the cell. To investigate, we performed both western blot and immunofluorescence analysis.

The chimeric receptors all include a Myc tag, providing a simple method to compare total receptor levels by Western blot. Interestingly, based on Myc expression, the cell populations contained higher levels of the HER2-CD28TAC than the HER2-CD4TAC. Since the HER2-CD4TAC displays higher surface expression by flow cytometry, it appears that the HER2-CD28TAC is likely being retained within the cell. Unexpectedly, we could not measure the expression 41BBTAC by Western blot despite some evidence of surface expression by flow cytometry. Since the flow cytometry employs distinct probes (i.e. HER2 Fc) from the Western blot (i.e. anti-Myc), it is possible that differences in the reagents underpin the reduced sensitivity of the Western blot. (**Figure 20**).

To further characterize the protein localization of the chimeric TAC receptors, we employed immunofluorescence microscopy, once again probing for the Myc tag. Microscopic analysis clearly showed the HER2CAR and the HER2-CD4TAC on the cell surface (**Figure 21**). As expected from the Westen blot the HER2-4-1BBTAC was undetectable. The HER2-CD28TAC was clearly visible within the cell and co-localized with calnexin, a marker of the endoplasmic reticulum (ER). Therefore, these results indicate that the HER2-CD28TAC is trapped in the ER and fails to traffic to the cell surface.

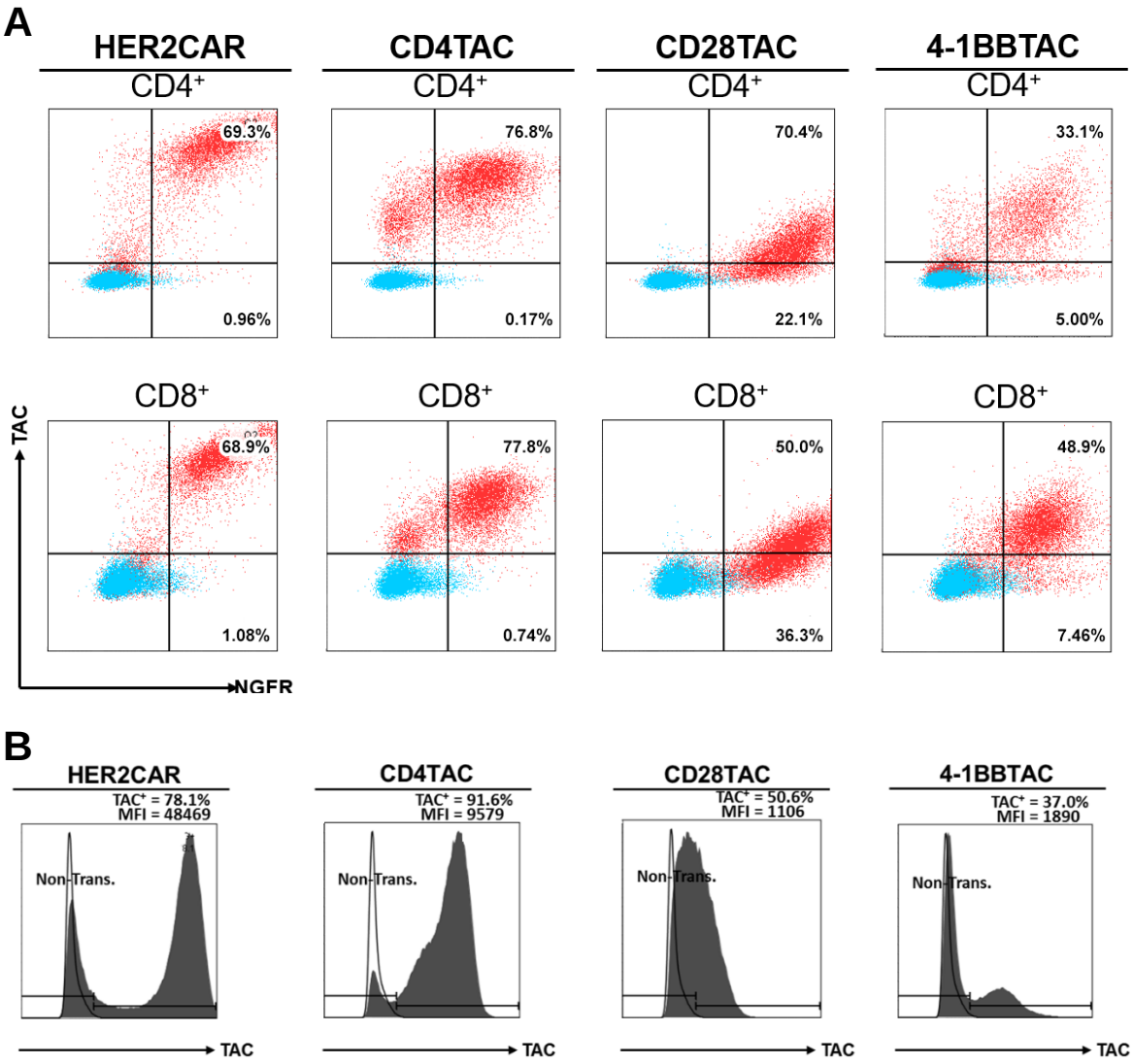

Figure 19. Primary human T cells poorly express modified TAC receptors. Example from one T cell batch. ***A*** PBMCs were transduced at an MOI of 10 and cultured for 14 days before phenotypic analysis by flow cytometry. Cells were incubated with recombinant HER2/Fc chimera and stained with anti-human IgG-PE, anti-NGFR-BV421, anti-CD4-AlexaFluor700 and anti-CD8-PerCP-Cy5.5. Plots show transduced cell population in red, overlaid with non-transduced controls in blue. ***B*** Histogram data of TAC expression displaying mean fluorescence intensity.

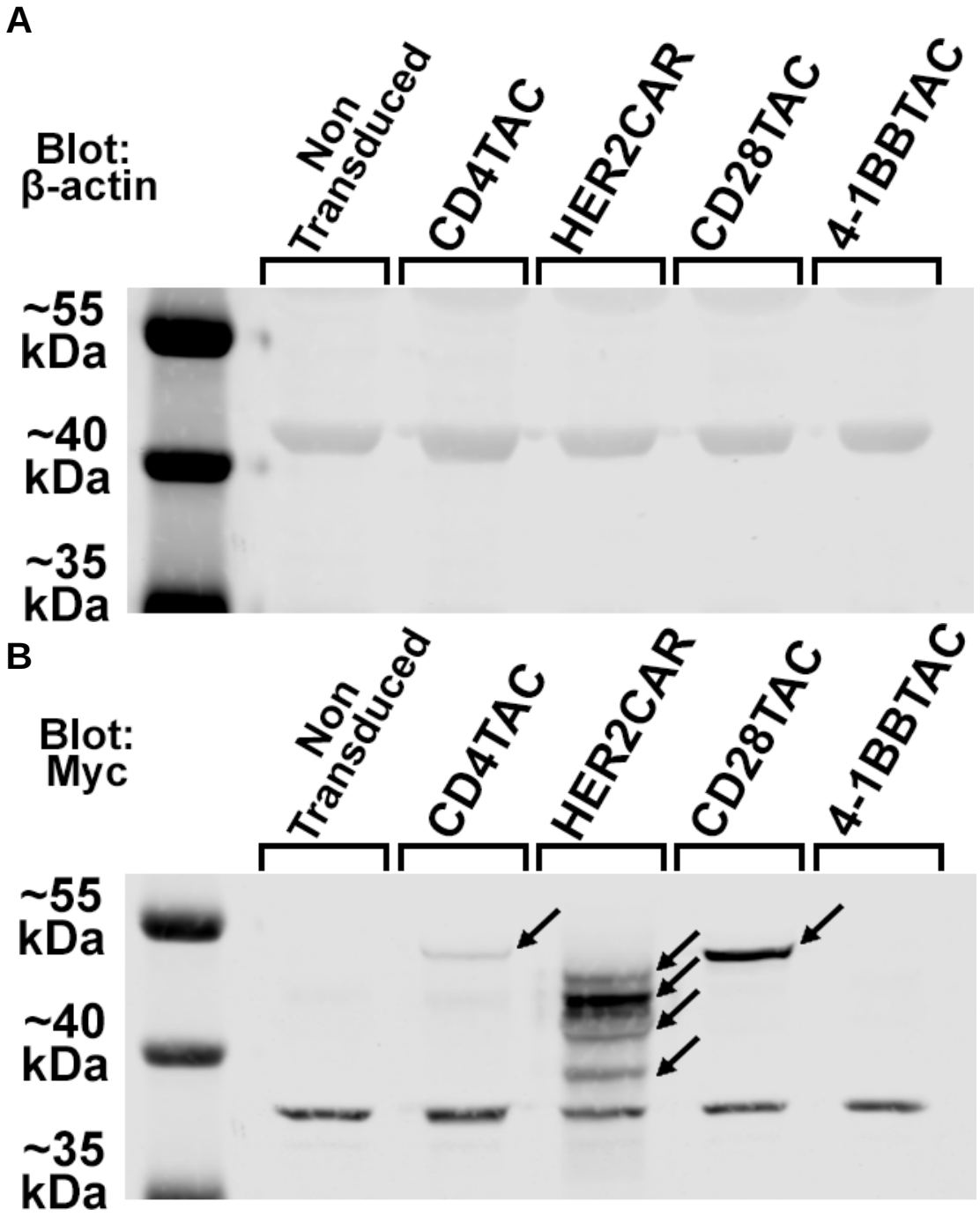

Figure 20. HER2-CD4TAC and HER2-CD28TAC, but not HER2-4-1BBTAC, expression is observable by western blot analysis. Half a million cells were loaded per well on a 10% acrylamide gel. Samples were then transferred to a nitrocellulose membrane and blotted with 1:5000 chicken anti-β-actin and 1:500 mouse anti-C-myc primary, and visualized with ***A*** 1:20,000 Li-Cor goat anti-mouse IRDye 800CW secondary or ***B*** 1:40,000 Li-Cor donkey anti-chicken IRDye 680RD secondary. Black arrow indicates proteins containing the Myc tag.

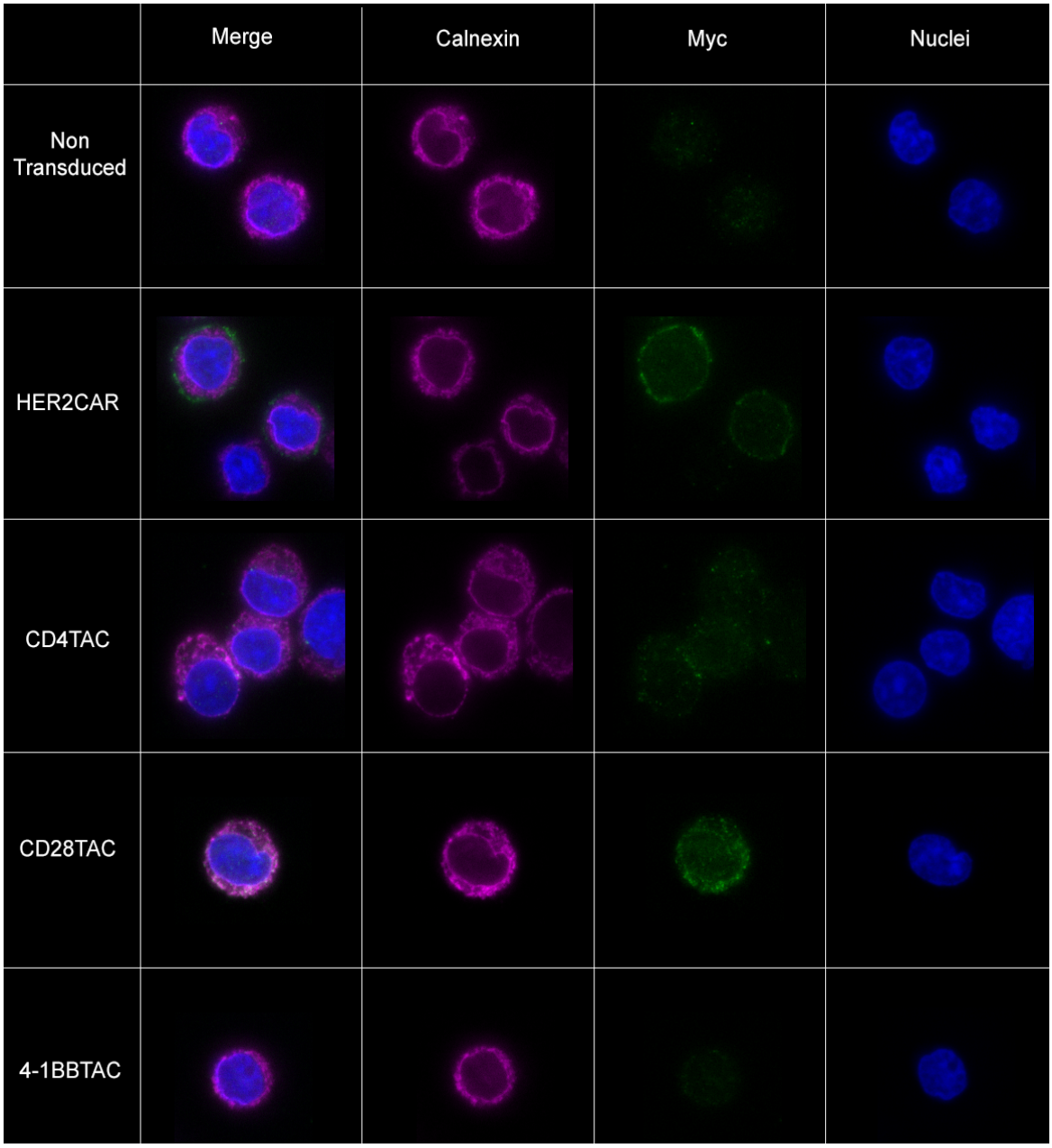

Figure 21. Immunofluorescence microscopy of CAR- and TAC-transduced T cells. T cells were cultured for 16 days before $1.5x10^6$ cells were stained for immunofluorescence with mouse anti-human c-Myc 1:20 and rabbit anti-calnexin 1:150. Secondary goat anti-mouse IgG (H+L) AlexaFluor 488 and goat anti-rabbit IgG (H+L) AlexaFluor 594 at 1:100 were utilized, followed with counterstain Hoechst 33342 dye 1:1000 to visualize nuclei. Samples were fixed on a slide utilizing Vector Technologies VectaShield and imaged by Life Technologies EVOS FL Auto Cell Imaging System at 60x magnification with oil immersion. The Pearson's correlation of co-localization between Myc and calnexin is provided.

5.0 Discussion

Adoptive transfer of anti-tumor CAR-engineered T cells is a rapidly expanding field of cancer immunotherapy with much promise. In particular, clinical trials treating hematological malignancies by targeting the CD19 antigen have shown the greatest clinical outcomes[105,178–181]. Arguably the most important aspect of this form of therapy is generation of an ideal T cell product. An optimal T cell response to cancer, or any harmful entity, is a robust, polyfunctional T cell population that efficiently proliferates, forms memory, and is resistant to exhaustion and apoptosis. There are many different factors and conditions that can alter the state of T cells, ranging from the way in which a T cell is activated, to its local microenvironment.

Recombinant chimeric receptors are an attractive modular platform to assemble one or more signaling components and assign their activation contingent upon binding of a chosen antigen. Second and third generation CARs have proven that inclusion of costimulatory domains can improve the anti-tumor functionality of CAR-T cells both *in vitro* and *in vivo*, as reviewed by Dotti *et al.*[117] and Jensen & Riddell[182]. In particular, costimulatory signals delivered by the CAR appear to enhance the persistence and expansion of CAR-engineered T cells in both pre-clinical models and human trials[114,120,130].

The HER2-CD4TAC designed in the Bramson lab provides only signal 1 to engineered-T cells. In principle, the addition of signal 2 via the TIGIT/CD28 CCR should augment certain T cell functions, such as improved survival and

proliferation. Our first tactic to bring costimulation to TAC-engineered T cells was to employ a split receptor system. Thus, we aimed to develop a novel chimeric costimulatory receptor. We chose to use the binding capacity of the T cell coinhibitory molecule, TIGIT, in our design. We speculate that the advantages to using TIGIT as the binding domain are two-fold. Primarily, the TIGIT ligands CD155 and CD112 are highly expressed on many cancers[139,141,142,144], therefore employing the TIGIT extracellular domain as a binding moiety to target tumors is an attractive idea. Furthermore, as a consequence of using TIGIT, there may potentially be an added benefit of redirecting the normal negative regulation imparted by TIGIT on T cell anti-tumor function[149,151], towards the CD28 costimulatory pathway because the TIGIT/CD28 chimera may compete with wild type TIGIT.

In designing the TIGIT/CD28 chimeric proteins, we chose to create three variants that differ only in the extracellular hinge region. Each TIGIT/CD28 fusion protein contains the entire CD28 transmembrane and cytoplasmic domains, and adjustments were made to the fusion point to determine the ideal hinge structure (**Figure 2**). Both the TIGIT/CD28*a* and *b*, but not the TIGIT/CD28*c,* constructs were well expressed on the surface of human T cells and HEK293TM cells (**Figure 4**). Removal of the TIGIT hinge region in the TIGIT/CD28*c* variant appeared to hinder expression of this chimera (**Figure 4**). Relative to their high ΔNGFR expression, TIGIT/CD28*c*-transduced T and HEK293TM cells had a low level of TIGIT expression. It is possible that this hinge region is necessary for surface expression

of the fusion protein. We chose not to pursue the TIGIT/CD28*c* variant and focused on the other chimeras, which demonstrated strong surface expression.

To determine whether the TIGIT/CD28 chimeras displayed costimulatory activity, we first investigated phosphorylation of the kinase Akt following CCR ligation, since the PI3K/Akt pathway is an important component of CD28 signaling. Our attempts at analysis of Akt phosphorylation by flow cytometry in response to T cell stimulation were unsuccessful as none of the stimulation conditions tested were able to reproducibly induce detectable phosphorylated Akt (**Figure 5**). As an alternative approach, we employed western blot analysis to assess Akt phosphorylation in our engineered T cells. Although we were able to detect Akt phosphorylation using this method, we failed to demonstrate Akt activation as a result of CD28 signaling. Stimulation of primary T cells with agonistic anti-CD3 mAb consistently yielded greater Akt phosphorylation than stimulations with both anti-CD3 and anti-CD28 mAbs (**Figure 8**). Furthermore, stimulation with plate-bound TIGIT ligand rhCD155 and anti-CD3 mAb did not appear to induce phosphorylation of Akt greater than with anti-CD3 alone (**Figure 8**). While these experiments failed to demonstrate evidence of costimulation following ligation of the TIGIT/CD28 chimera, our inability to confirm Akt phosphorylation as a result of CD28 signaling using an agonist antibody against CD28 render these experiments inconclusive. Given the considerable time investment and variation in generating engineered-primary T cells, we also attempted to use Jurkat cells to measure Akt activation. Jurkat cells were readily transduced to express the TIGIT/CD28*a* chimera, and

these cells were assessed for Akt activation in response to stimulation with rhCD155. Initial western blot results with TIGIT/CD28*a*-transduced Jurkat cells displayed a high basal Akt phosphorylation (data not shown). This phenotype may be due to a PTEN-deficiency present in Jurkat clones[183]. The absence of PTEN activity, a negative regulator of PI3K/Akt at steady-state, results in constitutive Akt phosphorylation[183]. We chose not to pursue signaling in Jurkat cells because of possible signaling abnormalities. Given our inability to observe Akt phosphorylation, we could not convincingly establish whether or not the TIGIT/CD28 CCR provided costimulatory signal. Other investigators have successfully induced Akt phosphorylation through the CD28 receptor using agonistic antibodies. However, these studies employed other agonistic clones different from the 28.2 clone used in this research, namely 9.3[52,167,184]. It is possible that switching to this mAb may resolve our issues. However, in addition to the issues faced with anti-CD28 stimulation, titration of an experimentally relevant concentration of rhCD155 for TIGIT/CD28 stimulation is difficult due to uncertainties in functionality of the receptor. Future experiments may benefit from titration of rhCD155 through examination of inhibitory effects from the natural TIGIT receptor. However, this is a laborious approach. Instead, a more robust method of stimulation may be to utilize artificial APCs (aAPC). Stimulation of T cells by aAPCs has previously been used to specifically target ligands to CAR-engineered T cells to assess readouts such as signal transduction[130]. aAPCs based on the K562 cell line can be engineered to express the high affinity FcγRI, CD64, to allow loading

of agonistic antibodies such as anti-CD3, and optionally with the CD28 ligands CD80/86[185]. These cells may be used as positive inducers in experiments assessing CD28 signaling or function. Furthermore, K562 aAPCs naturally express the TIGIT ligands CD155 and CD112 (**Figure S2**) and thus can be used to stimulate through the TIGIT/CD28 chimeric receptor. Experiments may be set up such that TIGIT/CD28 chimera-transduced T cells are compared to ΔNGFR-transduced T cells. However, a recent report has shown that some second generation CARs containing the CD28 signaling domain undergo autoproliferation[132]. As one of the readouts for CD28 signaling is proliferation, it may be beneficial to create a true K562 negative control by knocking out expression of the TIGIT ligands to account for such a phenotype. A Cas9 with guide RNA ribonucleoprotein has successfully been used to knock out genes in primary T cells, and such a system may be applicable to these aAPCs[186]. Because this method is typically not highly efficient, any ligand subpopulation may provide a false positive signal when co-cultured with TIGIT/CD28-engineered T cells. Thus, knock-out cells may stained with anti-CD155 and anti-CD112 mAb and flow sorted on the negative population.

As an alternate way of demonstrating CD28 signaling, we exploited the reliance of multiple myeloma cells on CD28 signaling for survival in the absence of serum *in vitro.* When deprived of serum, the MM.1S multiple myeloma cells begin to die in culture. Stimulation via agonistic anti-CD28 mAb rescues these cells from death due to serum starvation[173,174]. Thus, we planned to engineer MM.1S cells

with the TIGIT/CD28 receptors and compare survival in serum-free conditions in the presence of CD28 agonist antibody or TIGIT ligand. MM.1S cells transduced with the ΔNGFR control or the TIGIT/CD28*a* chimera displayed high transduction efficiency (**Figure 9B**). However, the TIGIT/CD28*a* receptor itself was poorly expressed (**Figure 9B**). We reasoned that this low surface expression would not present an issue because the TIGIT/CD28-expressing cells should display survival benefit when cultured with TIGIT ligand during serum starvation, assuming the CCR was working. Unfortunately, in our experiments, the process of viral transduction increased the survival of MM.1S myeloma cells following serum starvation, rendering the transduced MM.1S cells unsuitable for our experiments (**Figure 9C**). To further complicate matters, inclusion of the TIGIT ligand, rhCD155, during serum-starvation rescued non-transduced MM.1S cells, similar to anti-CD28 mAb. Thus, we also cannot make conclusions regarding rescue from serum-starvation in the presence of TIGIT ligand (**Figure 9D**). Overall, these control experiments demonstrated that the MM.1S cells could not be used as a biological assay to measure CD28 signaling.

As an alternate biological assay for signaling via the TIGIT/CD28 CCRs, we choose to test their functional properties in combination with the HER2-CD4TAC receptor. To this end, we created lentiviruses for co-expression of the TIGIT/CD28 CCRs along with our prototypic HER2-specific HER2-CD4TAC (**Figure 11**) and investigated phenotypic improvements that CD28 costimulation should provide, such as IL-2 production, and other parameters of T cell function. We examined a

number of HER2-positive tumor lines and found high level expression of TIGIT ligands, indicating they would be good targets to evaluate the consequence of signaling via the CCRs along with the TAC (**Figure 13**). Our first attempt at transducing primary T cells with this lentivirus batch resulted in meager overall transduction (**Figure 12B**). Although a second attempt slightly improved transduction efficiency (mean±SD $\Delta NGFR^+$ $CD4^+$: 7.6%±1.8, $\Delta NGFR^+$ $CD8^+$: 6.6%±1.5 vs mean±SD $\Delta NGFR^+$ $CD4^+$: 11.2%±2.0, $\Delta NGFR^+$ $CD8^+$: 13.1%±2.0) and co-expression of the TIGIT/CD28*b* and *c* variants (data not shown), the TAC^+ $NGFR^+$ $TIGIT^+$ population remained below 10%. Compared to transduction efficiencies normally seen with the TIGIT/CD28 chimeras (50-80%) or HER2-CD4TAC (35-60%), these cells were poorly transduced. It is unclear to us why the two experiments varied in transduction efficiency as the same reagents were used in each experiment. It is possibly due to donor batch variation, the method of diluting virus within 10 µL PBS, or simply a stochastic event. Unsurprisingly, given the low transduction efficiency, co-culture with $HER2^+CD155^+$ tumor cells did not show any appreciable difference in %IL-2 producing cells or cytotoxic capacity when the TIGIT/CD28 CCR was coexpressed with the HER2-CD4TAC (**Figure 14-16**). (**Figure 16**). We chose not to further study these cells until we have resolved the poor transduction efficiency. It is possible that some property of the lentivirus batches created prevented high-efficiency transduction. We probed distinct lentivirus batches for Myc tag presence and saw that lentiviruses encoding the HER2-CD4TAC contain a protein within or on the virion that matches the size of

the TAC receptor (**Figure S1**). As lentiviral particles bud through lipid raft regions and can retain cell-associated receptors[187,188], it is probable that our lentivirus acquire the HER2-CD4TAC through this phenomena. The UCHT1 scFv present within the TAC molecule may retain the virus on the T cell surface by engagement to CD3ε and prevent viral entry. Unlike the HER2-CD4TAC-containing lentiviruses, the HER2-CD28TAC-expressing lentivirus consistently yields high transduction efficiencies, despite the fact that the HER2-CD28TAC utilizes the same UCHT1 moiety as the HER2-CD4TAC (**Figure 19**). Probing the HER2-CD28TAC lentivirus showed only a faint Myc band, suggesting little HER2-CD28TAC incorporation (**Figure S1**). We cannot explain why the HER2-CD4TAC is incorporated into the virion and the HER2-CD28TAC is not. Unlike in T cells, the HER2-CD28TAC is surface expressed in HEK293TM producer cells (data not shown). The lack of incorporation into the virion may reflect differential distribution of the HER2-CD4TAC and the HER2-CD28TAC on the cell membrane at the time of lentivirus budding. At this time, we cannot explain the poor transduction of the lentiviruses expressing the HER2-CD4TAC and the TIGIT/CD28 CCR.

Although many of our attempts at characterization did not demonstrate clear functionality, our investigation with the TIGIT/CD28 fusion receptors has so far proven inconclusive and I believe further investigation of the current designs is warranted. The greatest challenge lies in finding a suitable stimulation specific to the both CD28 and TIGIT. Switching to a cell-based co-culture should provide a more robust, and physiologically relevant form of stimulation. However, it is difficult

to distinguish between cell types using western blot analysis, so a more thorough investigation into phospho-flow cytometry is a feasible approach. The use of commercial buffer sets that are specifically designed for phospho-flow cytometry staining may provide greater sensitivity for measuring phosphorylated Akt. The ultimate test of the TIGIT/CD28 CCR will be the effect of combined signalling via the CCR and HER2-CD4TAC on engineered T cells. However, these viruses expressing these constructs do not transduce with high efficiency for reasons that we cannot explain. In the future, we can consider non-viral methods for engineering the T cells. mRNA nucleofection is a rapid and transient method of gene expression that has been utilized to investigate CAR design[189]. The advantage to this system is the ability to alter the design of the protein under investigation and test in T cells much quicker than through the lengthy process of lentivirus production. Thus, future experiments of combined TIGIT/CD28 and HER2-CD4TAC expression could employ mRNA nucleofection rather than lentivirus transduction.

In the latter part of my thesis, we explored an alternative approach to bringing costimulatory signaling to the TAC design. Akin to second generation CARs, we explored whether replacing the CD4 portion of the TAC with the transmembrane and signaling domains of the costimulatory molecules CD28 or 4-1BB would activate their respective signalling pathways (**Figure 17**). We chose to investigate both CD28 and 4-1BB, as these two molecules have robust, yet distinct, effects on $CD8^+$ T cells. In the context of conventional CARs, a recent publication highlighted the impact of the CD28 signaling domain on amplifying T cell

exhaustion in the case of tonic, antigen-independent, CD3ζ signaling as a result of CAR clustering[190]. In contrast, the 4-1BB signalling domain produced less tonic signalling and, as result, less T cell exhaustion. Whether such parameters (tonic signalling, T cell exhaustion) are relevant to therapeutic activity remains unknown. Further, CARs that employ either 4-1BB or CD28 signaling domains have demonstrated impressive clinical results[105,178,180]. Thus, we chose to investigate both CD28 and 4-1BB in the design of a costimulatory TAC receptor.

The HER2-CD4TAC is the prototypic TAC and was used as a baseline within our study. The findings described in this thesis with the HER2-CD4TAC are consistent with other data generated in the Bramson lab - the receptor is expressed at a low level per cell, as seen by the MFI (**Figure 19C**). This is especially evident when comparing the HER2-CD4TAC to the HER2CAR, a typical second generation CAR. In comparison to the HER2-CD4TAC, T cells transduced to express either the HER2-CD28TAC or HER2-4-1BBTAC display poor surface expression (**Figure 19**) suggesting that our initial design, although well-rationalized, would not be suitable for our purposes.

In the case of the HER2-4-1BBTAC construct, the chimeric receptor could only be measured on a subpopulation of cells by flow cytometry (**Figure 19C**) and, we were unable to visualize the receptor itself through either western blot analysis or immunofluorescence microscopy (**Figure 20** and **21**). It is not evident why we observed with a lower transduction with the HER2-4-1BBTAC lentiviral vector when compared with other TAC constructs at the same MOI. One possibility is that the

receptor may be toxic to T cells and only cells that are either resistant or express low levels of the chimera can survive the culture conditions. A simple way to approach this hypothesis is to employ an inducible expression system for this receptor. In this way, 4-1BB TAC expression can be induced after transduction in a controlled manner and the viability of the culture can be monitored following induction. Alternatively, we could employ mRNA nucleofection, as described above, to express the 4-1BB TAC and measure viability following nucleofection.

In the case of the HER2-CD28TAC construct, we observed a phenotype suggestive of a defect in receptor trafficking. Although we achieved high level of T cell transduction with this lentivirus, as revealed by ΔNGFR expression, the HER2-CD28TAC receptor was not expressed well on the T cell membrane (**Figure 19**) despite high levels of the protein in the cell as measured by western blot analysis (**Figure 20**). Indeed, immunofluorescence demonstrated that the protein co-localized with calnexin, a marker of the ER (**Figure 21**). The anti-CD3 scFv utilized by the TAC receptors is derived from mAb clone UCHT1 and associates with the TCR/CD3 complex with high affinity[191]**.** It is possible that the HER2-CD28TAC is retained within the cell due to complex formation of TAC dimers with the TCR/CD3 complex within the ER. This scenario is plausible, as CD3 begins complex assembly within the ER[192]. A similar setting is seen when CD4 and HIV-1 gp120 are co-expressed within a cell, preventing surface expression of CD4[193]. It is notable that the HER2-CD4TAC, which uses the same scFv as the HER2-CD28TAC, has greater surface expression than the HER2-CD28TAC and shows

little retention within the cell by immunofluorescence microscopy. Furthermore, one would expect downregulation of TCRαβ if the HER2-CD28TAC was binding the TCR complex within the ER, but this was not observed (data not shown). It is possible that differences in trafficking or localization of CD4 and CD28 may be the explanation; whereas CD28 is mostly contained in non-raft regions and mobilizes to lipid rafts upon ligation, CD4 is known to locate with lipid rafts and may influence surface expression of the HER2-CD4TAC[154,194]. It is also possible that the monomeric nature of the HER2-CD4-TAC is preferred as the HER2-CD28-TAC contains the CD28 hinge and dimerization domain and likely exists as a dimer[164]. In such a scenario, dimer HER2-CD28TAC molecules may further complex with the TCR/CD3 complex as a result of the UCHT1 scFv, and form large oligomer structures that do not egress from the ER.

Regardless of which of the above hypotheses are correct, it will be necessary to redesign the HER2-CD28TAC receptor to pursue this line of research. Two changes that should be considered are: 1) mutation of the cysteines used for dimerization with the hinge region of CD28 hinge to prevent dimerization and 2) simply adding the CD28 intracellular signaling domain to the prototype CD4-TAC. With regard to the latter option, the orientation of the CD4 and CD28 intracellular domains must be considered. To date, no study has investigated the combination of one or more costimulatory domains in tandem with the CD4 transmembrane region or cytoplasmic domain. However, a study by Maher *et al.* found that the orientation of CD28 within the cytoplasmic tail of a CD28-CD3ζ CAR is critical for

functional properties of the receptor[195]. The authors found that placement of CD28 proximal, rather than distal, to the membrane, does not affect surface expression, but does impact the ability of the CAR to provide costimulation. With the limited knowledge available, investigating inclusion of CD4 both distal and proximal to the CD28 tail, as well as replacement of the CD28 hinge with that of the hinge utilized by the HER2-CD4TAC, is the most complete approach to identifying and creating a costimulatory CD28 TAC receptor capable of surface expression and function.

6.0 Conclusions

At this point, it is not possible to draw definite conclusions regarding the functionality of either the TIGIT/CD28 constructs or the costimulatory TAC receptors. To ultimately affirm our TIGIT/CD28 design, an alternative approach to achieve higher TAC and TIGIT/CD28 transgene expression is needed to examine the costimulatory capacity of this novel receptor; such alternate strategies were discussed above. Resolution of these issues and questions, as well as of the HER2-CD28TAC design, are the next steps in this research. Should the issue of expression be surmounted, the effects of costimulation, namely survival and proliferation, need to be assessed. Should these receptors show promise *in vitro*, the natural progression will then to test in an *in vivo* model to readily allow observation of increased persistence and maintained antitumor functionality over time.

7.0 Appendix

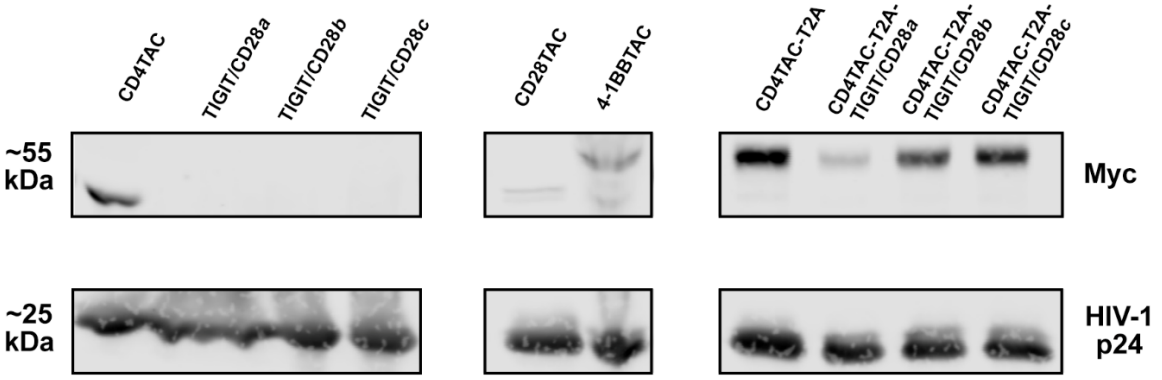

Figure S1. Lentiviruses containing the HER2-CD4TAC, and to a lesser degree the HER2-CD28TAC, contain the TAC receptor protein. Lentivirus was boiled in 1x sample buffer for 30 minutes and ~$7.0x10^6$ TU were loaded into a 10% polyacrylamide gel and samples were electrophoresed at 200V for 1 hour. Samples were then transferred to nitrocellulose membrane by the wet-method of transfer at 400 mA for 70 minutes. Membranes were blocked in 1:1 1x TBS:Odyssey Block Buffer (TBS) for one hour and stained with 1:500 mouse anti-C-myc primary and 1:2500 rabbit anti-HIV-1 p24 , and then 1:20,000 Li-Cor goat anti-mouse IRDye 680LT secondary and 1:20,000 Li-Cor goat anti-rabbit IRDye 800CW secondary.

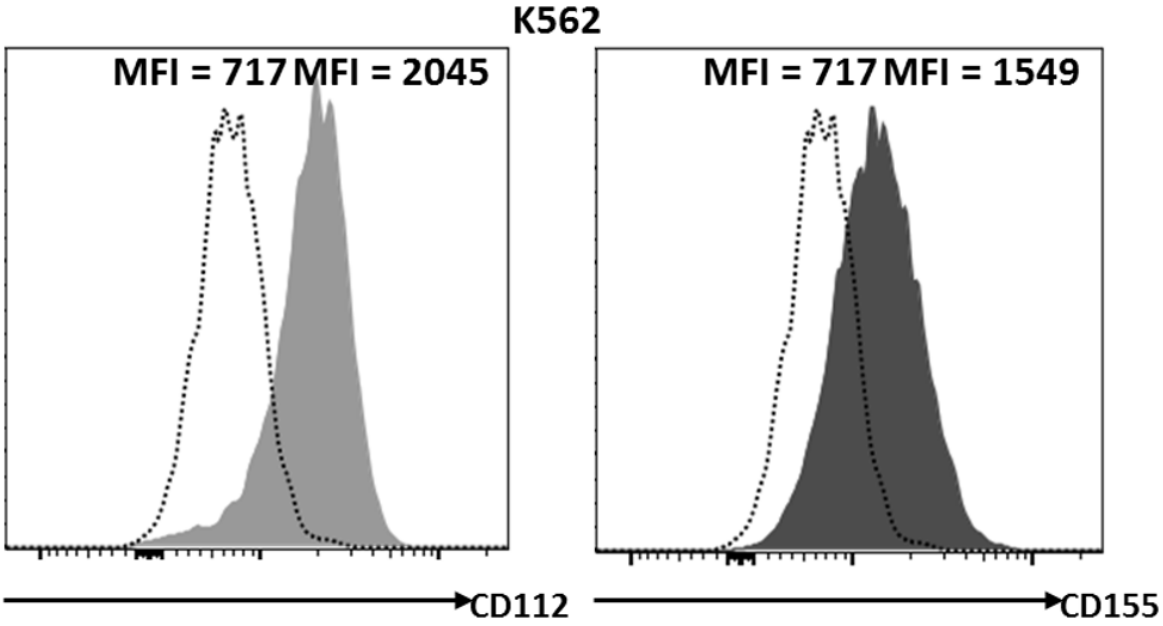

Figure S2. The cell line K562 expresses the surface antigens CD112 and CD155. K562 cells were stained with either 1:80 anti-CD155-PE or 1:20 anti-CD112-PE and run on a BD FACSCanto flow cytometry and analyzed with FlowJo software. Dotted line indicates unstained K562 cells.

References

1. Hanahan, D. & Weinberg, R. a. Hallmarks of cancer: The next generation. *Cell* **144,** 646–674 (2011).

2. Nowell, P. C. The clonal evolution of tumor cell populations. *Science* **194,** 23–28 (1976).

3. Knudson, a G. Two genetic hits (more or less) to cancer. *Nat. Rev. Cancer* **1,** 157–162 (2001).

4. Barrett, J. C. Mechanisms of multistep carcinogenesis and carcinogen risk assessment. *Environ. Health Perspect.* **100,** 9–20 (1993).

5. Loeb, K. R. & Loeb, L. a. Significance of multiple mutations in cancer. *Carcinogenesis* **21,** 379–385 (2000).

6. Cornfield, J. *et al.* Smoking and lung cancer: Recent evidence and a discussion of some questions. *Int. J. Epidemiol.* **38,** 1175–1191 (2009).

7. Lazovich, D. *et al.* Indoor tanning and risk of melanoma: A case-control study in a highly exposed population. *Cancer Epidemiol. Biomarkers Prev.* **19,** 1557–1568 (2010).

8. Zhang, M. *et al.* Use of tanning beds and incidence of skin cancer. *J. Clin. Oncol.* **30,** 1588–1593 (2012).

9. Wehner, M. R. *et al.* Indoor tanning and non-melanoma skin cancer: systematic review and meta-analysis. *Bmj* **345,** e5909 (2012).

10. Pfeifer, G. P. *et al.* Tobacco smoke carcinogens, DNA damage and p53 mutations in smoking-associated cancers. *Oncogene* **21,** 7435–7451 (2002).

11. Wels, J., Kaplan, R. N., Rafii, S. & Lyden, D. Migratory neighbors and distant invaders: Tumor-associated niche cells. *Genes Dev.* **22,** 559–574 (2008).

12. Hanahan, D. & Coussens, L. M. Accessories to the Crime: Functions of Cells Recruited to the Tumor Microenvironment. *Cancer Cell* **21,** 309–322 (2012).

13. Ghoshal, S. *The Emperor of All Maladies: A Biography of Cancer*. *Journal of Postgraduate Medicine Education and Research* **46,** (Simon and Schuster, 2012).

14. Canadian Cancer Society's Steering Comittee on Cancer Statistics. *Canadian Cancer Statistics 2014*. (2014).

15. Alizadeh, A. a *et al.* Toward understanding and exploiting tumor heterogeneity. *Nat. Med.* **21,** 846–853 (2015).

16. Burrell, R. a, McGranahan, N., Bartek, J. & Swanton, C. The causes and consequences of genetic heterogeneity in cancer evolution. *Nature* **501,** 338–45 (2013).

17. Michor, F. & Polyak, K. The origins and implications of intratumor heterogeneity. *Cancer Prev. Res.* **3,** 1361–1364 (2010).

18. Bedard, P. L., Hansen, A. R., Ratain, M. J. & Siu, L. L. Tumour heterogeneity in the clinic. *Nature* **501,** 355–64 (2013).

19. Alexandrov, L. B. *et al.* Signatures of mutational processes in human cancer. *Nature* **500,** 415–21 (2013).

20. DeVita, V. T. & Rosenberg, S. a. Two Hundred Years of Cancer Research. *N. Engl. J. Med.* **366,** 2207–2214 (2012).

21. Overgaard, M. *et al.* Postoperative radiotherapy in high-risk premenopausal women with breast cancer who receive adjuvant chemotherapy. Danish Breast Cancer Cooperative Group 82b Trial. *N. Engl. J. Med.* **337,** 949–955 (1997).

22. Visvader, J. E. & Lindeman, G. J. Cancer stem cells in solid tumours: accumulating evidence and unresolved questions. *Nat. Rev. Cancer* **8,** 755–768 (2008).

23. Vidal, S. J., Rodriguez-Bravo, V., Galsky, M., Cordon-Cardo, C. & Domingo-Domenech, J. Targeting cancer stem cells to suppress acquired chemotherapy resistance. *Oncogene* **33,** 1–13 (2013).

24. Kottke, T. *et al.* Detecting and targeting tumor relapse by its resistance to innate effectors at early recurrence. *Nat Med* **19,** 1625–1631 (2013).

25. Aguirre-Ghiso, J. a. Models, mechanisms and clinical evidence for cancer dormancy. *Nat. Rev. Cancer* **7,** 834–846 (2007).

26. Goss, P. E. & Chambers, A. F. Does tumour dormancy offer a therapeutic target? *Nat. Rev. Cancer* **10,** 871–877 (2010).

27. Huber, S. M. *et al.* Ionizing radiation, ion transports, and radioresistance of cancer cells. *Front. Physiol.* **4,** 212 (2013).

28. Pajonk, F., Vlashi, E. & McBride, W. H. Radiation resistance of cancer stem cells: The 4 R's of radiobiology revisited. *Stem Cells* **28,** 639–648 (2010).

29. Baguley, B. C. Multiple drug resistance mechanisms in cancer. *Mol. Biotechnol.* **46,** 308–316 (2010).

30. Garneau, J. E. *et al.* The CRISPR/Cas bacterial immune system cleaves bacteriophage and plasmid DNA. *Nature* **468,** 67–71 (2010).

31. Benhar, I., London, A. & Schwartz, M. The privileged immunity of immune privileged organs: The case of the eye. *Front. Immunol.* **3,** 296 (2012).

32. Akira, S., Uematsu, S. & Takeuchi, O. Pathogen Recognition and Innate Immunity. *Cell* **124,** 783–801 (2006).

33. Shankaran, V. *et al.* IFNgamma and lymphocytes prevent primary tumour development and shape tumour immunogenicity. *Nature* **410,** 1107–1111 (2001).

34. Girardi, M. *et al.* Regulation of cutaneous malignancy by gammadelta T cells. *Science* **294,** 605–609 (2001).

35. Kim, R., Emi, M. & Tanabe, K. Cancer immunoediting from immune surveillance to immune escape. *Immunology* **121,** 1–14 (2007).

36. Dunn, G. P., Bruce, A. T., Ikeda, H., Old, L. J. & Schreiber, R. D. Cancer immunoediting: from immunosurveillance to tumor escape. *Nat. Immunol.* **3,** 991–998 (2002).

37. Gallagher, M. P. *et al.* Long-term cancer risk of immunosuppressive regimens after kidney transplantation. *J. Am. Soc. Nephrol.* **21,** 852–858 (2010).

38. Engels, E. a. Spectrum of Cancer Risk Among US Solid Organ Transplant Recipients. *JAMA J. Am. Med. Assoc.* **306,** 1891 (2011).

39. Jochems, C. & Schlom, J. Tumor-infiltrating immune cells and prognosis: the potential link between conventional cancer therapy and immunity. *Exp. Biol. Med. (Maywood).* **236,** 567–579 (2011).

40. Clemente, C. G. *et al.* Prognostic value of tumor infiltrating lymphocytes in the vertical growth phase of primary cutaneous melanoma. *Cancer* **77,** 1303–1310 (1996).

41. Swann, J. B. & Smyth, M. J. Review series Immune surveillance of tumors. *J. Clin. Invest.* **117,** 1137–1146 (2007).

42. Neefjes, J., Jongsma, M. L. M., Paul, P. & Bakke, O. Towards a systems understanding of MHC class I and MHC class II antigen presentation. *Nat. Rev. Immunol.* **11,** 823–36 (2011).

43. Koch, U. & Radtke, F. Mechanisms of T cell development and transformation. *Annu. Rev. Cell Dev. Biol.* **27,** 539–62 (2011).

44. Germain, R. N. T-cell development and the CD4-CD8 lineage decision. *Nat. Rev. Immunol.* **2,** 309–22 (2002).

45. Appleman, L. J. & Boussiotis, V. a. T cell anergy and costimulation. *Immunol. Rev.* **192,** 161–180 (2003).

46. Macián, F., Im, S. H., García-Cózar, F. J. & Rao, A. T-cell anergy. *Curr. Opin. Immunol.* **16,** 209–216 (2004).

47. Alegre, M. L., Frauwirth, K. a & Thompson, C. B. T-cell regulation by CD28 and CTLA-4. *Nat. Rev. Immunol.* **1,** 220–228 (2001).

48. Smith-Garvin, J. E., Koretzky, G. a & Jordan, M. S. T cell activation. *Annu. Rev. Immunol.* **27,** 591–619 (2009).

49. Boomer, J. S. & Green, J. M. An enigmatic tail of CD28 signaling. *Cold Spring Harb. Perspect. Biol.* **2,** a002436 (2010).

50. Jones, R. G. *et al.* Protein kinase B regulates T lymphocyte survival, nuclear factor kappaB activation, and Bcl-X(L) levels in vivo. *J. Exp. Med.* **191,** 1721–1734 (2000).

51. Marko, A. J., Miller, R. a., Kelman, A. & Frauwirth, K. a. Induction of glucose metabolism in stimulated T lymphocytes is regulated by mitogen-activated protein kinase signaling. *PLoS One* **5,** (2010).

52. Frauwirth, K. a *et al.* The CD28 signaling pathway regulates glucose metabolism. *Immunity* **16,** 769–777 (2002).

53. Sanchez-Lockhart, M. *et al.* Cutting edge: CD28-mediated transcriptional and posttranscriptional regulation of IL-2 expression are controlled through different signaling pathways. *J. Immunol.* **173,** 7120–7124 (2004).

54. Acuto, O. & Michel, F. CD28-mediated co-stimulation: a quantitative support for TCR signalling. *Nat. Rev. Immunol.* **3,** 939–951 (2003).

55. Boesteanu, A. C. & Katsikis, P. D. Memory T cells need CD28 costimulation to remember. *Semin. Immunol.* **21,** 69–77 (2009).

56. Borowski, A. B. *et al.* Memory CD8+ T cells require CD28 costimulation. *J. Immunol.* **179,** 6494–6503 (2007).

57. Martínez-Llordella, M. *et al.* CD28-inducible transcription factor DEC1 is required for efficient autoreactive CD4+ T cell response. *J. Exp. Med.* **210,** 1603–19 (2013).

58. Guermonprez, P., Valladeau, J., Zitvogel, L., Théry, C. & Amigorena, S. Antigen presentation and T cell stimulation by dendritic cells. *Annu. Rev. Immunol.* **20,** 621–67 (2002).

59. Wiedemann, A., Depoil, D., Faroudi, M. & Valitutti, S. Cytotoxic T lymphocytes kill multiple targets simultaneously via spatiotemporal uncoupling of lytic and stimulatory synapses. *Proc. Natl. Acad. Sci. U. S. A.* **103,** 10985–90 (2006).

60. Duke, R. C. Self recognition by T cells. I. Bystander killing of target cells bearing syngeneic MHC antigens. *J. Exp. Med.* **170,** 59–71 (1989).

61. Groscurth, P. & Filgueira, L. Killing Mechanisms of Cytotoxic T Lymphocytes. *News Physiol Sci* **13,** 17–21 (1998).

62. Appay, V. The physiological role of cytotoxic CD4(+) T-cells: the holy grail? *Clin. Exp. Immunol.* **138,** 10–3 (2004).

63. Quezada, S. A. *et al.* Tumor-reactive CD4(+) T cells develop cytotoxic activity and eradicate large established melanoma after transfer into lymphopenic hosts. *J. Exp. Med.* **207,** 637–50 (2010).

64. Kennedy, R. & Celis, E. Multiple roles for CD4+ T cells in anti-tumor immune responses. *Immunol. Rev.* **222,** 129–144 (2008).

65. Schoenberger, S. P., Toes, R. E., van der Voort, E. I., Offringa, R. & Melief, C. J. T-cell help for cytotoxic T lymphocytes is mediated by CD40-CD40L interactions. *Nature* **393,** 480–483 (1998).

66. Janssen, E. M. *et al.* CD4+ T-cell help controls CD8+ T-cell memory via TRAIL-mediated activation-induced cell death. *Nature* **434,** 88–93 (2005).

67. Van Horssen, R., Ten Hagen, T. L. M. & Eggermont, A. M. M. TNF-alpha in cancer treatment: molecular insights, antitumor effects, and clinical utility. *Oncologist* **11,** 397–408 (2006).

68. Calzascia, T. *et al.* TNF-α is critical for antitumor but not antiviral T cell immunity in mice. *J. Clin. Invest.* **117,** 3833–3845 (2007).

69. Zaidi, M. R. & Merlino, G. The two faces of interferon-γ in cancer. *Clin. Cancer Res.* **17,** 6118–6124 (2011).

70. Ikeda, H., Old, L. J. & Schreiber, R. D. The roles of IFN?? in protection against tumor development and cancer immunoediting. *Cytokine Growth Factor Rev.* **13,** 95–109 (2002).

71. Kumar, V., Kono, D. H., Urban, J. L. & Hood, L. The T-cell receptor repertoire and autoimmune diseases. *Annu. Rev. Immunol.* **7,** 657–682 (1989).

72. Coulie, P. G., Van den Eynde, B. J., van der Bruggen, P. & Boon, T. Tumour antigens recognized by T lymphocytes: at the core of cancer immunotherapy. *Nat. Rev. Cancer* **14,** 135–46 (2014).

73. Gubin, M. M., Artyomov, M. N., Mardis, E. R. & Schreiber, R. D. Tumor neoantigens: building a framework for personalized cancer immunotherapy. *J. Clin. Invest.* **125,** 1–9 (2015).

74. Schumacher, T. N. & Schreiber, R. D. Neoantigens in cancer immunotherapy. *Science (80-.).* **348,** 69–74 (2015).

75. McCarthy, E. F. The toxins of William B. Coley and the treatment of bone and soft-tissue sarcomas. *Iowa Orthop. J.* **26,** 154–158 (2006).

76. Meyer, J., Persad, R. & Gillatt, D. Use of bacille Calmette-Guérin in superficial bladder cancer. *Postgrad. Med. J.* **78,** 449–454 (2002).

77. Pardoll, D. M. The blockade of immune checkpoints in cancer immunotherapy. *Nat. Rev. Cancer* **12,** 252–264 (2012).

78. Wolchok, J. D. *et al.* Nivolumab plus ipilimumab in advanced melanoma. *N. Engl. J. Med.* **369,** 122–33 (2013).

79. Hodi, F. S. *et al.* Improved survival with ipilimumab in patients with metastatic melanoma. *N. Engl. J. Med.* **363,** 711–723 (2010).

80. Shin, D. S. & Ribas, A. The evolution of checkpoint blockade as a cancer therapy: what's here, what's next? *Curr. Opin. Immunol.* **33,** 23–35 (2015).

81. Postow, M. a., Callahan, M. K. & Wolchok, J. D. Immune Checkpoint Blockade in Cancer Therapy. *J. Clin. Oncol.* **33,** 1974–1982 (2015).

82. Ansell, S. M. *et al.* Phase I study of ipilimumab, an anti-CTLA-4 monoclonal antibody, in patients with relapsed and refractory B-cell non-Hodgkin lymphoma. *Clin. Cancer Res.* **15,** 6446–6453 (2009).

83. Corsello, S. M. *et al.* Endocrine side effects induced by immune checkpoint inhibitors. *J. Clin. Endocrinol. Metab.* **98,** 1361–1375 (2013).

84. Fecher, L. a, Agarwala, S. S., Hodi, F. S. & Weber, J. S. Ipilimumab and its toxicities: a multidisciplinary approach. *Oncologist* **18,** 733–43 (2013).

85. Overwijk, W. W. *et al.* Vaccination with a recombinant vaccinia virus encoding a 'self' antigen induces autoimmune vitiligo and tumor cell destruction in mice: Requirement for CD4+ T lymphocytes. *Proc. Natl. Acad. Sci.* **96,** 2982–2987 (1999).

86. Ludewig, B. *et al.* Immunotherapy with Dendritic Cells Directed against Tumor Antigens Shared with Normal Host Cells Results in Severe Autoimmune Disease. *J. Exp. Med.* **191,** 795–804 (2000).

87. Lane, C. *et al.* Vaccination-induced autoimmune vitiligo is a consequence of secondary trauma to the skin. *Cancer Res.* **64,** 1509–14 (2004).

88. Eggermont, a. M. M. Immunostimulation versus immunosuppression after multiple vaccinations: The woes of therapeutic vaccine development. *Clin. Cancer Res.* **15,** 6745–6747 (2009).

89. McGray, a J. R. *et al.* Immunotherapy-induced CD8(+) T Cells Instigate Immune Suppression in the Tumor. *Mol. Ther.* **22,** 206–18 (2014).

90. June, C. H. Adoptive T cell therapy for cancer in the clinic. *J. Clin. Invest.* **117,** 1466–1476 (2007).

91. Hinrichs, C. S. & Rosenberg, S. a. Exploiting the curative potential of adoptive T-cell therapy for cancer. *Immunol. Rev.* **257,** 56–71 (2014).

92. Klebanoff, C. a, Gattinoni, L. & Restifo, N. P. Sorting through subsets: which T-cell populations mediate highly effective adoptive immunotherapy? *J. Immunother.* **35,** 651–60 (2012).

93. Gattinoni, L., Klebanoff, C. a. & Restifo, N. P. Paths to stemness: building the ultimate antitumour T cell. *Nat. Rev. Cancer* **12,** 671–684 (2012).

94. Bonini, C. & Mondino, A. Adoptive T-cell therapy for cancer: The era of engineered T cells. *Eur. J. Immunol.* **45,** 2457–69 (2015).

95. Bubeník, J. MHC class I down-regulation: tumour escape from immune surveillance? (review). *Int. J. Oncol.* **25,** 487–491 (2004).

96. Leone, P. *et al.* MHC class i antigen processing and presenting machinery: Organization, function, and defects in tumor cells. *J. Natl. Cancer Inst.* **105,** 1172–1187 (2013).

97. Ferris, R. L., Whiteside, T. L. & Ferrone, S. Immune escape associated with functional defects in antigen-processing machinery in head and neck cancer. *Clin. Cancer Res.* **12,** 3890–3895 (2006).

98. Cooke, T., Reeves, J., Lanigan, A. & Stanton, P. HER2 as a prognostic and predictive marker for breast cancer. *Ann. Oncol.* **12,** S23–S28 (2001).

99. Menard, S. *et al.* HER2 overexpression in various tumor types, focussing on its relationship to the development of invasive breast cancer. *Ann. Oncol.* **12,** S15–S19 (2001).

100. Eshhar, Z., Waks, T., Gross, G. & Schindler, D. G. Specific activation and targeting of cytotoxic lymphocytes through chimeric single chains consisting of antibody-binding domains and the gamma or zeta subunits of the immunoglobulin and T-cell receptors. *Proc. Natl. Acad. Sci. U. S. A.* **90,** 720–724 (1993).

101. Stancovski, I. *et al.* Targeting of T lymphocytes to Neu/HER2-expressing cells using chimeric single chain Fv receptors. *J. Immunol.* **151,** 6577–6582 (1993).

102. Sentman, C. L. & Meehan, K. R. NKG2D CARs as cell therapy for cancer. *Cancer J.* **20,** 156–9 (2014).

103. Barber, A. *et al.* Chimeric NKG2D receptor-bearing T cells as immunotherapy for ovarian cancer. *Cancer Res.* **67,** 5003–5008 (2007).

104. Song, D.-G. *et al.* Chimeric NKG2D CAR-expressing T cell-mediated attack of human ovarian cancer is enhanced by histone deacetylase inhibition. *Hum. Gene Ther.* **24,** 295–305 (2013).

105. Maude, S. L. *et al.* Chimeric Antigen Receptor T Cells for Sustained Remissions in Leukemia. *N. Engl. J. Med.* **371,** 1507–1517 (2014).

106. Gajewski, T. F. *et al.* Immune resistance orchestrated by the tumor microenvironment. *Immunol. Rev.* **213,** 131–145 (2006).

107. Lindau, D., Gielen, P., Kroesen, M., Wesseling, P. & Adema, G. J. The immunosuppressive tumour network: Myeloid-derived suppressor cells, regulatory T cells and natural killer T cells. *Immunology* **138,** 105–115 (2013).

108. Whiteside, T. L. The tumor microenvironment and its role in promoting tumor growth. *Oncogene* **27,** 5904–5912 (2008).

109. Jiang, Y., Li, Y. & Zhu, B. T-cell exhaustion in the tumor microenvironment. *Cell Death Dis.* **6,** e1792 (2015).

110. Driessens, G., Kline, J. & Gajewski, T. F. Costimulatory and coinhibitory receptors in anti-tumor immunity. *Immunol. Rev.* **229,** 126–144 (2009).

111. Norde, W. J., Hobo, W., Van Der Voort, R. & Dolstra, H. Coinhibitory molecules in hematologic malignancies: Targets for therapeutic intervention. *Blood* **120,** 728–736 (2012).

112. Koehler, H., Kofler, D., Hombach, A. & Abken, H. CD28 costimulation overcomes transforming growth factor-β-mediated repression of proliferation of redirected human CD4+ and CD8 + T cells in an antitumor cell attack. *Cancer Res.* **67,** 2265–2273 (2007).

113. Li, Q., Carr, A., Ito, F., Teitz-Tennenbaum, S. & Chang, A. E. Polarization effects of 4-1BB during CD28 costimulation in generating tumor-reactive T cells for cancer immunotherapy. *Cancer Res.* **63,** 2546–2552 (2003).

114. Savoldo, B. *et al.* CD28 costimulation improves expansion and persistence of chimeric antigen receptor-modified T cells in lymphoma patients. *J. Clin. Invest.* **121,** 1822–1826 (2011).

115. Moeller, M. *et al.* A functional role for CD28 costimulation in tumor recognition by single-chain receptor-modified T cells. *Cancer Gene Ther.* **11,** 371–379 (2004).

116. Porter, D. L. *et al.* Chimeric antigen receptor T cells persist and induce sustained remissions in relapsed refractory chronic lymphocytic leukemia. *Sci. Transl. Med.* **7,** 303ra139–303ra139 (2015).

117. Dotti, G., Gottschalk, S., Savoldo, B. & Brenner, M. K. Design and development of therapies using chimeric antigen receptor-expressing T cells. *Immunol. Rev.* **257,** 107–126 (2014).

118. Kowolik, C. M. *et al.* CD28 costimulation provided through a CD19-specific chimeric antigen receptor enhances in vivo persistence and antitumor efficacy of adoptively transferred T cells. *Cancer Res.* **66,** 10995–11004 (2006).

119. Finney, H. M., Akbar, A. N. & Lawson, A. D. G. Activation of resting human primary T cells with chimeric receptors: costimulation from CD28, inducible costimulator, CD134, and CD137 in series with signals from the TCR zeta chain. *J. Immunol.* **172,** 104–113 (2004).

120. Song, D. G. *et al.* In vivo persistence, tumor localization, and antitumor activity of CAR-engineered T cells is enhanced by costimulatory signaling through CD137 (4-1BB). *Cancer Res.* **71,** 4617–4627 (2011).

121. Hombach, A. a., Heiders, J., Foppe, M., Chmielewski, M. & Abken, H. OX40 costimulation by a chimeric antigen receptor abrogates CD28 and IL-2 induced IL-10 secretion by redirected CD4+ T cells. *Oncoimmunology* **1,** 458–466 (2012).

122. Song, D. G. *et al.* CD27 costimulation augments the survival and antitumor activity of redirected human T cells in vivo. *Blood* **119,** 696–706 (2012).

123. Guedan, S. *et al.* ICOS-based chimeric antigen receptors program bipolar TH17/TH1 cells. *Blood* **124,** 1070–80 (2014).

124. Condomines, M. *et al.* Tumor-Targeted Human T Cells Expressing CD28-Based Chimeric Antigen Receptors Circumvent CTLA-4 Inhibition. *PLoS One* **10,** e0130518 (2015).

125. Stephan, M. T. *et al.* T cell-encoded CD80 and 4-1BBL induce auto- and transcostimulation, resulting in potent tumor rejection. *Nat. Med.* **13,** 1440–1449 (2007).

126. Kofler, D. M. *et al.* CD28 costimulation Impairs the efficacy of a redirected t-cell antitumor attack in the presence of regulatory t cells which can be overcome by preventing Lck activation. *Mol. Ther.* **19,** 760–767 (2011).

127. Loskog, a *et al.* Addition of the CD28 signaling domain to chimeric T-cell receptors enhances chimeric T-cell resistance to T regulatory cells. *Leukemia* **20,** 1819–1828 (2006).

128. Krause, a *et al.* Antigen-dependent CD28 signaling selectively enhances survival and proliferation in genetically modified activated human primary T lymphocytes. *J. Exp. Med.* **188,** 619–626 (1998).

129. Kloss, C. C., Condomines, M., Cartellieri, M., Bachmann, M. & Sadelain, M. Combinatorial antigen recognition with balanced signaling promotes selective tumor eradication by engineered T cells. *Nat. Biotechnol.* **31,** 71–5 (2013).

130. Zhong, X.-S., Matsushita, M., Plotkin, J., Riviere, I. & Sadelain, M. Chimeric antigen receptors combining 4-1BB and CD28 signaling domains augment PI3kinase/AKT/Bcl-XL activation and CD8+ T cell-mediated tumor eradication. *Mol. Ther.* **18,** 413–420 (2010).

131. Milone, M. C. *et al.* Chimeric receptors containing CD137 signal transduction domains mediate enhanced survival of T cells and increased antileukemic efficacy in vivo. *Mol. Ther.* **17,** 1453–1464 (2009).

132. Frigault, M. J. *et al.* Identification of chimeric antigen receptors that mediate constitutive or inducible proliferation of T cells. *Cancer Immunol. Res.* **3,** 356–367 (2015).

133. Sadelain, M., Brentjens, R. & Rivière, I. The promise and potential pitfalls of chimeric antigen receptors. *Curr. Opin. Immunol.* **21,** 215–223 (2009).

134. Joller, N. *et al.* Cutting edge: TIGIT has T cell-intrinsic inhibitory functions. *J. Immunol.* **186,** 1338–1342 (2011).

135. Levin, S. D. *et al.* Vstm3 is a member of the CD28 family and an important modulator of T-cell function. *Eur. J. Immunol.* **41,** 902–915 (2011).

136. Chan, C. J., Andrews, D. M. & Smyth, M. J. Receptors that interact with nectin and nectin-like proteins in the immunosurveillance and immunotherapy of cancer. *Curr. Opin. Immunol.* **24,** 246–251 (2012).

137. Stengel, K. F. *et al.* Structure of TIGIT immunoreceptor bound to poliovirus receptor reveals a cell-cell adhesion and signaling mechanism that requires cis-trans receptor clustering. *Proc. Natl. Acad. Sci.* **109,** 5399–5404 (2012).

138. Lozano, E., Dominguez-Villar, M., Kuchroo, V. & Hafler, D. a. The TIGIT/CD226 axis regulates human T cell function. *J. Immunol.* **188,** 3869–75 (2012).

139. Masson, D. *et al.* Overexpression of the CD155 gene in human colorectal carcinoma. *Gut* **49,** 236–240 (2001).

140. Carlsten, M. *et al.* DNAX accessory molecule-1 mediated recognition of freshly isolated ovarian carcinoma by resting natural killer cells. *Cancer Res.* **67,** 1317–1325 (2007).

141. Oshima, T. *et al.* Nectin-2 is a potential target for antibody therapy of breast and ovarian cancers. *Mol. Cancer* **12,** 60 (2013).

142. Pende, D. *et al.* Analysis of the receptor-ligand interactions in the natural killer-mediated lysis of freshly isolated myeloid or lymphoblastic leukemias: Evidence for the involvement of the Polio virus receptor (CD 155) and Nectin-2 (CD 112). *Blood* **105,** 2066–2073 (2005).

143. El-Sherbiny, Y. M. *et al.* The requirement for DNAM-1, NKG2D, and NKp46 in the natural killer cell-mediated killing of myeloma cells. *Cancer Res.* **67,** 8444–8449 (2007).

144. Castriconi, R. *et al.* Natural killer cell-mediated killing of freshly isolated neuroblastoma cells: Critical role of DNAX accessory molecule-1-poliovirus receptor interaction. *Cancer Res.* **64,** 9180–9184 (2004).

145. Bottino, C. *et al.* Identification of PVR (CD155) and Nectin-2 (CD112) as cell surface ligands for the human DNAM-1 (CD226) activating molecule. *J. Exp. Med.* **198,** 557–567 (2003).

146. Carlsten, M. *et al.* Primary human tumor cells expressing CD155 impair tumor targeting by down-regulating DNAM-1 on NK cells. *J. Immunol.* **183,** 4921–4930 (2009).

147. Sloan, K. E., Stewart, J. K., Treloar, A. F., Matthews, R. T. & Jay, D. G. CD155/PVR enhances glioma cell dispersal by regulating adhesion signaling and focal adhesion dynamics. *Cancer Res.* **65,** 10930–10937 (2005).

148. Sloan, K. E. *et al.* CD155/PVR plays a key role in cell motility during tumor cell invasion and migration. *BMC Cancer* **4,** 73 (2004).

149. Chauvin, J.-M. *et al.* TIGIT and PD-1 impair tumor antigen-specific $CD8^+$ T cells in melanoma patients. *J. Clin. Invest.* **125,** 2046–58 (2015).

150. Grogan, J. *et al.* TIGIT inhibits CD8+ T cell effector function during chronic viral infection and cancer (TUM7P.933). *J. Immunol.* **192,** 203.15 (2014).

151. Johnston, R. J. *et al.* Article The Immunoreceptor TIGIT Regulates Antitumor and Antiviral CD8 + T Cell Effector Function. *Cancer Cell* **26,** 923–937 (2014).

152. Dennehy, K. M. *et al.* Cutting edge: monovalency of CD28 maintains the antigen dependence of T cell costimulatory responses. *J. Immunol.* **176,** 5725–5729 (2006).

153. Sanchez-Lockhart, M., Kim, M. & Miller, J. Cutting edge: A role for inside-out signaling in TCR regulation of CD28 ligand binding. *J. Immunol.* **187,** 5515–9 (2011).

154. Sadra, A., Cinek, T. & Imboden, J. B. Translocation of CD28 to lipid rafts and costimulation of IL-2. *Proc. Natl. Acad. Sci. U. S. A.* **101,** 11422–11427 (2004).

155. Viola, a, Schroeder, S., Sakakibara, Y. & Lanzavecchia, a. T lymphocyte costimulation mediated by reorganization of membrane microdomains. *Science* **283,** 680–682 (1999).

156. Tavano, R. *et al.* CD28 and lipid rafts coordinate recruitment of Lck to the immunological synapse of human T lymphocytes. *J. Immunol.* **173,** 5392–5397 (2004).

157. Hofinger, E. & Sticht, H. Multiple modes of interaction between Lck and CD28. *J. Immunol.* **174,** 3839–3840; author reply 3840 (2005).

158. Zufferey, R. *et al.* Self-inactivating lentivirus vector for safe and efficient in vivo gene delivery. *J. Virol.* **72,** 9873–9880 (1998).

159. Dull, T. *et al.* A third-generation lentivirus vector with a conditional packaging system. *J. Virol.* **72,** 8463–8471 (1998).

160. Cronin, J., Zhang, X.-Y. & Reiser, J. Altering the tropism of lentiviral vectors through pseudotyping. *Curr. Gene Ther.* **5,** 387–398 (2005).

161. Krutzik, P. O. & Nolan, G. P. Intracellular phospho-protein staining techniques for flow cytometry: monitoring single cell signaling events. *Cytometry. A* **55,** 61–70 (2003).

162. Kurien, B. T. & Scofield, R. H. Protein blotting: A review. *J. Immunol. Methods* **274,** 1–15 (2003).

163. Pulè, M. a. *et al.* A chimeric T cell antigen receptor that augments cytokine release and supports clonal expansion of primary human T cells. *Mol. Ther.* **12,** 933–941 (2005).

164. Lazar-Molnar, E., Almo, S. C. & Nathenson, S. G. The interchain disulfide linkage is not a prerequisite but enhances CD28 costimulatory function. *Cell. Immunol.* **244,** 125–129 (2006).

165. Linsley, P. S. *et al.* Binding stoichiometry of the cytotoxic T lymphocyte-associated molecule-4 (CTLA-4): A disulfide-linked homodimer binds two CD86 molecules. *J. Biol. Chem.* **270,** 15417–15424 (1995).

166. Finney, H. M., Lawson, a D., Bebbington, C. R. & Weir, a N. Chimeric receptors providing both primary and costimulatory signaling in T cells from a single gene product. *J. Immunol.* **161,** 2791–2797 (1998).

167. Kane, L. P., Andres, P. G., Howland, K. C., Abbas, a K. & Weiss, a. Akt provides the CD28 costimulatory signal for up-regulation of IL-2 and IFN-gamma but not TH2 cytokines. *Nat. Immunol.* **2,** 37–44 (2001).

168. Dodson, L. F. *et al.* Targeted knock-in mice expressing mutations of CD28 reveal an essential pathway for costimulation. *Mol. Cell. Biol.* **29,** 3710–3721 (2009).

169. Jones, R. G. *et al.* CD28-dependent activation of protein kinase B/Akt blocks Fas-mediated apoptosis by preventing death-inducing signaling complex assembly. *J. Exp. Med.* **196,** 335–348 (2002).

170. Sarbassov, D. D., Guertin, D. a, Ali, S. M. & Sabatini, D. M. Phosphorylation and regulation of Akt/PKB by the rictor-mTOR complex. *Science* **307,** 1098–1101 (2005).

171. Manning, B. D. & Cantley, L. C. AKT/PKB Signaling: Navigating Downstream. *Cell* **129,** 1261–1274 (2007).

172. Perez, O. D. & Nolan, G. P. Simultaneous measurement of multiple active kinase states using polychromatic flow cytometry. *Nat. Biotechnol.* **20,** 155–162 (2002).

173. Bahlis, N. J. *et al.* CD28-mediated regulation of multiple myeloma cell proliferation and survival. *Blood* **109,** 5002–5010 (2007).

174. Nair, J. R. *et al.* CD28 expressed on malignant plasma cells induces a prosurvival and immunosuppressive microenvironment. *J. Immunol.* **187,** 1243–1253 (2011).

175. Murray, M. E. *et al.* CD28-mediated pro-survival signaling induces chemotherapeutic resistance in multiple myeloma. *Blood* **123,** 3770–3779 (2014).

176. Kim, J. H. *et al.* High cleavage efficiency of a 2A peptide derived from porcine teschovirus-1 in human cell lines, zebrafish and mice. *PLoS One* **6,** e18556 (2011).

177. Zahnd, C. *et al.* A Designed Ankyrin Repeat Protein Evolved to Picomolar Affinity to Her2. *J. Mol. Biol.* **369,** 1015–1028 (2007).

178. Lee, D. W. *et al.* T cells expressing CD19 chimeric antigen receptors for acute lymphoblastic leukaemia in children and young adults : a phase 1 dose-escalation trial. *Lancet* **385,** 517–528 (2014).

179. Maude, S. L., Teachey, D. T., Porter, D. L. & Grupp, S. a. CD19-targeted chimeric antigen receptor T cell therapy for acute lymphoblastic leukemia. *Blood* **125,** 4017–4023 (2015).

180. Kochenderfer, J. N. *et al.* Chemotherapy-Refractory Diffuse Large B-Cell Lymphoma and Indolent B-Cell Malignancies Can Be Effectively Treated With Autologous T Cells Expressing an Anti-CD19 Chimeric Antigen Receptor. *J. Clin. Oncol.* **33,** 540–549 (2014).

181. Grupp, S. a *et al.* Chimeric antigen receptor-modified T cells for acute lymphoid leukemia. *N. Engl. J. Med.* **368,** 1509–18 (2013).

182. Jensen, M. C. & Riddell, S. R. Design and implementation of adoptive therapy with chimeric antigen receptor-modified T cells. *Immunol. Rev.* **257,** 127–144 (2014).

183. Shan, X. *et al.* Deficiency of PTEN in Jurkat T cells causes constitutive localization of Itk to the plasma membrane and hyperresponsiveness to CD3 stimulation. *Mol. Cell. Biol.* **20,** 6945–6957 (2000).

184. Parry, R. V *et al.* CTLA-4 and PD-1 receptors inhibit T-cell activation by distinct mechanisms. *Mol. Cell. Biol.* **25,** 9543–9553 (2005).

185. Suhoski, M. M. *et al.* Engineering artificial antigen-presenting cells to express a diverse array of co-stimulatory molecules. *Mol. Ther.* **15,** 981–988 (2007).

186. Schumann, K. *et al.* Generation of knock-in primary human T cells using Cas9 ribonucleoproteins. *Proc. Natl. Acad. Sci.* **112,** 201512503 (2015).

187. Brügger, B. *et al.* The HIV lipidome: a raft with an unusual composition. *Proc. Natl. Acad. Sci. U. S. A.* **103,** 2641–2646 (2006).

188. Nguyen, D. H. & Hildreth, J. E. Evidence for budding of human immunodeficiency virus type 1 selectively from glycolipid-enriched membrane lipid rafts. *J. Virol.* **74,** 3264–3272 (2000).

189. Beatty, G. L. *et al.* Mesothelin-specific Chimeric Antigen Receptor mRNA-Engineered T cells Induce Anti-Tumor Activity in Solid Malignancies. *Cancer Immunol. Res.* **2,** 112–20 (2014).

190. Long, A. H. *et al.* 4-1BB costimulation ameliorates T cell exhaustion induced by tonic signaling of chimeric antigen receptors. *Nat. Med.* **21,** 581–590 (2015).

191. Salmerón, a, Sánchez-Madrid, F., Ursa, M. a, Fresno, M. & Alarcón, B. A conformational epitope expressed upon association of CD3-epsilon with either CD3-delta or CD3-gamma is the main target for recognition by anti-CD3 monoclonal antibodies. *J. Immunol.* **147,** 3047–3052 (1991).

192. Alarcon, B., Berkhout, B., Breitmeyer, J. & Terhorst, C. Assembly of the human T cell receptor-CD3 complex takes place in the endoplasmic reticulum and involves intermediary complexes between the CD3-gamma.delta.epsilon core and single T cell receptor alpha or beta chains. *J. Biol. Chem.* **263,** 2953–2961 (1988).

193. Crise, B., Buonocore, L. & Rose, J. K. CD4 is retained in the endoplasmic reticulum by the human immunodeficiency virus type 1 glycoprotein precursor. *J. Virol.* **64,** 5585–5593 (1990).

194. Fragoso, R. *et al.* Lipid raft distribution of CD4 depends on its palmitoylation and association with Lck, and evidence for CD4-induced lipid raft aggregation as an additional mechanism to enhance CD3 signaling. *J. Immunol.* **170,** 913–921 (2003).

195. Maher, J., Brentjens, R. J., Gunset, G., Rivière, I. & Sadelain, M. Human T-lymphocyte cytotoxicity and proliferation directed by a single chimeric TCRzeta /CD28 receptor. *Nat. Biotechnol.* **20,** 70–75 (2002).